ESTIMATION OF SHEAR WAVE VELOCITY PROFILE FROM EXPLOSION SOURCE

Mr. Pithan Pairojn

จุฬาลงกรณ์มหาวิทยาลัย
Chulalongkorn University

บทคัดย่อและแฟ้มข้อมูลฉบับเต็มของวิทยานิพนธ์ตั้งแต่ปีการศึกษา 2554 ที่ให้บริการในคลังปัญญาจุฬาฯ (CUIR)
เป็นแฟ้มข้อมูลของนิสิตเจ้าของวิทยานิพนธ์ ที่ส่งผ่านทางบัณฑิตวิทยาลัย
The abstract and full text of theses from the academic year 2011 in Chulalongkorn University Intellectual Repository (CUIR)
are the thesis authors' files submitted through the University Graduate School.

A Dissertation Submitted in Partial Fulfillment of the Requirements

for the Degree of Doctor of Philosophy Program in Civil Engineering

Department of Civil Engineering

Faculty of Engineering

Chulalongkorn University

Academic Year 2014

Copyright of Chulalongkorn University

การหาค่าความเร็วคลื่นเฉือนจากแหล่งกำเนิดคลื่นวัตถุระเบิด

นายพิธาน ไพโรจน์

จุฬาลงกรณ์มหาวิทยาลัย
Chulalongkorn University

วิทยานิพนธ์นี้เป็นส่วนหนึ่งของการศึกษาตามหลักสูตรปริญญาวิศวกรรมศาสตรดุษฎีบัณฑิต
สาขาวิชาวิศวกรรมโยธา ภาควิชาวิศวกรรมโยธา
คณะวิศวกรรมศาสตร์ จุฬาลงกรณ์มหาวิทยาลัย
ปีการศึกษา 2557
ลิขสิทธิ์ของจุฬาลงกรณ์มหาวิทยาลัย

Thesis Title	ESTIMATION OF SHEAR WAVE VELOCITY PROFILE FROM EXPLOSION SOURCE
By	Mr. Pithan Pairojn
Field of Study	Civil Engineering
Thesis Advisor	Associate Professor Supot Teachavorasinskun, D.Eng.

Accepted by the Faculty of Engineering, Chulalongkorn University in Partial Fulfillment of the Requirements for the Doctoral Degree

.....Dean of the Faculty of Engineering

(Professor Bundhit Eua-arporn, Ph.D.)

THESIS COMMITTEE

.....Chairman

(Associate Professor Tirawat Boonyatee, D.Eng.)

.....Thesis Advisor

(Associate Professor Supot Teachavorasinskun, D.Eng.)

.....Examiner

(Associate ProfessorBoonchai Ukritchon, Sc.D)

.....Examiner

(Professor Suched Likitlersuang, D.Phil.)

.....External Examiner

(Assistant Professor Siam Yimsiri, Ph.D.)

จุฬาลงกรณ์มหาวิทยาลัย
CHULALONGKORN UNIVERSITY

พิธาน ไพโรจน์ : การหาค่าความเร็วคลื่นเฉือนจากแหล่งกำเนิดคลื่นวัตถุระเบิด (ESTIMATION OF SHEAR WAVE VELOCITY PROFILE FROM EXPLOSION SOURCE) อ.ที่ปรึกษาวิทยานิพนธ์หลัก: รศ. ดร.สุพจน์ เตชวรสินสกุล, 110 หน้า.

การศึกษานี้มีวัตถุประสงค์เพื่อนำเสนอการหาสหสัมพันธ์ของความเร็วคลื่นเฉือนจากแหล่งกำเนิดคลื่นวัตถุระเบิดในพื้นที่ 5 จังหวัด ได้แก่ จังหวัดมหาสารคาม จังหวัดสุรินทร์ จังหวัดอุดรธานี จังหวัดสุพรรณบุรี และจังหวัดสุราษฎร์ธานี โดยใช้การวิเคราะห์ 3 วิธี วิธีแรกเป็นวิธีการวิเคราะห์อย่างง่ายซึ่งวิธีนี้เป็นเทคนิคซึ่งง่ายต่อประมาณค่าความเร็วคลื่นเฉือนโดยนำมาวิเคราะห์การสั่นสะเทือนแล้วสร้างโค้งการกระจาย วิธีที่สองเป็นวิธีการวิเคราะห์คลื่นผิวแบบหลายช่องสัญญาณซึ่งวิธีนี้มีข้อจำกัดด้านความลึกในการสำรวจเนื่องจากมีแหล่งกำเนิดคลื่นจากค้อนเหล็ก และวิธีที่สามเป็นวิธีการวิเคราะห์หาความเร็วคลื่นเฉือนในหลุมเจาะซึ่งเป็นวิธีที่มีราคาในการตรวจวัดสูง ดังนั้นการศึกษานี้จึงหาค่าความเร็วคลื่นเฉือนจากแหล่งกำเนิดคลื่นวัตถุระเบิด จากผลการศึกษาพบว่าเมื่อเปรียบเทียบค่าความเร็วคลื่นเฉือนจากวิธีวิเคราะห์อย่างง่ายกับวิธีการวิเคราะห์คลื่นผิวแบบหลายช่องสัญญาณและวิธีการวิเคราะห์หาความเร็วคลื่นเฉือนในหลุมเจาะแล้วมีค่าใกล้เคียงกัน จากผลดังกล่าวทำให้ทราบว่าผลจากการสั่นสะเทือนจากการใช้วัตถุระเบิดใต้ผิวดิน (จากโครงการสำรวจคลื่นไหวสะเทือน) สามารถนำมาใช้ในการประมาณค่าความเร็วเฉือนในพื้นที่ที่สนใจ โดยเฉพาะอย่างยิ่ง ข้อมูลจากโครงการสำรวจคลื่นไหวสะเทือนซึ่งมีจำนวนมาก โดยการศึกษานี้มีประโยชน์ในการประเมินพื้นที่ที่มีการขยายตัวจากคลื่นสั่นสะเทือน พื้นที่ที่อาจเกิดปรากฏการณ์ทรายเดือด การศึกษาอันตรายจากแรงสั่นสะเทือน และการวางผังเมืองต่อไป

Chulalongkorn University

ภาควิชา วิศวกรรมโยธา ลายมือชื่อนิสิต .....

สาขาวิชา วิศวกรรมโยธา ลายมือชื่อ อ.ที่ปรึกษาหลัก .....

ปีการศึกษา 2557

5471455321 : MAJOR CIVIL ENGINEERING

KEYWORDS: SHEAR WAVE VELOCITY / EXPLOSION SOURCE / SIMPLE METHOD / MULTICHANNEL ANALYSIS OF SURFACE WAVE METHOD / DOWNHOLE SEISMIC TEST

PITHAN PAIROJN: ESTIMATION OF SHEAR WAVE VELOCITY PROFILE FROM EXPLOSION SOURCE. ADVISOR: ASSOC. PROF. SUPOT TEACHAVORASINSKUN, D.Eng., 110 pp.

This study aimed to propose a simple correlation of shear wave velocity derived from explosion source at five locations located in Mahasarakham, Surin, Udonthani, Suphanburi and Suratthani province. First, the Simple Method (SM) was been a simple technique for shear wave velocity survey and was applied to analyze vibration records of ground surface through the established dispersion curve. Second, the Multichannel Analysis of Surface Wave Method (MASW) has limited in terms of the depth because the shear wave velocity was generated by a sledgehammer. Third, the Downhole Seismic Test (DH) was not often been economically feasible to carry out the shear wave velocity measurements; therefore, the present study was adopted to evaluate shear wave velocity profile from the underground explosion source. The results of SM were in fairly well agreement with those obtained from MASW and DH test. Required parameters were then obtained through the calibration with the result from MASW and DH test. This result is implied that the ground surface vibration record from the deep underground explosion (from seismic survey project) can be properly used to estimate the shear velocity profile of the interested site. This is very important because there are considerable amount of such information especially from the seismic survey projects. The SM method has been for site amplification evaluation, liquefaction potential, seismic hazard study and city planning.

Department:	Civil Engineering	Student's Signature	.....
Field of Study:	Civil Engineering	Advisor's Signature	.....
Academic Year:	2014		

ACKNOWLEDGEMENTS

The research would not have been possible without the supported by Assoc. Prof. Dr. Supot Teachavorasinskun who it is appropriate to acknowledge, and many thanks for the most importantly the support staff and friends in the Geotechnical Engineering group at Chulalongkorn University. Finally, this research was supported by CU.GRADUATE SCHOOL THESIS GRANT.

จุฬาลงกรณ์มหาวิทยาลัย
Chulalongkorn University

CONTENTS

Page

THAI ABSTRACT iv

ENGLISH ABSTRACT v

ACKNOWLEDGEMENTS vi

CONTENTS vii

LIST OF TABLES xii

LIS OF FIGURES xiii

CHAPTER 1 1

INTRODUCTION 1

1.1 Background 1

1.2 Research objectives 1

1.3 Scopes of study 1

1.4 Research outcome 2

CHAPTER 2 3

LITERATURE REVIEW 3

2.1 Introduction 3

2.2 Seismic exploration 4

2.2.1 Refraction seismic survey 6

2.2.1.1 Intercept time 9

2.2.1.2 Critical distance 12

2.2.2 Reflection seismic survey 13

2.2.3 The Simple Analysis of Surface Wave Method (SM) 15

2.2.3.1 Procedure of surface wave analysis 15

จุฬาลงกรณ์มหาวิทยาลัย
Chulalongkorn University

Page

2.2.3.2 Estimated shear wave velocity by inversion 16
2.2.4 The Multichannel Analysis of Surface Wave Method (MASW) 16
2.2.4.1 Procedure of surface wave analysis 16
2.2.4.2 Estimated shear wave velocity by inversion 17
2.2.5 Down-hole Seismic Method (DH) 19
2.2.5.1 Interpretation Methods of Down-hole Seismic Test Data 20
2.2.5.1.1 Direct Method 20
2.2.5.1.2 Snell's Law Ray-Path Method 21
2.3 Seismic waves 23
2.3.1 Body waves 23
2.3.1.1 Longitudinal wave 23
2.3.1.2 Transverse wave 24
2.3.2 Surface waves 25
2.3.2.1 Rayleigh wave 25
2.3.2.2 Love wave 25
2.4 Seismic data acquisition 28
2.5 Seismic sources on shore 29
2.5.1 Vibroseis 29
2.5.2 Dynamite 31
2.6 Field layouts 34
2.6.1 Spilt- dip spread 34
2.6.2 Spilt- dip spread with source point gap 34

จุฬาลงกรณ์มหาวิทยาลัย
Chulalongkorn University

Page

2.6.3 End on spread 35
2.6.4 In line offset spread 35
2.6.5 Broadside-T spread 35
2.6.6 Cross spreads 36
CHAPTER 3 37
METHODOLOGY 37
3.1 Introduction 37
3.2 Research Framework 40
3.3 Data Acquisition 40
3.4 Acquisition instruments and setting 43
3.5 Data processing and interpretation 45
3.5.1 Pre-processing 45
3.5.2 Surface-wave analysis 45
CHAPTER 4 47
RESULTS 47
4.1 Overview 47
4.2 Information of subsurface 47
4.2.1 Mahasarakham province 47
4.2.2 Surin province 48
4.2.3 Udonthani province 49
4.2.4 Suphanburi province 51
4.2.5 Suratthani province 52

จุฬาลงกรณ์มหาวิทยาลัย
Chulalongkorn University

Page

4.3 Data acquisition 53
4.3.1 Mahasarakham province 53
4.3.2 Surin province 54
4.3.3 Udonthani province 55
4.3.4 Suphanburi province 57
4.3.5 Suratthani province 57
4.4 Processing and interpretation 58
4.4.1 Estimation of shear wave velocity profile at Mahasarakham province 58
4.4.1.1 Refraction seismic survey 58
4.4.1.2 Reflection seismic survey 59
4.4.1.3 The Simple Analysis of Surface Wave Method (SM) 60
4.4.1.4 The Multichannel Analysis of Surface Wave Method (MASW) 65
4.4.1.5 Down-hole Seismic Method (DH) 65
4.4.2 Estimation of shear wave velocity profile at Surin province 66
4.4.2.1 Refraction seismic survey 66
4.4.2.2 Reflection seismic survey 67
4.4.2.3 The Simple Analysis of Surface Wave Method (SM) 68
4.4.2.4 The Multichannel Analysis of Surface Wave Method (MASW) 72
4.4.2.5 Down-hole Seismic Method (DH) 72
4.4.3 Estimation of shear wave velocity profile at Udonthani province 73
4.4.3.1 Refraction seismic survey 73
4.4.3.2 Reflection seismic survey 74

จุฬาลงกรณ์มหาวิทยาลัย
Chulalongkorn University

Page

4.4.3.3 The Simple Analysis of Surface Wave Method (SM) 75
4.4.3.4 The Multichannel Analysis of Surface Wave Method (MASW) 79
4.4.3.5 Down-hole Seismic Method (DH) 79
4.4.4 Estimation of shear wave velocity profile at Suphanburi province 81
4.4.4.1 Refraction seismic survey 81
4.4.4.2 Reflection seismic survey 81
4.4.4.3 The Simple Analysis of Surface Wave Method (SM) 82
4.4.4.4 The Multichannel Analysis of Surface Wave Method (MASW) 89
4.4.5 Estimation of shear wave velocity profile at Suratthani province 90
4.4.5.1 Refraction seismic survey 90
4.4.5.2 Reflection seismic survey 91
4.4.5.3 The Simple Analysis of Surface Wave Method (SM) 92
4.4.5.4 The Multichannel Analysis of Surface Wave Method (MASW) 96
4.5 The comparison of shear wave velocity profile between SM, MASW and DH 98
4.6 The correlations between Vs and SPT-N value 103
CHAPTER 5 105
CONCLUSIONS AND RECOMMENDATIONS 105
5.1 Conclusions 105
5.2 Recommendations 105
REFERENCES 107
VITA 110

จุฬาลงกรณ์มหาวิทยาลัย
Chulalongkorn University

LIST OF TABLES

Table 1 Important differences between refraction and reflection seismic 14

Table 2 Relation between density P-wave and S-wave velocity of soil and rock (Clark & Emerson, 1999) 27

Table 3 Advantages and disadvantages of vibroseis and dynamite 33

Table 4 Geophones set at Mahasarakham province 41

Table 5 Geophones set at Surin province 42

Table 6 Geophones set at Udonthani province 42

Table 7 Geophones set at Suphanburi province 42

Table 8 Geophones set at Suratthani province 43

จุฬาลงกรณ์มหาวิทยาลัย
Chulalongkorn University

LIS OF FIGURES

Figure 1 Seismic exploration (Sattarak, 2007) 5

Figure 2 Refraction and reflection of seismic waves moving through an intermediary (Sattarak, 2007) 5

Figure 3 Schematic of seismic refraction survey (Lippus, 2007) 7

Figure 4 Snell's Law and critical incidence 7

Figure 5 Simple two-layer case with plane (Bruce, 1973) 9

Figure 6 Schematically illustrates the multiple layer case and corresponding time-distance curve (Bruce, 1973) 11

Figure 7 Reflection seismic survey (Sattarak, 2007) 14

Figure 8 A Simple Analysis of Surface Wave 16

Figure 9 Transformation from shot gather to phase velocity image 17

Figure 10 Relation between Poisson's ratio and velocity of propagation of primary (P), shear (S) and Rayleigh (R) waves in a linear elastic homogeneous half space (Foti, 2000) 19

Figure 11 Diagram of down-hole tests (Kim, Bang, & Kim, 2008) 20

Figure 12 Illustration of the Direct Method (Kim et al., 2008) 20

Figure 13 Illustration of the Snell's Law Ray-Path Method (Teachavorasinskun & Lukkunaprasit, 2004) 22

Figure 14 Primary wave and secondary wave movement (SV and SH-component) (Sattarak, 2007) 24

Figure 15 Secondary wave movements (Sattarak, 2007) 24

Figure 16 Rayleigh wave movements (Sattarak, 2007) 25

Figure 17 Love wave movements (Sattarak, 2007) 26

จุฬาลงกรณ์มหาวิทยาลัย
Chulalongkorn University

Figure 18 Seismic acquisition on land using a dynamite source and a cable of geophones (Dobrin & Savit, 1988)..... 29

Figure 19 The force-generating mechanism of the seismic vibrator source (Dobrin & Savit, 1988)..... 30

Figure 20 Schematic view of the Vibroseis truck with the air springs, the baseplate..... 31

Figure 21 The behaviour of dynamite: (a) the characteristic zones in space and (b) the radius as a function of time with its characteristic zones (Dobrin & Savit, 1988)..... 32

Figure 22 Spilt- dip spread (Telford, Geldart, & Sheriff, 1990) 34

Figure 23 Spilt- dip spread with source point gap (Telford et al., 1990) 34

Figure 24 End on spread (Telford et al., 1990)..... 35

Figure 25 In line offset spread (Telford et al., 1990) 35

Figure 26 Broadside-T spread (Telford et al., 1990) 35

Figure 27 Cross spread (Telford et al., 1990)..... 36

Figure 28 Location map of Phayakkhaphumphisai, Mahasarakham province 38

Figure 29 Location map of Chumphonburi, Surin province 38

Figure 30 Location map of Nongwuaso, Udonthani province..... 39

Figure 31 Location map of Uthong, Suphanburi province 39

Figure 32 Location map of Phunphin, Suratthani province 39

Figure 33 Flow chart of research framework 40

Figure 34 Geophones spread line 41

Figure 35 Geophone 44

Figure 36 Loading profile (Apico (Korat) ltd., 2005)..... 44

Figure 37 Notebook and data logger 45

จุฬาลงกรณ์มหาวิทยาลัย
CHULALONGKORN UNIVERSITY

Figure 38 Subsoil profile at Mahasarakham 48

Figure 39 Subsoil profile at Surin 49

Figure 40 Subsoil profile at Udonthani 50

Figure 41 Subsoil profile at Suphanburi (Department of Public Works and Town & Country Planning, 2002) 51

Figure 42 Subsoil profile at Suratthani (Department of Public Works and Town & Country Planning, 1985) 52

Figure 43 Seismic data in the space-time domain by SM and MASW at Mahasarakham 53

Figure 44 Seismic data in the time – depth by DH at Mahasarakham 54

Figure 45 Seismic data in the space-time domain by SM and MASW at Surin 54

Figure 46 Seismic data in the time – depth by DH at Surin 55

Figure 47 Seismic data in the space-time domain by SM and MASW at Udonthani 56

Figure 48 Seismic data in the time – depth by DH at Udonthani 56

Figure 49 Seismic data in the space-time domain by SM and MASW at Suphanburi 57

Figure 50 Seismic data in the space-time domain by SM and MASW at Suratthani 58

Figure 51 Data processing by Refraction seismic survey at Mahasarakham 59

Figure 52 Data processing by Reflection seismic survey at Mahasarakham 60

Figure 53 The SM data processing from field test (d5397) 61

Figure 54 The SM data processing from field test (d5398) 61

Figure 55 The SM data processing from field test (d5399) 62

Figure 56 The SM data processing from field test (d5402) 62

Figure 57 The SM data processing from field test (d5406) 63

Figure 58 The SM data processing from field test (d5408) 63

Figure 59 The SM data processing from field test (d5410) 64

Figure 60 Shear wave velocity profile by SM at Mahasarakham 64

Figure 61 Shear wave velocity profile by MASW at Mahasarakham 65

Figure 62 Shear wave velocity profile by DH at Mahasarakham 66

Figure 63 Data processing by Refraction seismic survey at Surin 67

Figure 64 Data processing by Reflection seismic survey at Surin 68

Figure 65 The SM data processing from field test (d5935) 69

Figure 66 The SM data processing from field test (d5939) 69

Figure 67 The SM data processing from field test (d5940) 70

Figure 68 The SM data processing from field test (d5946) 70

Figure 69 The SM data processing from field test (d5949) 71

Figure 70 Shear wave velocity profile by SM at Surin 71

Figure 71 Shear wave velocity profile by MASW at Surin 72

Figure 72 Shear wave velocity profile by DH at Surin 73

Figure 73 Data processing by Refraction seismic survey at Udonthani 74

Figure 74 Data processing by Reflection seismic survey at Udonthani 75

Figure 75 The SM data processing from field test (d95) 76

Figure 76 The SM data processing from field test (d01) 76

Figure 77 The SM data processing from field test (d2392) 77

Figure 78 The SM data processing from field test (d2394) 77

Figure 79 The SM data processing from field test (d2396) 78

Figure 80 Shear wave velocity profile by SM at Udonthani 78

Figure 81 Shear wave velocity profile by MASW at Udonthani 79

จุฬาลงกรณ์มหาวิทยาลัย
CHULALONGKORN UNIVERSITY

Figure 82 Shear wave velocity profile by DH at Udonthani 80

Figure 83 Data processing by Refraction seismic survey at Suphanburi 81

Figure 84 Data processing by Reflection seismic survey at Suphanburi 82

Figure 85 The SM data processing from field test (d650858) 83

Figure 86 The SM data processing from field test (d650860) 83

Figure 87 The SM data processing from field test (d650862) 84

Figure 88 The SM data processing from field test (d650872) 84

Figure 89 The SM data processing from field test (d650876) 85

Figure 90 The SM data processing from field test (d730876) 85

Figure 91 The SM data processing from field test (d890872) 86

Figure 92 The SM data processing from field test (d890876) 86

Figure 93 The SM data processing from field test (d890878) 87

Figure 94 The SM data processing from field test (d970874) 87

Figure 95 The SM data processing from field test (d970876) 88

Figure 96 The SM data processing from field test (d970878) 88

Figure 97 Primary wave velocity profile by SM at Suphanburi 89

Figure 98 Primary wave velocity profile by MASW at Suphanburi 90

Figure 99 Data processing by Refraction seismic survey at Suratthani 91

Figure 100 Data processing by Reflection seismic survey at Suratthani 92

Figure 101 The SM data processing from field test (d5070) 93

Figure 102 The SM data processing from field test (d5072) 93

Figure 103 The SM data processing from field test (d5074) 94

Figure 104 The SM data processing from field test (d5078) 94

จุฬาลงกรณ์มหาวิทยาลัย
CHULALONGKORN UNIVERSITY

Figure 105 The SM data processing from field test (d5080) 95

Figure 106 The SM data processing from field test (d5081) 95

Figure 107 Primary wave velocity profile by SM at Suratthani 96

Figure 108 Primary wave velocity profile by MASW at Suratthani 97

Figure 109 The comparison of shear wave velocity profile between SM, MASW and DH method at Mahasarakham 98

Figure 110 The comparison of shear wave velocity profile between SM, MASW and DH method at Surin 99

Figure 111 The comparison of shear wave velocity profile between SM, MASW and DH method at Udonthani 100

Figure 112 The comparison of primary wave velocity profile between SM and MASW method at Suphanburi 101

Figure 113 The comparison of primary wave velocity profile between SM and MASW method at Suratthani 102

Figure 114 The correlations between Vs and SPT-N value at Mahasarakham province 103

Figure 115 The correlations between Vs and SPT-N value at Surin province 104

Figure 116 The correlations between Vs and SPT-N value at Udonthani province 104

จุฬาลงกรณ์มหาวิทยาลัย
Chulalongkorn University

CHAPTER 1

INTRODUCTION

1.1 Background

Seismic surveying is a vital process employed by concession companies as a means of studying geological structures beneath the ground surface using a signal transmitted along the shallow surface level. The intensity of vibration levels used during this method depends on several factors including; type, quantity and depth of the object used to generate these seismic waves. Distance from the center of the quake and geological conditions such as vibrations occur with the frequency and amplitude at a specific characteristic that results from the combination of the surface waves and body waves can be determined shear wave velocity with depth from the surface wave theory.

1.2 Research objectives

1.2.1 To investigate the shear wave velocity profiles of subsoil in Thailand within 30 m depth from seismic survey on shore.

1.2.2 To verify the validity of MASWM by comparing its shear wave velocity profiles from five sites with those of boring reports and down-hole test.

1.2.3 To presents the development of empirical correlations between Vs and SPT-N value for different categories of subsoil in Thailand.

1.3 Scopes of study

The scopes of this study are as follows:

1.3.1 Measuring the seismic waves from the explosive source at

(1) Phayakkhaphumphisai, Mahasarakham province.

จุฬาลงกรณ์มหาวิทยาลัย
Chulalongkorn University

(2) Chumphonburi, Surin province.

(3) Nongwuaso, Udonthani province.

(4) Uthong, Suphanburi province.

(5) Phunphin, Suratthani province.

1.3.2 The equipment used in the experiment are:

Source: 1-4 kg explosive charge

Receiver: sixteen 4.5 Hz geophones spikes

Seismograph: Data logger

1.3.3 The expected depth of investigation is around 30 m due to limitation of energy source and geophones.

1.4 Research outcome

1.4.1 The shear wave velocity profiles from explosive source for different categories of subsoil in Thailand from seismic survey on shore.

1.4.2 The variation of shear wave velocity profiles from boring reports and down-hole test.

1.4.3 The empirical correlations between Vs and SPT-N value for different categories of subsoil in Thailand.

จุฬาลงกรณ์มหาวิทยาลัย
Chulalongkorn University

CHAPTER 2

LITERATURE REVIEW

2.1 Introduction

The propagation of seismic waves near the surface is strongly influenced by the presence of unconsolidated loose sediments overlying the bedrock resulting in modifications of the ground motion characteristics at the surface. The ground motion parameters at the surface are generally obtained by conducting one dimensional ground response analysis considering only the upward propagating shear waves. In these analyses, the shear wave velocity (Vs) is one of the most important input parameter to represent the stiffness of the soil layers. Hence, it is important to determine the shear wave velocity for the estimation of ground motion parameters at the surface. Field measurements of shear wave velocity include cross-hole tests, down-hole tests, suspension logging, seismic reflection, seismic refraction and surface waves tests (Kramer, 1996). Surface waves test is a simple and an efficient technique compared to other in situ tests to measure the shear wave velocity in the field. But, it is not often economically feasible to carry out the shear wave velocity measurements in all cases particularly in urban areas for microzonation studies. The penetration tests have been widely accepted in Thailand as routine tests in geotechnical site investigation and abundant SPT data is available.

Several researchers have proposed empirical correlations based on standard penetration test to evaluate the dynamic soil properties of the soils (Ohta & Goto, 1978) (Imai & Tonouchi, 1982) (Sykora & Stokoe, 1983) (Mayne & Rix, 1995). These empirical relationships seem to be site specific and require thorough process of validation before using them for Thailand.

2.2 Seismic exploration

The basic technique of seismic exploration consists of generating seismic waves and measuring the time required for the waves to travel from sources to a series of geophones, usually disposed along a straight line directed toward the source. From a knowledge of travel times and the velocity of the waves, one attempts to reconstruct the path of seismic waves. Structural information is derived principally from path that fall into two main categories; head wave or refracted paths, in which the principal portion of the path is along the interface between two rock layers and hence is approximately horizontal, and reflected path, in which the wave travel downward initially and at some point is reflected back to the surface, the overall path being essentially vertical. For both types of path (Figure 1 and 2) the travel times depend on the physical properties of the rock and the attitudes of the beds. The objective of seismic exploration is to deduce information about the rocks, especially about attitudes of the beds from the observed arrival times and from variations in amplitude, frequency, phase and wave shape.

Despite the indirectness of the method most seismic work results in the mapping of geological structure rather than finding petroleum directly. The likelihood of a successful venture is improved more than enough to pay for the seismic work. Likewise, engineering surveys, mapping of water resources, and other studies requiring accurate knowledge of subsurface structure derive valuable information from seismic data.

Chulalongkorn University

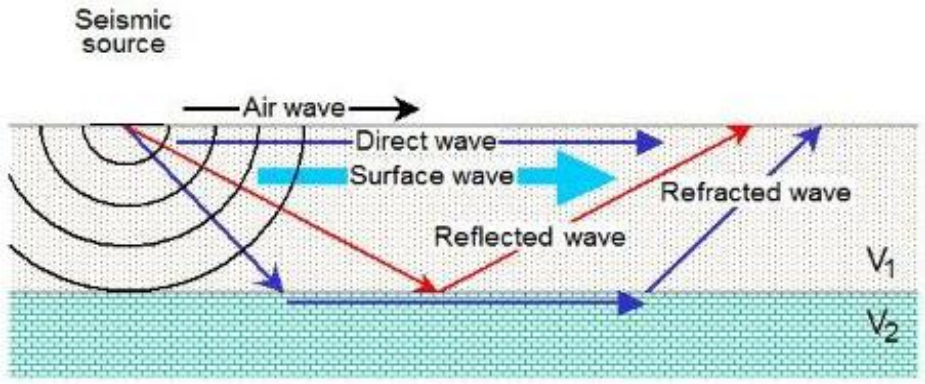

Figure 1 Seismic exploration (Sattarak, 2007)

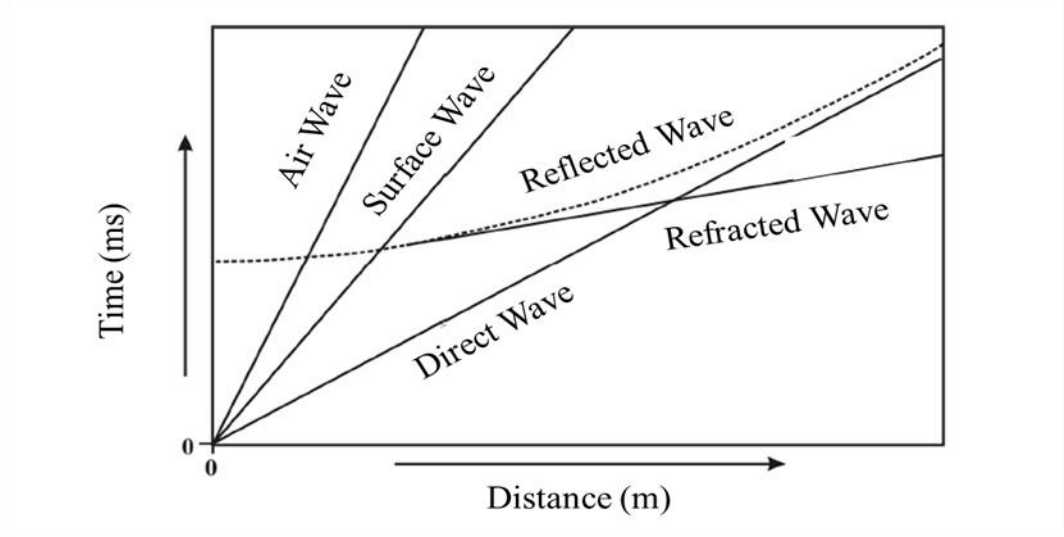

Figure 2 Refraction and reflection of seismic waves moving through an intermediary (Sattarak, 2007)

2.2.1 Refraction seismic survey

Seismic refraction theory is used in a bid to help develop methods of interpretation that are used extensively. There are many textbooks on geophysics that discuss the principles and applications of refraction surveys; however, most of them are oriented towards exploration for oil and give only passing attention to detailed shallow investigations (American Society for Testing and Materials, 2011).

The refraction method consists of measuring (at known points along the surface of the ground) the travel times of compression waves generated by an impulsive energy source. The energy source is usually a small explosive charge and the energy is detected, amplified, and recorded by special equipment designed for this purpose. The instant of the explosion, or "zero-time," is recorded on the record of arriving pulses. The unprocessed data, therefore, consists of travel times and distances, and this time-distance information is then manipulated to convert it into the format of velocity variations with depth. The interpretation of said unprocessed data will be developed as we go along.

The process is schematically illustrated in Figure 3. All measurements are made at the surface of the ground, and the subsurface structure is inferred from interpretation methods based on the laws of energy propagation (Huntera et al., 2002).

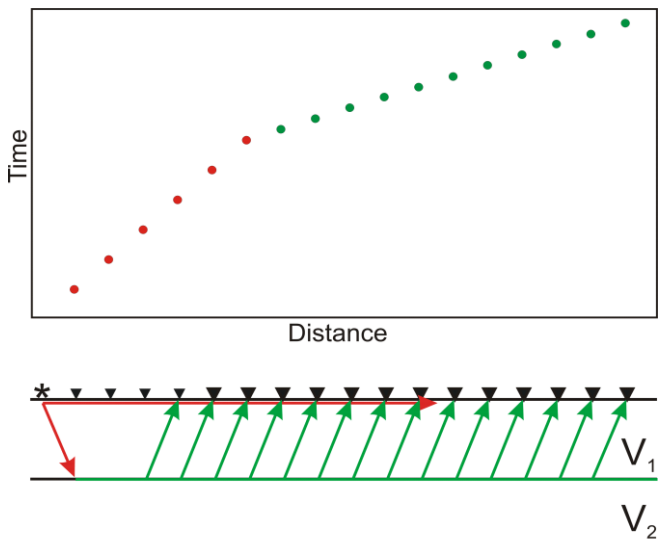

Figure 3 Schematic of seismic refraction survey (Lippus, 2007)

The propagation of seismic energy through subsurface layers is described by essentially the same rules that govern the propagation of light rays through transparent media. The refraction or angular deviation that a light ray or seismic pulse undergoes when passing from one material to another depends upon the ratio of the transmission velocities of the two materials. The fundamental law that describes the refraction of light rays is Snell's Law, and this, together with the phenomenon of “critical incidence,” is the physical foundation of seismic refraction surveys.

Snell's Law and critical incidence are illustrated in Figure 4, which shows a medium with a velocity V_1, underlain by a medium with a higher velocity V_2.

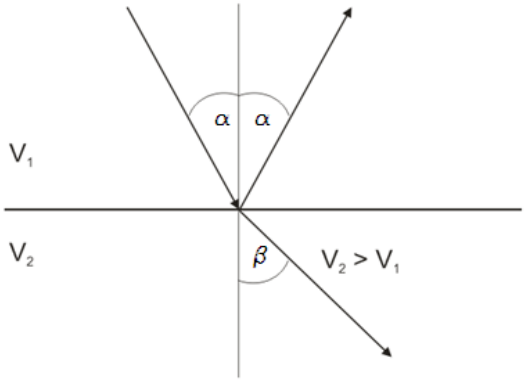

Figure 4 Snell's Law and critical incidence

The particular case of the critical angle of incidence is fundamental to the derivation of the formulas for refraction exploration. Although the exact mathematical and physical description of what occurs when a ray is incident at the critical angle is complex, it is entirely adequate to assume that the critically refracted ray travels along the boundary between the two media at the higher of the two velocities. Further, as the critically refracted ray travels along the boundary, it continually generates seismic waves in the lower-velocity (upper) layer that depart from the boundary at the angle of critical incidence. In the literature these waves are frequently referred to as head waves. If the

velocities of the layers increase with depth, a portion of the energy will eventually be refracted back to the surface where it can be detected.

We begin with the simplest of all cases: two layers with plane and parallel boundaries as illustrated in Figure 5. A small explosive charge is detonated in a deep hole at A and the energy is detected by a set of detectors laid out in a straight line along the surface. The arrival times of the impulses are plotted against the corresponding shot-to-detector distances as shown in Figure 5. The first few arrival times are those of direct arrivals through the first layer, and the slope of the line through these points, $\Delta T/\Delta X$, is simply the reciprocal of the velocity of that layer; i.e., $1/V_1$. At some distance from the shot, a distance called the critical distance, it takes less time for the energy to travel down to the top of the second layer, refract along the interface at the higher velocity V_2 and travel back up to the surface, than it does for the energy to travel directly through the top layer. The energy that arrives at the detectors beyond the critical distance will plot along a line with a slope of $1/V_2$. The line through these refracted arrivals will not pass through the origin, but rather will project back to the time axis to intersect it at a time called the intercept time. Because both the intercept time and the critical distance are directly dependent upon the velocities of the two materials and the thickness of the top layer, they can be used to determine the depth to the top of the second layer.

Chulalongkorn University

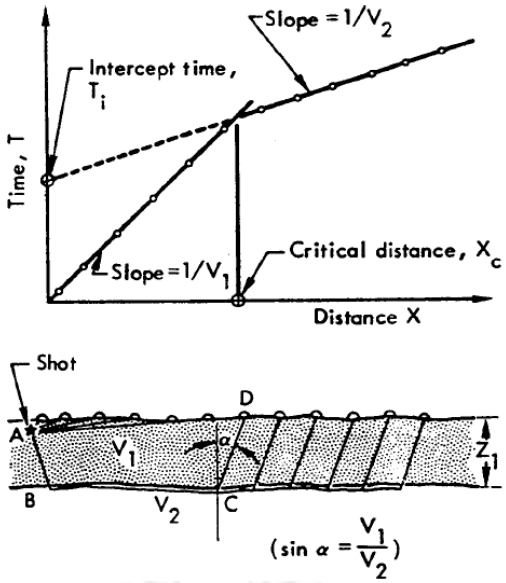

Figure 5 Simple two-layer case with plane (Bruce, 1973)

2.2.1.1 Intercept time

Referring to Figure 5, let us compute the arrival time of the refracted impulse at a detector. Consider the travel path ABCD;

$$\overline{AB} = \overline{CD} = \frac{Z_1}{\cos(\alpha)} \tag{1}$$

$$\overline{BC} = x - 2Z_1 \tan(\alpha) \tag{2}$$

where Z_1 is the thickness of the top layer, and a is the critical angle of incidence. The travel time is therefore given by:

$$T = \frac{\overline{AB}}{V_1} + \frac{\overline{BC}}{V_2} + \frac{\overline{CD}}{V_1} \tag{3}$$

$$T = 2Z_1\left(\frac{1}{V_1\cos(\alpha)} - \frac{\sin(\alpha)}{V_2\cos(\alpha)}\right) + \frac{x}{V_2} \tag{4}$$

Snell's law defines the critical angle of incidence, α by:

$$\sin\alpha = \frac{V_1}{V_2} \tag{5}$$

And selectively substituting Eq. (5) into the previous equation:

$$T = \frac{2Z_1\cos(\alpha)}{V_1} + \frac{x}{V_2} \tag{6}$$

If we now let $X = 0$, then T becomes the intercept time, Ti, and we can rewrite the last expression as:

$$Z_1 = \frac{T_i V_1}{2\cos(\sin^{-1}\frac{V_1}{V_2})} \tag{7}$$

For the situation we have assumed in Figure 5, Eq. (7) can be determined from the time-distance plot; therefore, the depth to the second layer can be computed. The depth of the shot has been ignored in the derivation above and the true depth to the second layer is determined simply by adding one-half the shot depth to the value of Z_1 computed by Eq. (7). In the particular example of Figure 5, the depth computed by Eq. (7) is the depth along the entire seismic line because we stipulated that the layers were plane and parallel. A very important point to bring out at this time is that all depths determined in refraction surveys are measured normal to the boundary between layers and are not necessarily vertical depths beneath the ground surface. The intercept-time analysis can be extended to the case of multiple layers; however, only the resulting formulas will be given here because their derivations are redundant and may be found in a number of references. Figure 6 schematically illustrates the multiple layer case and corresponding time-distance plot. Note that the intercept times and layer

thicknesses have been identified by a subscript corresponding to the number of the layer.

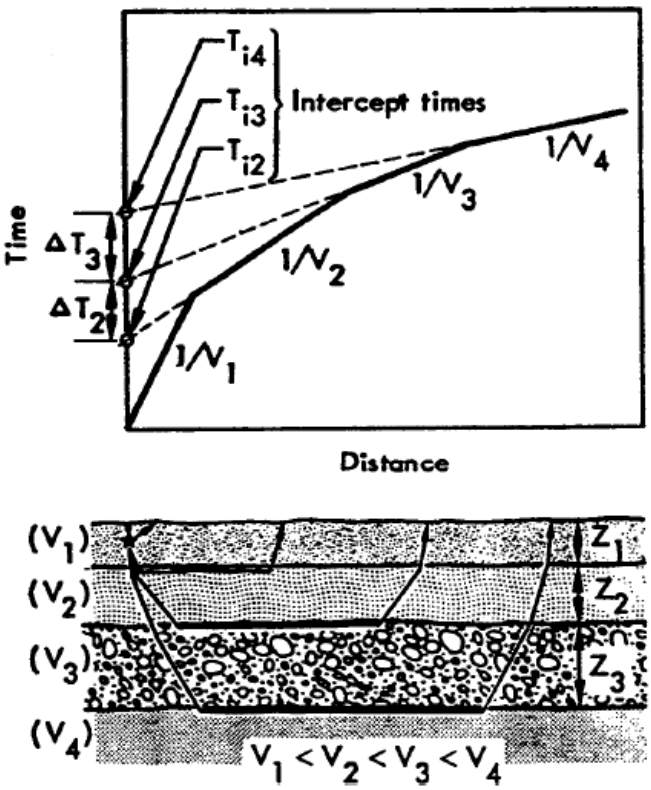

Figure 6 Schematically illustrates the multiple layer case and corresponding time-distance curve (Bruce, 1973)

$$Z_1 = \frac{T_{i2}V_1}{2\cos(\sin^{-1}\frac{V_1}{V_2})} \tag{8}$$

$$Z_2 = \frac{\left[T_{i3} - T_{i2}\frac{\cos(\sin^{-1}V_1/V_3)}{\cos(\sin^{-1}V_1/V_2)}\right]V_2}{2\cos(\sin^{-1}V_2/V_3)} + Z_1 \tag{9}$$

$$Z_3 = \frac{\left[T_{i4} - T_{i2}\frac{\cos(\sin^{-1}V_1/V_4)}{\cos(\sin^{-1}V_1/V_2)} - \frac{2h_2\cos(\sin^{-1}{}_2/V_4)}{V_2}\right]V_3}{2\cos(\sin^{-1}V_3/V_4)} + Z_1 + Z_2 \tag{10}$$

If the velocity contrasts between layers are high enough; say 2 to 1, and only approximate depths are required, then the following formulas can be used:

$$Z_2 = \frac{\Delta T_2 V_2}{2\cos(\sin^{-1}\frac{V_2}{V_3})} \quad (11)$$

$$Z_3 = \frac{\Delta T_3 V_3}{2\cos(\sin^{-1}\frac{V_3}{V_4})} \quad (12)$$

Where ΔT_2 and ΔT_3 are as indicated in Figure 6, Equations (11) and (12) will give thicknesses that are greater than actual, and it is suggested that thicknesses initially be computed both ways to learn whether the error is significant in a particular situation.

2.2.1.2 Critical distance

The critical-distance method for determining depth will receive only brief attention here because it is analogous to the intercept-time method, and offers no advantages significant enough to warrant further detail. Its primary application is to compute the depth of the first layer and to estimate the length of the seismic line required for a particular exploration task. The critical distance is the distance from the shot point to the point at which the refracted energy arrives at the same time as the energy traveling directly through the top layer. The critical distance (*Xc*) is illustrated in Figure 5; it is the breakpoint in the graph of arrival times. By an approach similar to the one used in deriving the intercept-time formulas, it can be shown that the depth of the first layer is given by:

$$Z_1 = \frac{Xc}{2}\frac{1-(V_1/V_2)}{\cos(\sin^{-1}V_1/V_2)} \quad (13)$$

where Xc is the critical distance

2.2.2 Reflection seismic survey

Reflection seismic survey (Figure 7) explore the subsurface geology based on the properties of the reflected wave (American Society for Testing and Materials, 2010). Wave was released to the media on the boundaries of two media with different acoustic impedance, which is the product of the density (ρ) with the wave velocity V, i.e., ρV. When a ray encounters a boundary, some energy will be reflected back, and some will be transmitted to the next layer. The amount of energy reflected back is characterized by the reflection coefficient (R).

$$R = \frac{\rho_2 V_2 - \rho_1 V_1}{\rho_2 V_2 + \rho_1 V_1} \tag{14}$$

In this instance wave is reflected back to the surface after the signal has been released. Then time and amplitude of the reflected wave is then recorded as a wave that is on par with the difference of the time and amplitude. We can interpret the depth of soil/rocks from the reflection of the wave. The depth of the boundary layer of soil/rock, the angle of incidence and the angle of the reflected waves are equal to 90° or direction of the incident wave and the reflected wave is calculated from the vertical equation:

$$D = \frac{Vt_0}{2} \tag{15}$$

Where V is wave velocity of the medium, t_0 is two-way travel time.

จุฬาลงกรณ์มหาวิทยาลัย
Chulalongkorn University

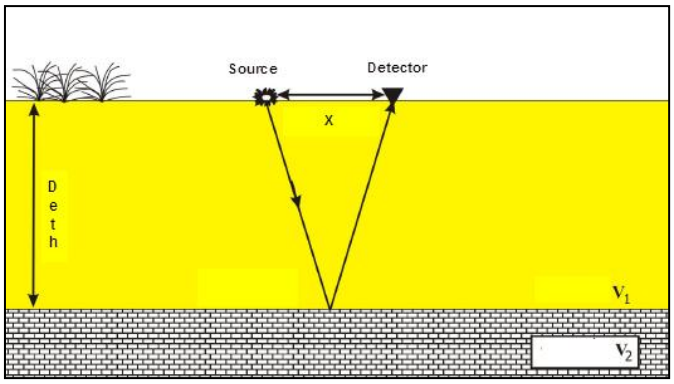

Figure 7 Reflection seismic survey (Sattarak, 2007)

Notice that it is the impedance contrast which determines whether energy is reflected back or not; it may happen that the velocities and densities are different between two layers, but that the impedance is nearly the same. In that case we will see no reflection. We can now state another difference between refraction and reflection seismic. With refraction seismic we are only interested in travel times of the waves, so this means that we are interested in contrasts in velocities. This is different in reflection seismic. Then we are interested in the amplitude of the waves, and we will only measure amplitude if there is a contrast in acoustic impedance in the subsurface.

Table 1 Important differences between refraction and reflection seismic

Advantages	Disadvantages
Based on contrasts in : seismic wave speed	Based on contrasts in : seismic wave impedances
Material property determined : wave speed only	Material property determined : wave speed and wave impedance
Only travel times used	Travel times and amplitudes used
No need to record amplitudes completely : relatively cheap instruments	Must record amplitudes correctly : relatively expensive instruments
Source-receiver distances large compared	Source-receiver distances small

to investigation depth	compared to investigation depth

2.2.3 The Simple Analysis of Surface Wave Method (SM)

2.2.3.1 Procedure of surface wave analysis

This is the procedure of transformation from shot gather to phase velocity. First, shot gather data is converted to period by Eq. (16). And then converted to frequency (17) and phase velocity (18) is the dispersion curve.

$$T = t_2 - t_1 \quad (16)$$

$$f = 1/T \quad (17)$$

$$V_R = \Delta x/\Delta t \quad (18)$$

Where t is time (s)

T is period (s)

f is frequency (s^{-1})

x is geophone array (m)

V_R is phase velocity of surface waves (m/s)

Chulalongkorn University

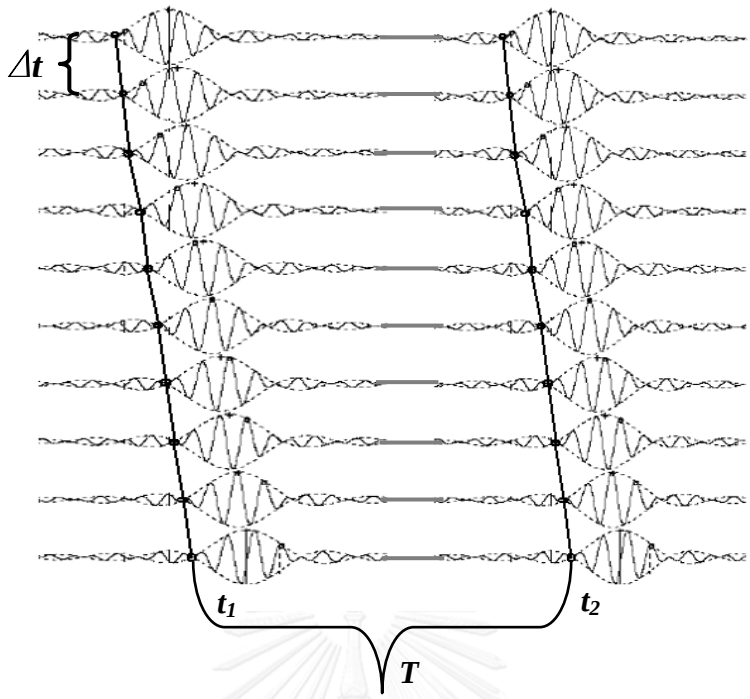

Figure 8 A Simple Analysis of Surface Wave

2.2.3.2 Estimated shear wave velocity by inversion

Shear wave velocity can be derived by inverting the dispersive phase velocity of surface waves. Surface wave dispersion can be significant in the presence of velocity layering by using Eq. (21) - (23).

จุฬาลงกรณ์มหาวิทยาลัย
Chulalongkorn University

2.2.4 The Multichannel Analysis of Surface Wave Method (MASW)

2.2.4.1 Procedure of surface wave analysis

This is the procedure of transformation from shot gather to phase velocity image. First, shot gather data is converted to phase and amplitude by Fourier transform Eq. (19). And then applying phase shift and stacking technique (Park, Miller, & Xia, 1999) by Eq. (20), and established a phase velocity image and the maximum amplitude value of each frequency is the dispersion curve (Zhang, Chan, & Xia, 2004).

$$E(\omega, v) = \left| \sum_{j=1}^{N} A(\omega)_j e^{i(\phi(\omega)_j + \Delta\phi(\omega)_j)} \right| \quad (19)$$

$$\Delta\phi(\omega)_j = \omega x_j / v \quad (20)$$

Where A is amplitude spectrum

$\emptyset$ is phase from Fourier transformation

i is Imaginary number

ω is frequency in radian

x is geophone array (m)

v is phase velocity for frequency (ω)

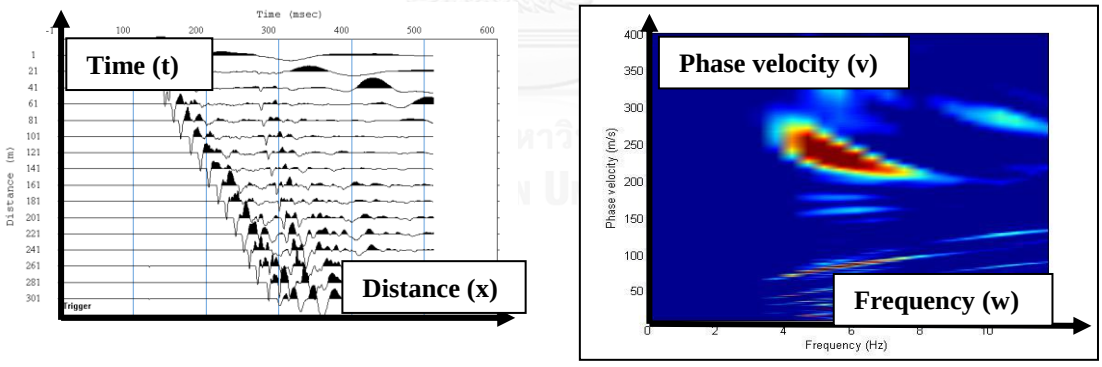

Figure 9 Transformation from shot gather to phase velocity image

2.2.4.2 Estimated shear wave velocity by inversion

Dispersion, or change in phase velocity with frequency, is the fundamental property utilized in surface wave methods. Shear wave velocity can be derived by inverting the dispersive phase velocity of surface waves. Surface wave dispersion can be significant in the presence of velocity layering, which is common in

the near-surface environment (upper 100 meters). There are other types of surface waves (waves that propagate along the earth's surface), but for this application we are concerned with the Rayleigh wave, also known as "ground roll". Although there are other wave types, the term "surface wave" when used in the MASW (Multichannel Analysis of Surface Waves) context has come to mean the Raleigh wave from the phase velocity of Rayleigh wave V_R and the frequency f is determined the wavelength λ_R by:

$$\lambda_R = \frac{V_R}{f} \tag{21}$$

and a direct conversion from V_R - λ_R domain to shear wave velocity and depth (Xia, Miller, & Park, 1999) from Figure 10 it is evident that the difference between shear wave velocity and Rayleigh wave velocity is very limited, being the latter slightly smaller than the former. In particular the exact range of variation is given by:

$$V_S \approx 1.1 V_R \tag{22}$$

$$z \approx \frac{\lambda}{3} \; or \; z \approx \frac{\lambda}{2} \tag{23}$$

จุฬาลงกรณ์มหาวิทยาลัย
Chulalongkorn University

Surface wave energy decays exponentially with depth beneath the surface. The energy or amplitude of any particular frequency is dependent on the ratio of depth to wavelength. Thus, for each frequency, the amplitude decreases by the same factor when the depth increases by a wavelength. This means that the longer wavelength (longer-period, lower-frequency) surface waves travel deeper and therefore contain more information about deeper velocity structure. Shorter wavelength (shorter-period, higher-frequency) surface waves travel shallower and thus contain more information about shallower velocity structure.

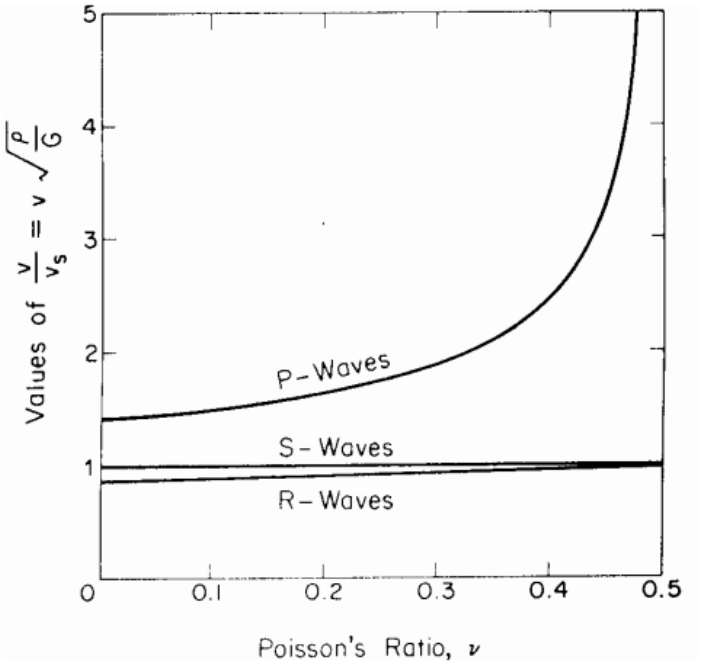

Figure 10 Relation between Poisson's ratio and velocity of propagation of primary (P), shear (S) and Rayleigh (R) waves in a linear elastic homogeneous half space (Foti, 2000)

2.2.5 Down-hole Seismic Method (DH)

The down-hole test is performed in one borehole. In the down-hole test (Figure 11), the receiver is in the borehole which can be moved to different depths to measure different layers, and the source in located on the surface near the borehole. Standard is the standard test methods for down-hole seismic testing (American Society for Testing and Materials, 2014). The down-hole test detected layers which can be hidden in the seismic refraction surveys. It also requires only one borehole, which is less costly and complicated than seismic cross-hole test. On the other hand, drilling of the borehole, like other tests which need boreholes, can disturb the soils around it. Also uncertainties can result from background noise effect, groundwater table effects.

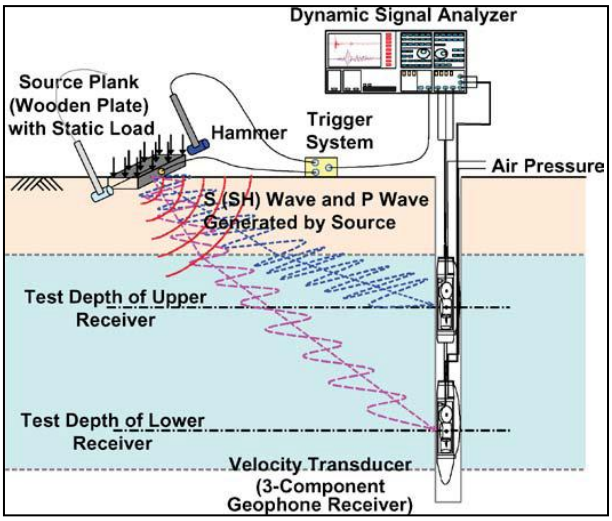

Figure 11 Diagram of down-hole tests (Kim, Bang, & Kim, 2008)

2.2.5.1 Interpretation Methods of Down-hole Seismic Test Data

2.2.5.1.1 Direct Method

The first arrival time of an elastic wave from the source to a receiver at each testing depth can be obtained from the down-hole seismic test. The measured travel time (t) in the inclined path can be corrected to the travel time (t_c) in the vertical path by using Eq. (24) as shown in Figure 12.

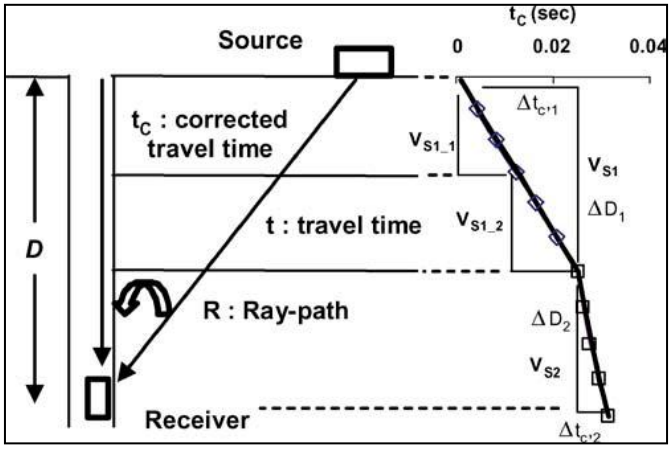

Figure 12 Illustration of the Direct Method (Kim et al., 2008)

$$t_c = D\frac{t}{R} \tag{24}$$

Where t_c is the corrected travel time;

D is the testing depth from ground surface;

t is the first arrival time from test; and

R is the distance between the source and receiver.

By plotting the corrected travel time versus depth, the velocity of each layer can be obtained from the slope of the fitting curve using the data points that have similar trend by Eq (25). The slope of the fitting curve represents the wave velocity in each covered range. As shown in Figure 12, the corrected travel times can be fitted by two straight lines, and the velocity profiles of the site can be classified as two layers in an average sense. For the detailed velocity profiling, subdivision of ΔD can be applied, but the potential errors in travel time measurement and data interpretation can be increased.

$$\mathrm{V}_d = \frac{\Delta D}{\Delta t_c} \tag{25}$$

จุฬาลงกรณ์มหาวิทยาลัย
Chulalongkorn University

2.2.5.1.2 Snell's Law Ray-Path Method

This method is assumed that the wave propagates along a refracted ray path based on Snell's Law, and the following relations should be satisfied as shown in Figure 13 (Teachavorasinskun & Lukkunaprasit, 2004).

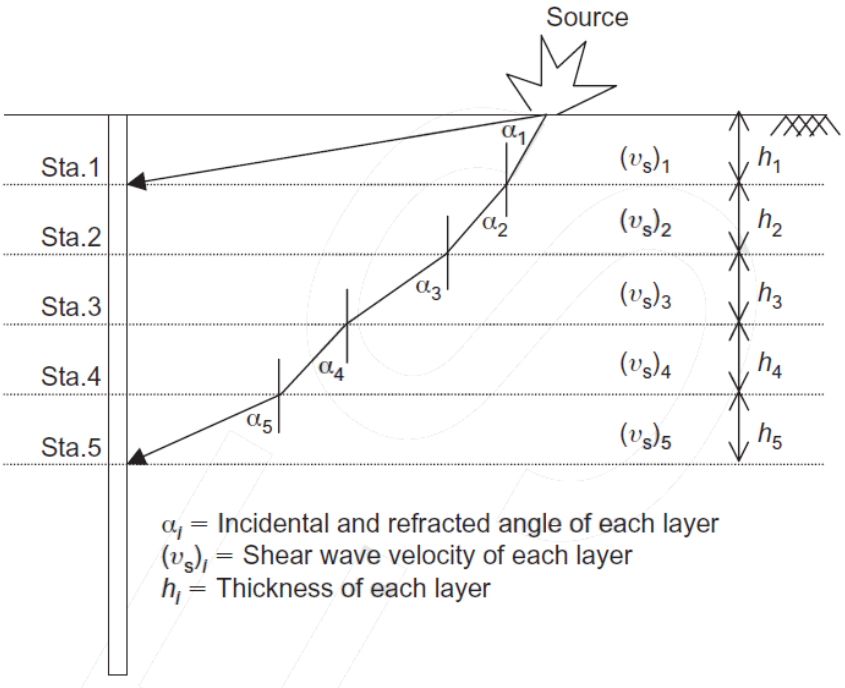

Figure 13 Illustration of the Snell's Law Ray-Path Method (Teachavorasinskun & Lukkunaprasit, 2004)

Snell's Law:

$$\frac{\sin\alpha_1}{(Vs)_1} = \frac{\sin\alpha_2}{(Vs)_2} = \frac{\sin\alpha_3}{(Vs)_3} = \cdots = \frac{\sin\alpha_n}{(Vs)_n} \tag{26}$$

Geometrical equation:

$$x = \sum_{i=1}^{n} h_1 \tan\alpha_i \tag{27}$$

Travelling time equation:

$$t = \frac{1}{(Vs)_1}\sum_{i=1}^{n} \frac{h_i}{\cos\alpha_i}\frac{\sin\alpha_1}{\sin\alpha_{i_1}} \tag{28}$$

Where X is the horizontal distance on the ground surface from the source to the center of the borehole

hi is the thickness of each layer (depth interval of each measurement)

α_i is incidental or refraction angles

i is measurement stations equal to 1, 2, 3, …, n

n is the number of the layer under consideration

t is the recorded travel time at layer n and

$(Vs)_i$ is the shear wave velocity of each layer

$(Vs)_n$ is an unknown shear wave velocity

2.3 Seismic waves

2.3.1 Body waves

2.3.1.1 Longitudinal wave

Waves that cause particles of the medium through which the wave is oscillating compression and expansion waves move in the same direction. As shown in Figure 14 wave vibration is called a “Primary wave” or “P-wave” or the more common name for the “Compression wave”.

จุฬาลงกรณ์มหาวิทยาลัย
CHULALONGKORN UNIVERSITY

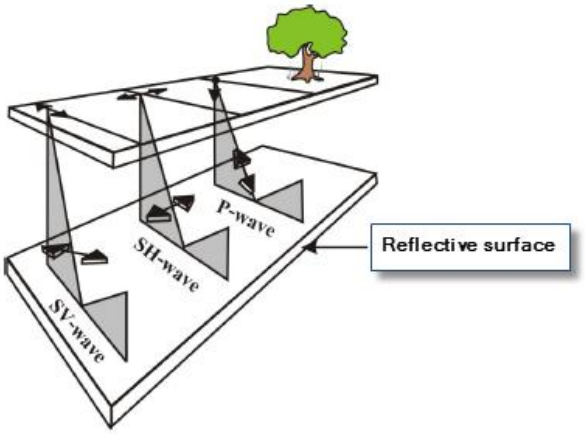

Figure 14 Primary wave and secondary wave movement (SV and SH-component) (Sattarak, 2007)

2.3.1.2 Transverse wave

Waves that cause particles of the medium the waves pass moving in the perpendicular to the direction of wave motion. As shown in Figure 15 is an example of a surface wave. These waves are called seismic because the particles are moving up or down, perpendicular to the direction of wave motion and the name of the wave is called the “Secondary wave” or “S-wave" or another name is "Shear wave". We can separate out the components of the direction of the wave in SV- component and SH-component as shown in Figure 15.

Chulalongkorn University

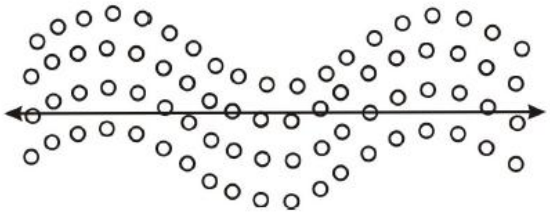

Figure 15 Secondary wave movements (Sattarak, 2007)

2.3.2 Surface waves

Surface waves (often called ground roll) are usually present on reflection record. For the most part, these are Rayleigh waves with velocities ranging from 100 to 1000 m/s or so. Ground roll frequencies usually are lower than those of reflections and refractions, often with the energy concentrated below 10 Hz. Ground roll alignments are straight, just as refractions are, but they represent lower velocities, the envelope of ground roll builds up and decay very slowly and often includes many cycles. Sometimes there is more than one ground roll wave train, each with different velocities. Occasionally where ground roll is exceptionally strong, in line offsets are used so that desired reflections can be recorded before the surface waves reach the spread.

2.3.2.1 Rayleigh wave

These waves require a medium to move parallel to the surface. The motion of the particles is elliptical. We can separate out the components of the direction of the wave in both vertical and horizontal as shown in Figure 16.

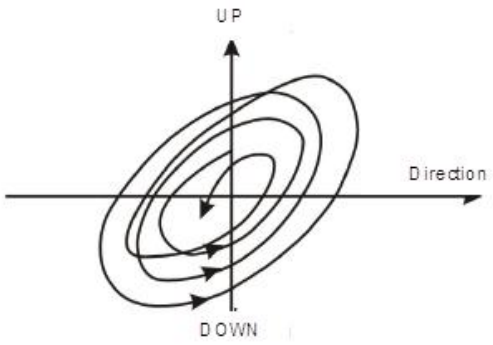

Figure 16 Rayleigh wave movements (Sattarak, 2007)

2.3.2.2 Love wave

Transverse wave is moving parallel to the surface of the air and the ground as shown in Figure 17.

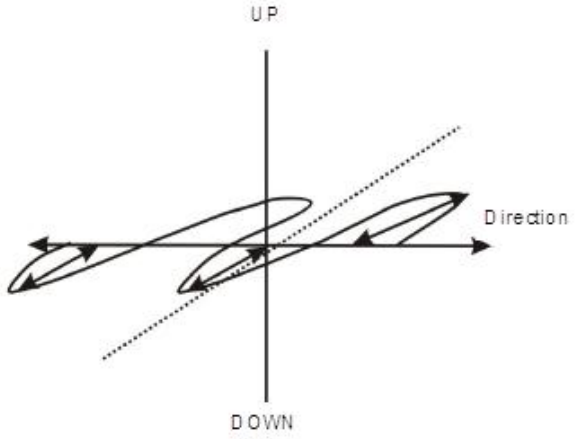

Figure 17 Love wave movements (Sattarak, 2007)

(Bruce, 1973) was introduced on the estimation of the S-wave when the waves below.

(1) Case is hard rock, the secondary wave velocity varies by about 0.6 times that of the primary wave for example if the primary wave velocity about 2500 m/s the secondary wave velocity about 1440 m/s.

(2) If the decay and sedimentary rocks, the secondary wave velocity is about 0.5 times the primary wave.

(3) If the soil, the secondary wave velocity is about 0.4 times the primary wave. During seismic wave exploration the surface waves are electromagnetic interference (noise) sometimes need to be separated or filtered from the primary wave. Surface waves consist of many wavelengths, however, the frequency of these waves are small. In refraction surveying, the surface wave velocity is less than the primary wave velocity which passes through the machine. Rayleigh wave velocity is about 0.9 times the shear wave velocity. Love wave velocity is equal to the shear wave velocity which moves in the horizontal direction (SH-component).

From the equation of V_P and V_S is that the velocity of the P-wave and S-wave depends on the density of the object. Table 2 shows relation between density P-wave and S-wave velocity of soil and rock.

Table 2 Relation between density P-wave and S-wave velocity of soil and rock (Clark & Emerson, 1999)

Material	Density (Kg/m^3)	P-wave velocity (m/s)	S-wave velocity (m/s)
Air	-	330-350	-
Water	1,000	1,400-1,600	0
Granite	2,600-2,700	4,500-5,500	2,500-3,300
Gneiss	2,500-2,700	3,500-4,800	1,700-2,800
Quartzite	2,500-2,700	5,000-5,800	2,900-3,600
Tuff	1,800-2,000	2,800-3,500	1,100-1,900
Basalt	2,800-2,900	5,000-6,000	2,800-3,600
Andysite	2,500-2,700	3,500-4,800	2,300-2,980
Rhyolite	2,500-2,600	3,800-5,000	2,400-3,050
Marble	2,700-2,800	3,500-5,800	2,355-3,250
Schist	2,700-2,800	4,500-5,200	2,860-2,900
Gabbro	2,900-3,050	5,000-5,500	3,200-3,500
Siltstone	2,400-2,500	2,200-2,500	1,520-1,750
Sandstone	2,400-2,700	1,400-4,200	700-2,200
Limestone	2,200-2,800	3,000-4,800	1,800-2,800

Diorite	2,400-2,800	3,500-4,800	2,000-3,000
Shale	2,200-2,700	1,800-2,800	800-1,600
Mud rock	2,000-2,400	1,500-2,400	-
Salt	2,100-2,200	4,200-5,000	2,100-2,800
Anhydrite	2,800-3,000	5,500-6,500	-
Wet sand	1,600-2,200	800-2,200	300-750
Dry sand	1,600-2,200	200-1,800	100-800
Wet sandy gravel	1,600-2,200	500-1,800	200-700
Dry sandy gravel	1,600-2,200	400-1,500	160-600
Sandy soil	1,400-1,800	250-600	120-300
Wet clay	1,900-2,000	1,200-1,800	400-600
Dry clay	1,900-2,000	700-1,200	300-600
loess	1,400-1,600	600-800	-
Silty clay	1,400-1,600	400-850	-

จุฬาลงกรณ์มหาวิทยาลัย
Chulalongkorn University

2.4 Seismic data acquisition

In seismic data acquisition, we concern ourselves only with the data gathering in the field, and making sure the data is of sufficient quality. In seismic acquisition, an elastic wave field is emitted by a seismic source at a certain location at the surface. The reflected wave field is measured by receivers that are located along lines (2D seismic) or on a grid (3D seismic). After each such a shot record experiment, the source is moved to another location and the measurement is repeated. Figure 18 gives an illustration of seismic acquisition in a land (onshore) survey. At sea (in a marine or offshore survey) the source and receivers are towed behind a vessel. In order to gather the data, many choices have to be made which are related to the physics of the

problem, the local situation and, of course, to economic considerations. For instance, a choice must made about the seismic source being used: on land, one usually has the choice between dynamite and vibroseis at sea, air guns are deployed. Also on the sensor side, choices have to be made, mainly with respect to their frequency characteristics. With respect to the recording equipment, one usually does not have a choice for each survey but one must be able to exploit its capabilities as much as possible.

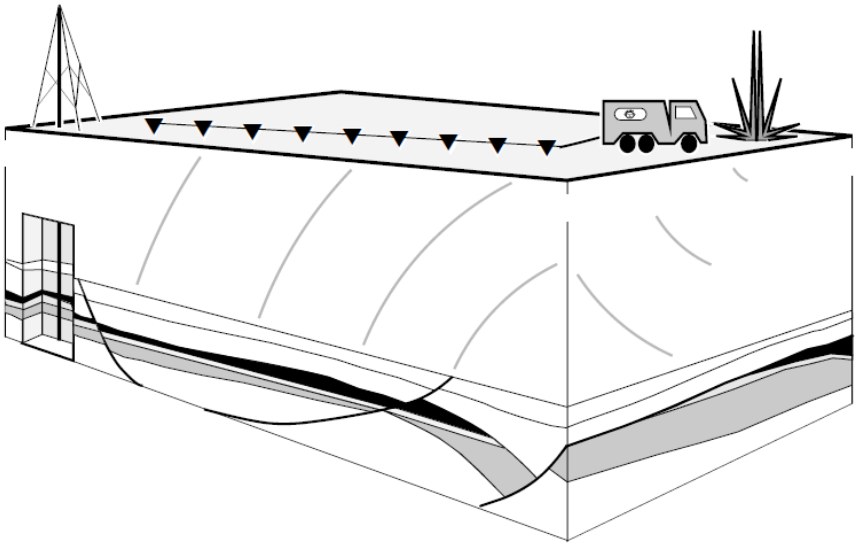

Figure 18 Seismic acquisition on land using a dynamite source and a cable of geophones (Dobrin & Savit, 1988)

2.5 Seismic sources on shore

2.5.1 Vibroseis

In seismic exploration, the use of a vibrator as a seismic source has become widespread ever since its introduction as a commercial technique in 1961. In the following the principles of the Vibroseis method are treated and the mechanism which allows the seismic vibrator to exert a pressure on the earth is explained. The basic features of the force generated by the seismic vibrator are the non-impulsive signal generated by a seismic vibrator having a duration of several seconds. The vibrator is a

surface source, and emits seismic waves by forcing vibrations of the vibrator baseplate which is kept in tight contact with the earth through a pull down weight. The driving force applied to the plate is supplied either by a hydraulic system, which is the most common system in use, or an electrodynamic system, or by magnetic levitation. The direction in which the plate vibrates can also vary: P-wave vibrators (where the motion of the plate is in the vertical direction) as well as S wave vibrators (vibrating in the horizontal direction) are used. Finally, a marine version of the seismic vibrator has been developed, however not in frequent use. For all these vibrator types, the general principle which governs the generation of the driving force applied to the plate (usually referred to as the baseplate) can be described by the configuration shown in Figure 19. The lowest frequency of operation in vibroseis seismic surveys for exploration purposes being usually not less than 5 Hz.

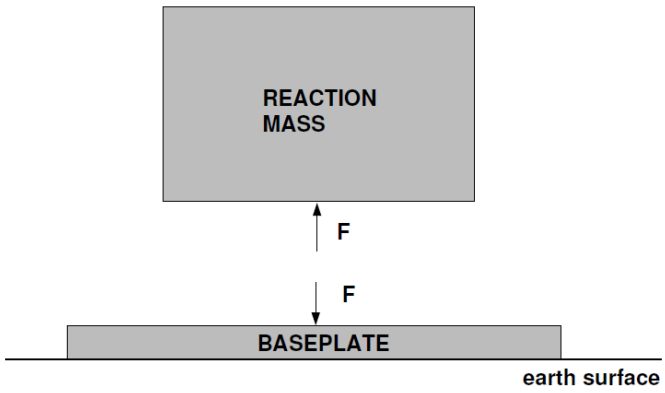

Figure 19 The force-generating mechanism of the seismic vibrator source (Dobrin & Savit, 1988)

Figure 20 Schematic view of the Vibroseis truck with the air springs, the baseplate and the vibrator actuator (Siam moeco limited, 2005)

2.5.2 Dynamite

Until the arrival of the vibroseis technique, dynamite was the mostly used seismic source on land. Dynamite itself is very cheap. The costs involved are mainly the costs of drilling the shot holes to place the dynamite. These costs may run up so high as to make the vibroseis a good competitor of the dynamite source. Dynamite is usually used in non-urban areas for obvious reasons. A positive characteristic of dynamite is that it resembles a (bandlimited) form of the delta pulse, something we would ideally like to have, since we are interested in the impulse response of the earth. Dynamite is a chemical composition which burns extremely fast when detonating. Typically, 1 kilogram of dynamite burns in about 20 microseconds. In this very short time it vaporizes and generates very high pressures and temperatures. The dynamite is usually ignited with a detonator which is a small-size charge of dynamite as well, but enough to ignite the larger charge. The detonator must obtain a large current in order to be set off. For safety reasons, the detonator is designed such that a large current has to be applied. A typical current strength is some 5 Amp. Explosives can be classified by their chemical composition. Dynamite itself consists of a combination of the explosives glyceroltrinitrate and glycoldinitrate. Since the combination of these two give a fluid, they are mixed with

celluloid-nitrate and then give a gelatinous material. Additives of certain (secret) components result in different types of dynamite.

The behaviour of the dynamite as a function of time is given in the lower of figure 21. In time, we first have an intense shock wave with a complete shattering of the rock or soil. Then, at a certain time, we get two effects, namely a cavity expansion and anelastic rock deformation, until we reach finally a time where we left a cavity which stays there, and an elastic wave originating from this area. So there will always be a cavity left when using dynamite. This cavity is not the same as the radius where the anelastic wave becomes an elastic wave. There has actually been some people who have dug out these cavities in order to see how the cavity changed with a different charge of dynamite. It turned out that the cavity radius was proportional to the cube root of the charge mass.

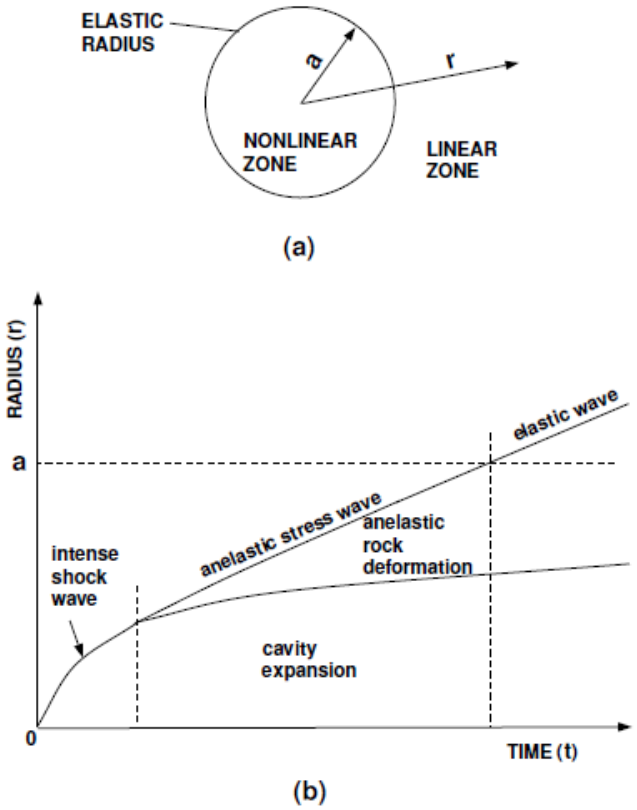

Figure 21 The behaviour of dynamite: (a) the characteristic zones in space and (b) the radius as a function of time with its characteristic zones (Dobrin & Savit, 1988)

The most well-known impulsive seismic source, dynamite, is indeed used very often in land seismic surveys. There are, however, some distinct disadvantages related to the use of an impulsive source like dynamite. Due to the high energy density of the dynamite explosion, severe harm can be done to the environment. In any case, the destructive nature of the dynamite source prohibits its use in densely populated areas. Second, a hole has to be drilled for every shot point in which the dynamite charge is placed. Third, the high energy-density of the explosion results in a non-linear zone surrounding the explosion. Although the ignition time of the dynamite itself is short compared with any time duration of interest in seismic exploration, this nonlinear zone results in a distorted wavelet. The high-frequency content of the signal decreases when the charge size is increased (the low frequency content increases). This yields a trade-off between penetration and resolution: a large charge size has better penetration, but lacks high frequencies. Another disadvantage of the creation of a nonlinear zone around the dynamite explosion is that effectively a wavelet is transmitted into the earth that is not an impulse, and has a shape which is not accurately known and cannot be measured easily. In table 3 the advantages and the disadvantages of the vibroseis and dynamite are tabulated.

จุฬาลงกรณ์มหาวิทยาลัย
Chulalongkorn University

Table 3 Advantages and disadvantages of vibroseis and dynamite

Source	Advantages	Disadvantages
Vibroseis	1. Less destructive than dynamite : can operate in urban areas 2. Not labour-intensive : cheap in operation 3. Some control over outgoing signal	1. One truck does not deliver enough energy : arrays, so directivity 2. Surface source : many Rayleigh waves 3. Can only operate in areas which can support 20 tons 4. Correlation imperfect : correlation

		noise
Dynamite	1. Buried source : much less surface waves generated than Vibroseis areas 2. Signal close to δ-pulse	1. Destructive : cannot operate in urban areas 2. Labour intensive for making shotholes : expensive in operation

2.6 Field layouts

2.6.1 Spilt- dip spread

Placing the source close to a geophone group often results in a noisy trace hence the source may be moved 15 to 50 m perpendicular to the seismic line is show in Figure 22.

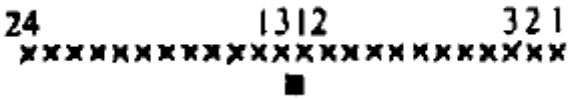

Figure 22 Spilt- dip spread (Telford, Geldart, & Sheriff, 1990)

จุฬาลงกรณ์มหาวิทยาลัย
CHULALONGKORN UNIVERSITY

2.6.2 Spilt- dip spread with source point gap

By spread we mean the relative location of the source point and the center of geophone groups used to record the energy from the source. In spilt-dip shooting the source point is at the center of a line of regularly spaced geophone groups is show in Figure 23.

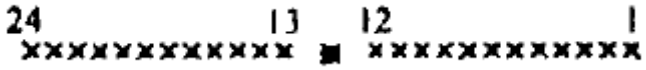

Figure 23 Spilt- dip spread with source point gap (Telford et al., 1990)

2.6.3 End on spread

Often the source is the end of the spread of active geophone groups is show in Figure 24.

Figure 24 End on spread (Telford et al., 1990)

2.6.4 In line offset spread

Source offset an appreciable distance along the line from the nearest active geophone group is show in Figure 25.

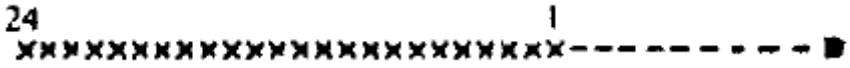

Figure 25 In line offset spread (Telford et al., 1990)

2.6.5 Broadside-T spread

The source point may be offset in the direction normal to the cable, either at one end of the active part to product the broadside-L or opposite the center to give a broadside-T is show in Figure 26.

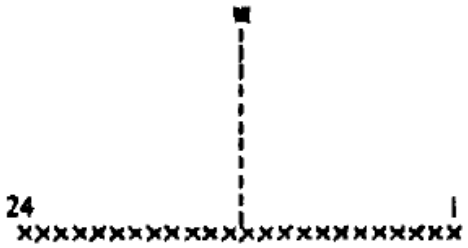

Figure 26 Broadside-T spread (Telford et al., 1990)

2.6.6 Cross spreads

Cross spreads consist of two lines of geophone groups roughly at right angles to each other, are used to record three dimensional dip information is show in Figure 27.

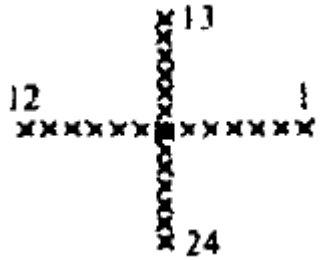

Figure 27 Cross spread (Telford et al., 1990)

จุฬาลงกรณ์มหาวิทยาลัย
Chulalongkorn University

CHAPTER 3

METHODOLOGY

3.1 Introduction

The object of exploration seismic is obtaining structural subsurface information from seismic data, i.e., data obtained by recording elastic wave motion of the ground. The main reason for doing this is the exploration for oil or gas fields (hydro-carbonates). In exploration seismic this wave motion is excited by an active source, the seismic source, e.g. for land seismic (onshore) dynamite. From the source elastic energy is radiated into the earth, and the earth reacts to this signal. The energy that is returned to the earth's surface, is then studied in order to infer the structure of the subsurface. Conventionally, three stages are discerned in obtaining the information of the subsurface, namely data acquisition, processing and interpretation.

To fulfill the objectives of this thesis, the researcher decided to perform the tests at five locations located in Mahasarakham, Surin, Udonthani, Suphanburi and Suratthani province. The specific addresses of the sites are as follows;

(1) Phayakkhaphumphisai, Mahasarakham province.

Coordinates: Latitude 15°31’18.79’’ N/ Longitude 103°7’24.98’’E (Figure 28)

(2) Chumphonburi, Surin province.

Coordinates: Latitude 15°21’32.8’’N/ Longitude 103°23’55.6’’E (Figure 29)

(3) Nongwuaso, Udonthani province.

Coordinates: Latitude 17°10’57.43’’N/ Longitude 102°39’59’’E (Figure 30)

(4) Uthong, Suphanburi province.

Coordinates: Latitude 14°20’18.78’’N/ Longitude 99°59’20.95’’E (Figure 31)

(5) Phunphin, Suratthani province.

จุฬาลงกรณ์มหาวิทยาลัย
CHULALONGKORN UNIVERSITY

Coordinates: Latitude 9°0’31.46’’N/ Longitude 99°5’19.21”E (Figure 32)

The sites (1) and (2) are in the lower northeastern of Thailand and assumed to have similar soil condition, the site (3) is in the upper northeastern of Thailand, the site (4) is in the central of Thailand and the site (5) is in the southern of Thailand, respectively.

Figure 28 Location map of Phayakkhaphumphisai, Mahasarakham province

Figure 29 Location map of Chumphonburi, Surin province

Figure 30 Location map of Nongwuaso, Udonthani province

Figure 31 Location map of Uthong, Suphanburi province

Figure 32 Location map of Phunphin, Suratthani province

3.2 Research Framework

The overall framework of this research is summarized in the flow chart below (Figure 33).

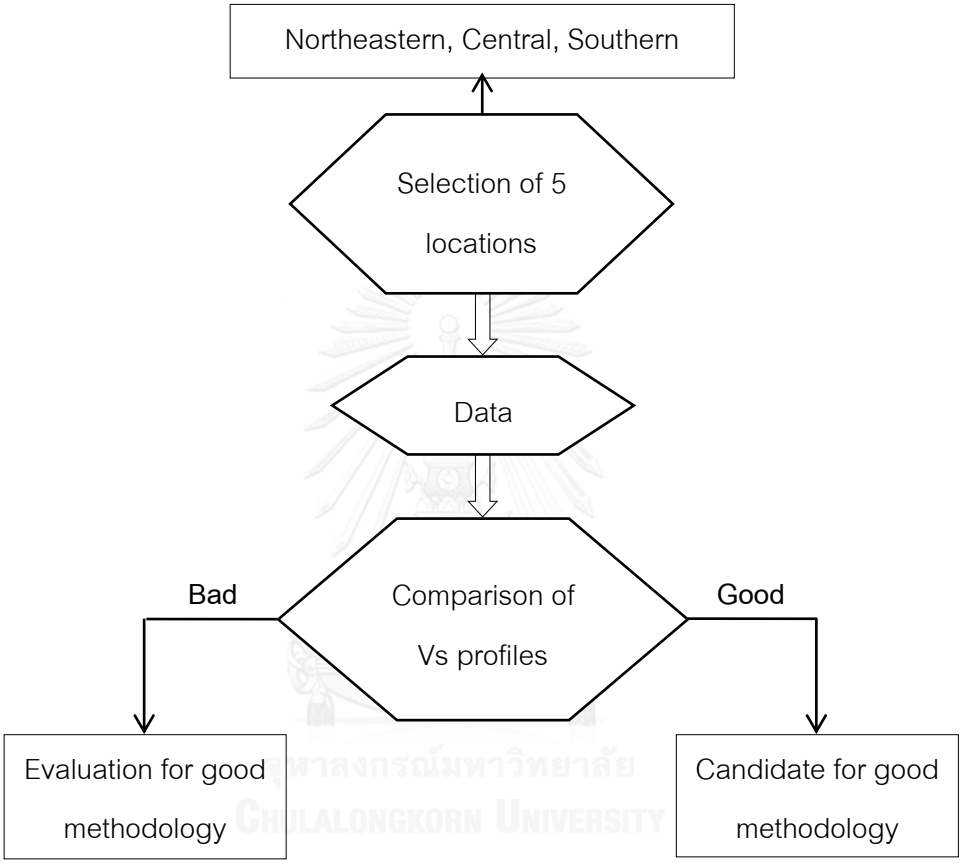

Figure 33 Flow chart of research framework

3.3 Data Acquisition

The maximum investigation depth of the project was around 30 m. As rule of thumb, the nearest offset is approximately equal to the maximum investigation depth. Because 16-channel system was available, I decided to set the nearest offset to 25-30% (75 - 90 m) of total spread to ensure high-frequency signals were recorded (Seng, 2009). The geophone interval was set to 20 m (d). With the 16-channel system, the geophone spread (Figure 34) is 300 m (D), which implies that in the best scenario the

longest recorded wavelength could be 300 m. The maximum investigation depth is normally half or by three of the longest wavelength (Seng, 2009). With this field setting, the maximum investigation depth could reach 100 m. In reality, the recorded longest wavelength is usually shorter than the geophone spread due to band-limited source and geophone, ambient noise, energy attenuation, and complexity of near-surface geology.

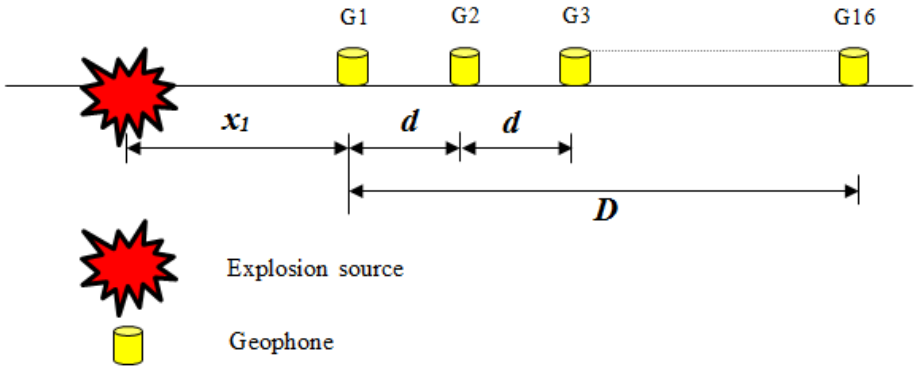

Figure 34 Geophones spread line

Table 4 Geophones set at Mahasarakham province

Shot point	Geophone, X_1 *(m)*	Explosive charge (kg)	*d (m)*	*D (m)*
d5397	G1, 130	3	20	300
d5398	G1, 90	3	20	300
d5399	G1, 50	3	20	300
d5402	Between G4&5, 10	3	20	300
d5406	Between G12&13, 10	3	20	300
d5408	G16, 10	3	20	300
d5410	G16, 90	3	20	300

Table 5 Geophones set at Surin province

Shot point	Geophone, X_1 *(m)*	Explosive charge (kg)	*d (m)*	*D (m)*
d5935	G1, 10	4	20	300
d5939	G1, 160	3	20	300
d5940	G1, 200	3	20	300
d5946	G1, 440	3	20	300
d5949	G1, 560	3	20	300

Table 6 Geophones set at Udonthani province

Shot point	Geophone, X_1 *(m)*	Explosive charge (kg)	*d (m)*	*D (m)*
d01	Between G4&5, 12.5	1.5	25	300
d95	G1, 12.5	1.5	25	300
d2392	G1, 990	1.5	25	300
d2394	G1, 941	1.5	25	300
d2396	G1, 1406	1.5	25	300

Table 7 Geophones set at Suphanburi province

Shot point	Geophone, X_1 *(m)*	Explosive charge (kg)	*d (m)*	*D (m)*
d650858	G11, 111	1	20	300
d650860	G11, 11	1	20	300
d650862	G12, 95	1	20	300
d650872	G16, 223	1	20	300
d650876	G16, 9	1	20	300

d730876	G7, 4	1	20	300
d890872	G1, 178	1	20	300
d890876	G1, 97	1	20	300
d890878	G1, 180	1	20	300
d970874	G1, 181	1	20	300
d970876	G1, 144	1	20	300
d970878	G1, 233	1	20	300

Table 8 Geophones set at Suratthani province

Shot point	Geophone, X_1 *(m)*	Explosive charge (kg)	*d (m)*	*D (m)*
d5070	G10, 3	2	20	300
d5072	G8, 8	2	20	300
d5074	G5, 3	2	20	300
d5078	G1, 18	2	20	300
d5080	G1, 68	2	20	300
d5081	G1, 93	2	20	300

จุฬาลงกรณ์มหาวิทยาลัย
Chulalongkorn University

3.4 Acquisition instruments and setting

Multichannel records were acquired using the end-on geophone (Figure 34) and sixteen 4.5-Hz vertical-component geophones (Figure 35). The source was an explosive 1-4 kg, installed 9-21 m from the ground (Figure 36). Data were recorded on a notebook directly (Figure 37). Recording time was 0.5-ms sample interval. No acquisition filter was applied during the recording to increase signal to noise (S/N) ratio.

Figure 35 Geophone

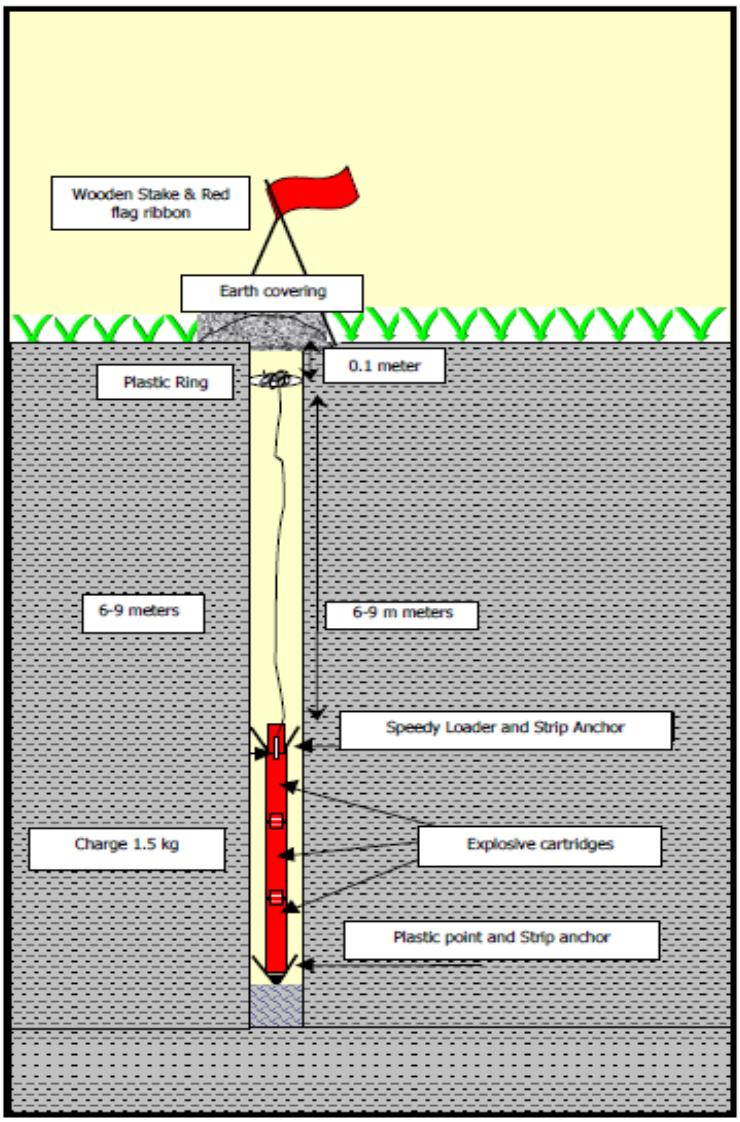

Figure 36 Loading profile (Apico (Korat) ltd., 2005)

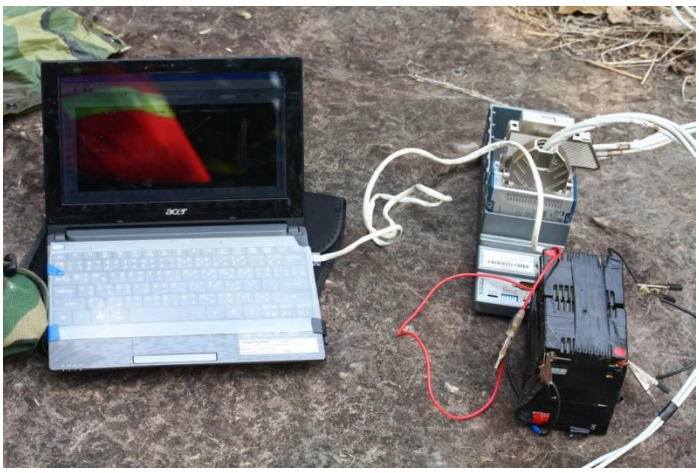

Figure 37 Notebook and data logger

3.5 Data processing and interpretation

Limited and uniform preprocessing was applied to the data to minimize processing artifacts.

3.5.1 Pre-processing

(1) Calibrate data from field test to the data.csv format.

(2) Data sorting: apply field geometry to data based on source and geophone locations.

(3) Spectrum analysis: define frequency ranges of surface-wave signals shot by shot and determine a common frequency range for all data.

(4) Velocity analysis: recognize and define surface wave velocity ranges shot by shot and determine a common velocity range using surface wave analysis.

3.5.2 Surface-wave analysis

(1) Dispersion property analysis of surface waves: determine the frequency range of surface waves, the wavelengths of surface waves, a range of surface wave velocity, and existence of modes.

(2) Dispersion curve picking: for each shot, surface wave phase velocities of the fundamental mode were manually picked normally frequency with an interval of 1 Hz point by point with assistance of velocity analysis of the shot gather in the time-distance domain. Based on the surface-wave components and drilling information.

(3) Inversion of dispersion curves: invert dispersion curves one by one to obtain shear wave velocity profiles (Vs and depth). The shear wave velocity profile was placed at the middle of the geophone spread.

(4) Find the empirical correlations between Vs and depth.

จุฬาลงกรณ์มหาวิทยาลัย
Chulalongkorn University

CHAPTER 4

RESULTS

4.1 Overview

This chapter showed the field investigation data and data analysis by procedure described in Chapter 2 to determine the shear wave velocity, and comparison between The Simple Analysis of Surface Wave Method (SM), The Multichannel Analysis of Surface Wave Method (MASW) and Down-hole Seismic Method (DH).

4.2 Information of subsurface

The researcher investigated soil profile at Mahasarakham, Surin and Udonthani province, respectively.

4.2.1 Mahasarakham province

Figure 38 shows the typical subsoil profile in the study area. There are 3 main soil types underlain the studied site as follows:

4.2.1.1 Silty very fine sand layer (SM): the layer extends from ground surface to depth of about 4.2 m. It mostly contains silt mixed with very fine sand. The relative density measured using split spoon ranged between loose to medium state.

4.2.1.2 Very fine sandy clay layer (CL): this layer of very fine sandy clay is found beneath the top silty very fine sand layer. It extends to depth of about 12 m from ground surface. The consistency ranged between medium to hard state.

4.2.1.3 Silty very fine-coarse sand layer (SM, SP-SM): this silty sand is underlain the studied site to depth of 32 m (end of boring) and underground water level at 2.42 m from surface. The relative density ranged between very dense to medium state.

จุฬาลงกรณ์มหาวิทยาลัย
Chulalongkorn University

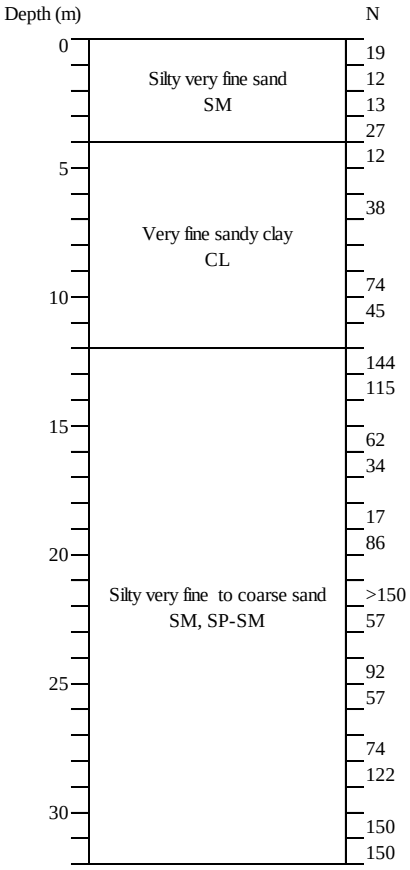

Figure 38 Subsoil profile at Mahasarakham

จุฬาลงกรณ์มหาวิทยาลัย
Chulalongkorn University

4.2.2 Surin province

Figure 39 shows the typical subsoil profile in the study area. There are 4 main soil types underlain the studied site as follows:

4.2.2.1 Silty sand layer (SM): the layer extends from ground surface to depth of about 4.5 m. It mostly contains silt mixed with very fine sand. The relative density measured using split spoon ranged between medium to dense state.

4.2.2.2 Fine to coarse sand layer (SP, SP-SM): this layer of medium to dense coarse sand is found beneath the top silty sand layer. It extends to depth of about 15 m from ground surface.

4.2.2.3 Silt-coarse sand layer (SM, SP-SM): this silty sand is found at depth from 15 m to 25 m from ground surface. The relative density ranged between medium to very dense state.

4.2.2.4 Cemented coarse sand layer: this very dense cemented coarse sand is underlain the studied site to depth of 32 m (end of boring) and underground water level at 2.68 m from surface.

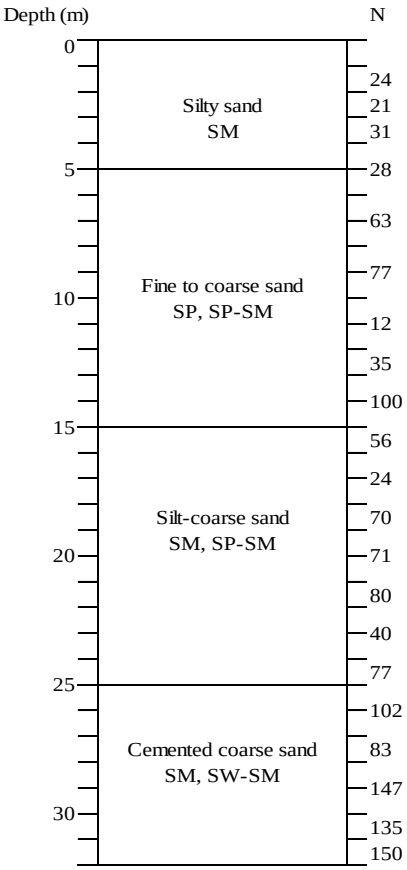

Figure 39 Subsoil profile at Surin

4.2.3 Udonthani province

Figure 40 shows the typical subsoil profile in the study area. There are 3 main soil types underlain the studied site as follows:

4.2.3.1 Silty very fine sand layer (SM): the layer extends from ground surface to depth of about 2 m. It mostly contains silt mixed with very fine sand. The relative density measured using split spoon ranged between dense to very dense state.

4.2.3.2 Compacted silty very fine sandy clay (CL): this layer of very fine sandy clay is found beneath the top silty very fine sand layer. It extends to depth of about 4.5 m from ground surface. The consistency ranged in hard state.

4.2.3.3 Compacted silty clay layer (ML-OL): this silty sand is underlain the studied site to depth of 6.45 m (end of boring) and underground water level at 2.6 m from surface. The relative density ranged in hard state.

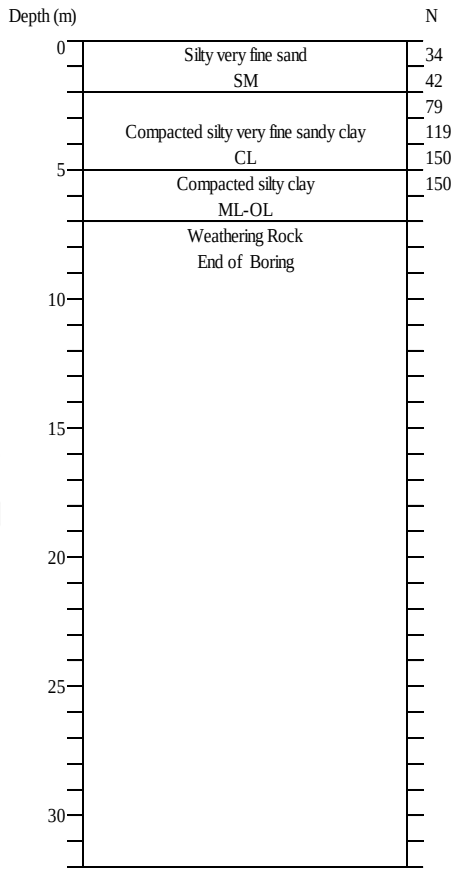

Figure 40 Subsoil profile at Udonthani

4.2.4 Suphanburi province

Figure 41 shows the typical subsoil profile in the study area. There are 4 main soil types underlain the studied site as follows:

4.2.2.1 Stiff silty clay layer (CL, OL-ML): the layer extends from ground surface to depth of about 2.75 m.

4.2.2.2 Hard silt with gravel layer (OL-ML): this layer is found beneath the top stiff silty clay layer. It extends to depth of about 4 m from ground surface.

4.2.2.3 Dense clayey sand with gravel layer (SC): this layer is found at depth from 4 m to 5.5 m from ground surface.

4.2.2.4 Hard clay with gravel layer (CL): this layer is found at depth from 5.5 m to 9.45 m (end of boring) and underground water level at 1.00 m from surface.

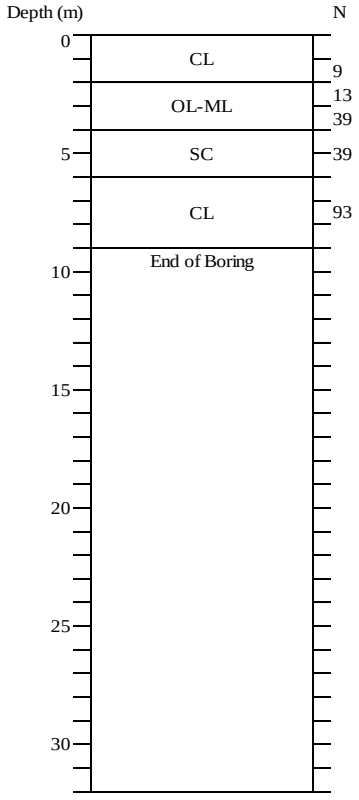

Figure 41 Subsoil profile at Suphanburi (Department of Public Works and Town & Country Planning, 2002)

4.2.5 Suratthani province

Figure 42 shows the typical subsoil profile in the study area. There are 3 main soil types underlain the studied site as follows:

4.2.2.1 Very soft to soft silty clay layer: the layer extends from ground surface to depth of about 1.5 m.

4.2.2.2 Very fine to fine sand layer: It extends to depth of about 1.5 m to 9 m.

4.2.2.3 Coarse sand and gravel: this layer is found at depth from 9 m to 14 m (end of boring) and underground water level at 0.20 m from surface.

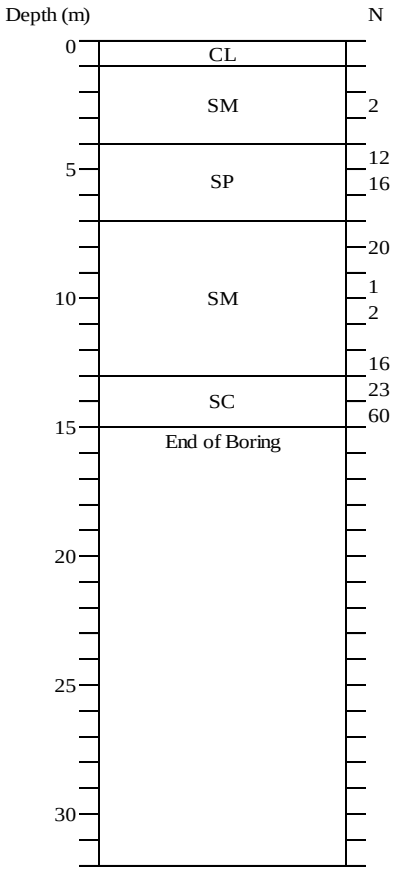

Figure 42 Subsoil profile at Suratthani (Department of Public Works and Town & Country Planning, 1985)

4.3 Data acquisition

4.3.1 Mahasarakham province

4.3.1.1 This example showed the path of the wave which is used to determine shear wave velocity for Refraction seismic survey, Reflection seismic survey, The Simple Analysis of Surface Wave Method (SM) and The Multichannel Analysis of Surface Wave Method (MASW).

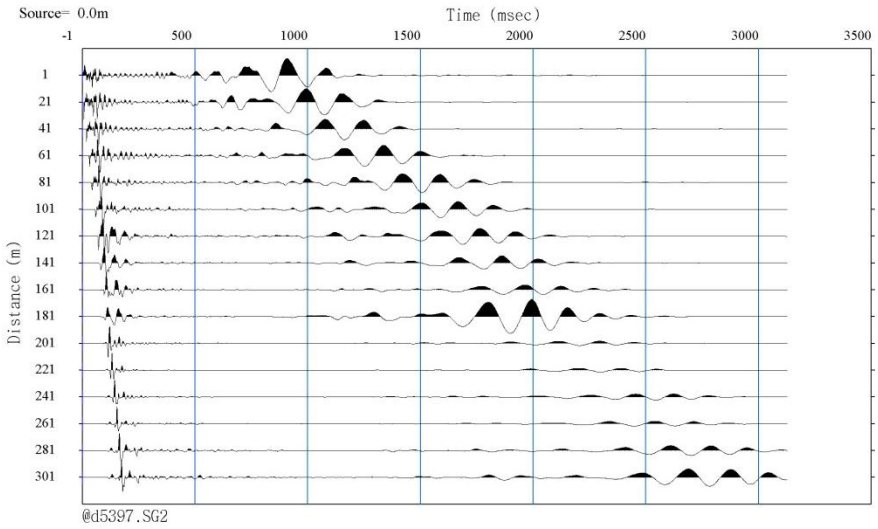

Figure 43 Seismic data in the space-time domain by SM and MASW at Mahasarakham

จุฬาลงกรณ์มหาวิทยาลัย
Chulalongkorn University

4.3.1.2 This figure showed the data acquisition from Down-hole Seismic Method (DH).

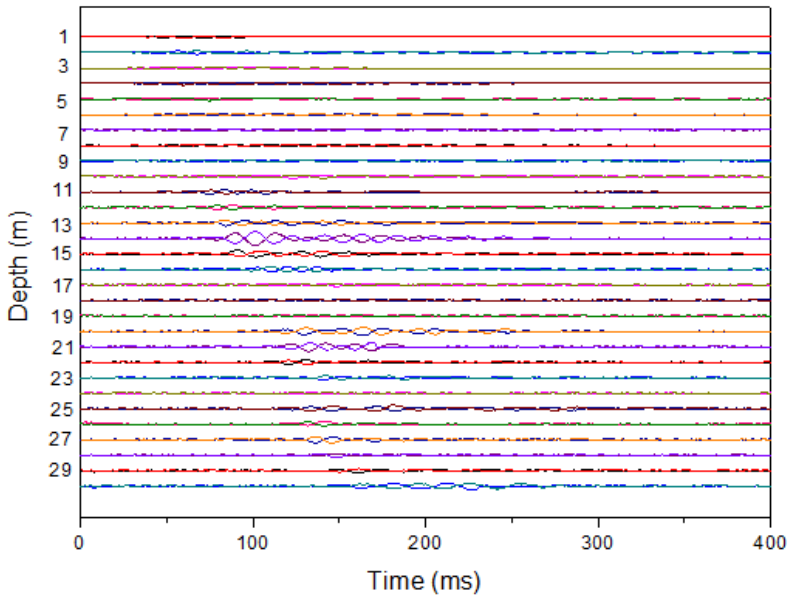

Figure 44 Seismic data in the time – depth by DH at Mahasarakham

4.3.2 Surin province

4.3.2.1 This example showed the path of the wave which is used to determine shear wave velocity for Refraction seismic survey, Reflection seismic survey, The Simple Analysis of Surface Wave Method (SM) and The Multichannel Analysis of Surface Wave Method (MASW).

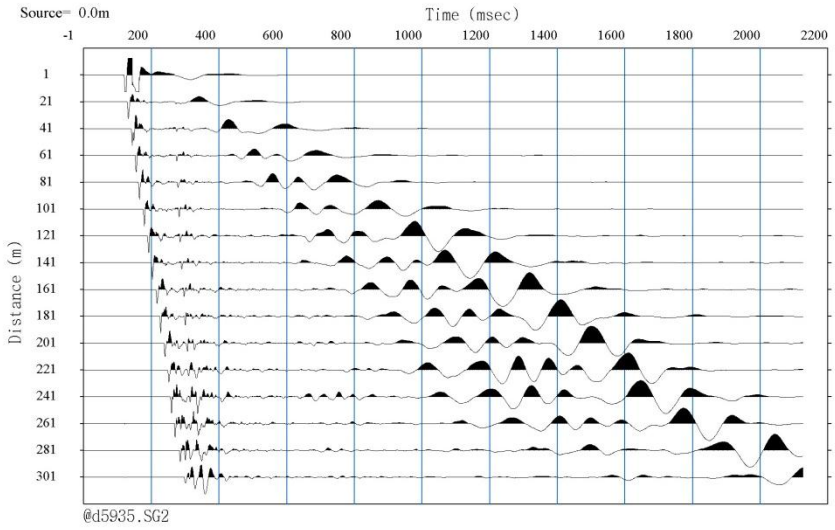

Figure 45 Seismic data in the space-time domain by SM and MASW at Surin

4.3.2.2 This figure showed the data acquisition from Down-hole Seismic Method (DH).

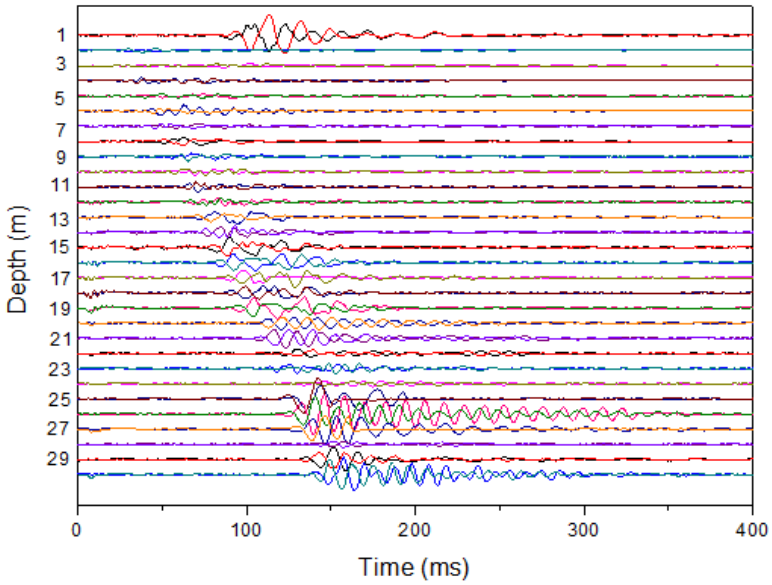

Figure 46 Seismic data in the time – depth by DH at Surin

4.3.3 Udonthani province

4.3.3.1 This example shows the path of the wave which is used to determine shear wave velocity for Refraction seismic survey, Reflection seismic survey, The Simple Analysis of Surface Wave Method (SM) and The Multichannel Analysis of Surface Wave Method (MASW).

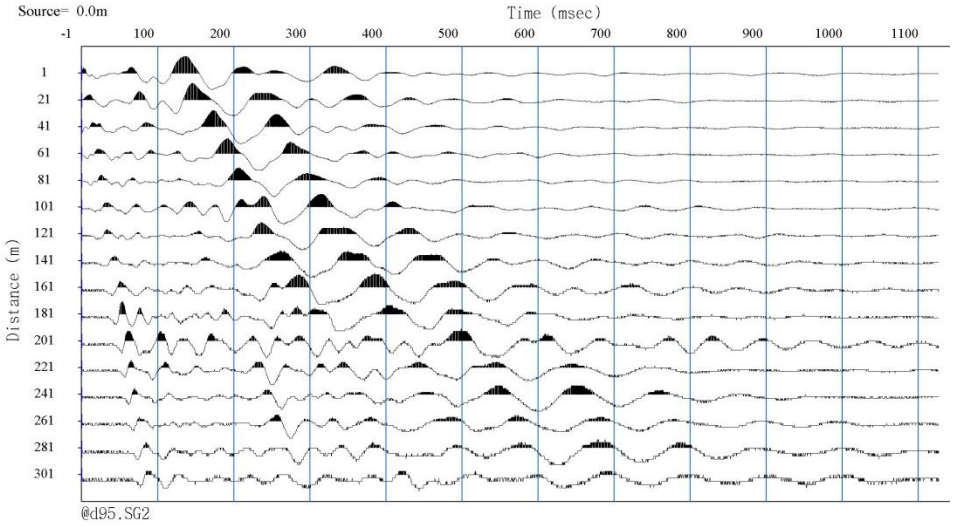

Figure 47 Seismic data in the space-time domain by SM and MASW at Udonthani

4.3.3.2 This figure showed the data acquisition from Down-hole Seismic Method (DH).

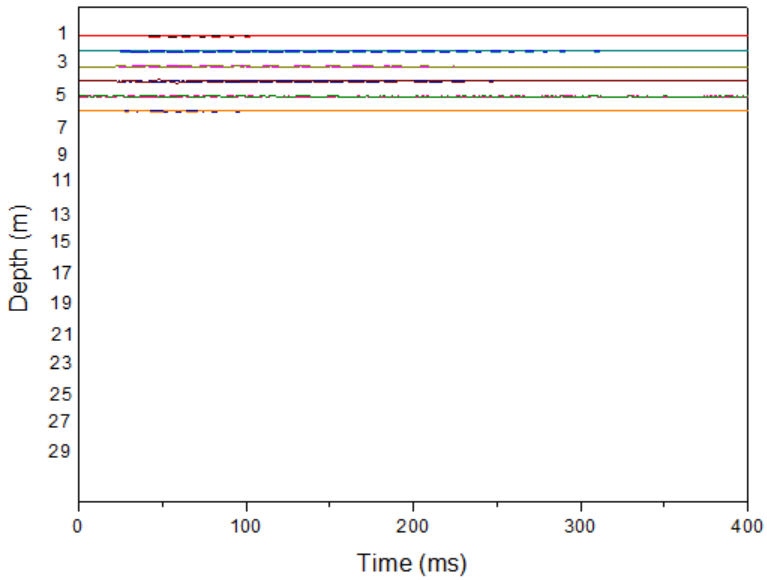

Figure 48 Seismic data in the time – depth by DH at Udonthani

4.3.4 Suphanburi province

4.3.4.1 This example shows the path of the wave which is used to determine shear wave velocity for Refraction seismic survey, Reflection seismic survey, The Simple Analysis of Surface Wave Method (SM) and The Multichannel Analysis of Surface Wave Method (MASW).

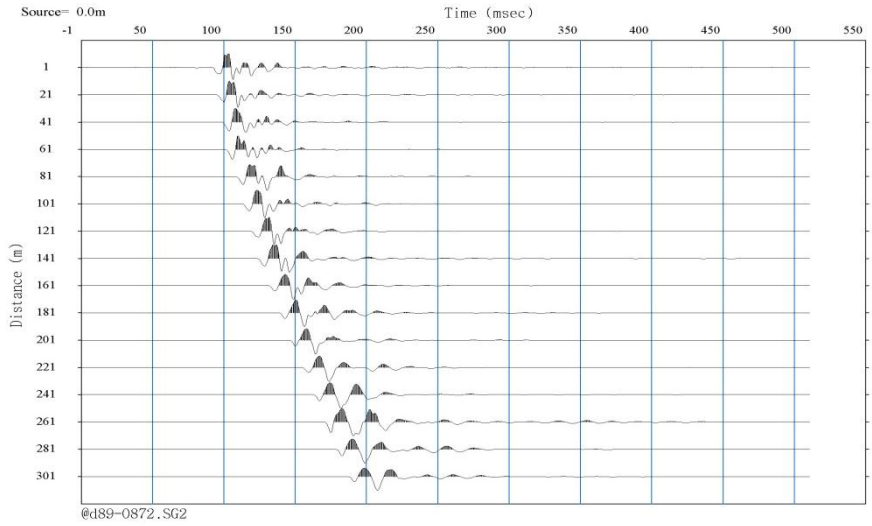

Figure 49 Seismic data in the space-time domain by SM and MASW at Suphanburi

4.3.4.2 No data acquisition from Down-hole Seismic Method (DH) because researcher did not drill the hole.

4.3.5 Suratthani province

4.3.5.1 This example shows the path of the wave which is used to determine shear wave velocity for Refraction seismic survey, Reflection seismic survey, The Simple Analysis of Surface Wave Method (SM) and The Multichannel Analysis of Surface Wave Method (MASW).

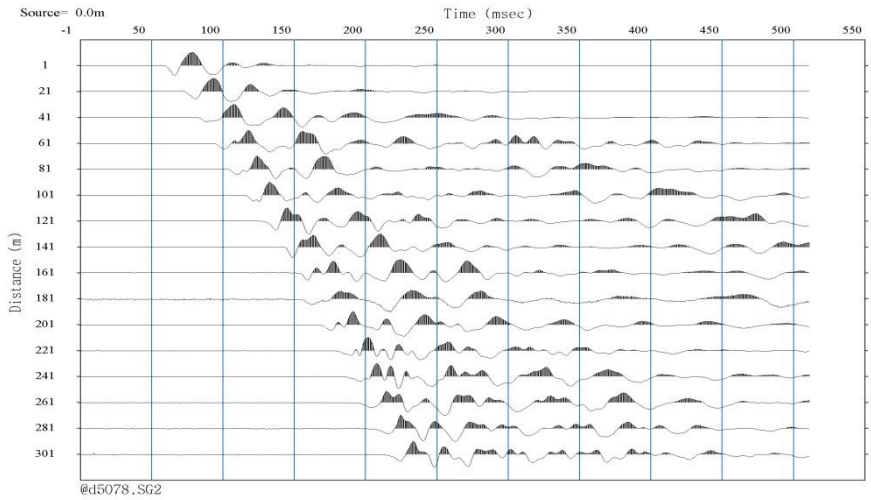

Figure 50 Seismic data in the space-time domain by SM and MASW at Suratthani

4.3.5.2 No data acquisition from Down-hole Seismic Method (DH) because researcher did not drill the hole.

4.4 Processing and interpretation

4.4.1 Estimation of shear wave velocity profile at Mahasarakham province

4.4.1.1 Refraction seismic survey

In this figure, the first arrival picks from the P-wave refraction survey shows one layer with a consistent P-wave velocity of 1,744.19 m/s. No second layer was found and it is postulated, due to the length of the line and weak energy source. With the absence of a second layer, the thickness of the initial layer cannot be calculated. Results from Refraction seismic survey, in this case velocity of the initial layer are used as input for the SM and MASW to drive inversion to more realistic results. From P-wave velocity can be classify as Wet sand, Dry sand or Wet sandy gravel (Table 2).

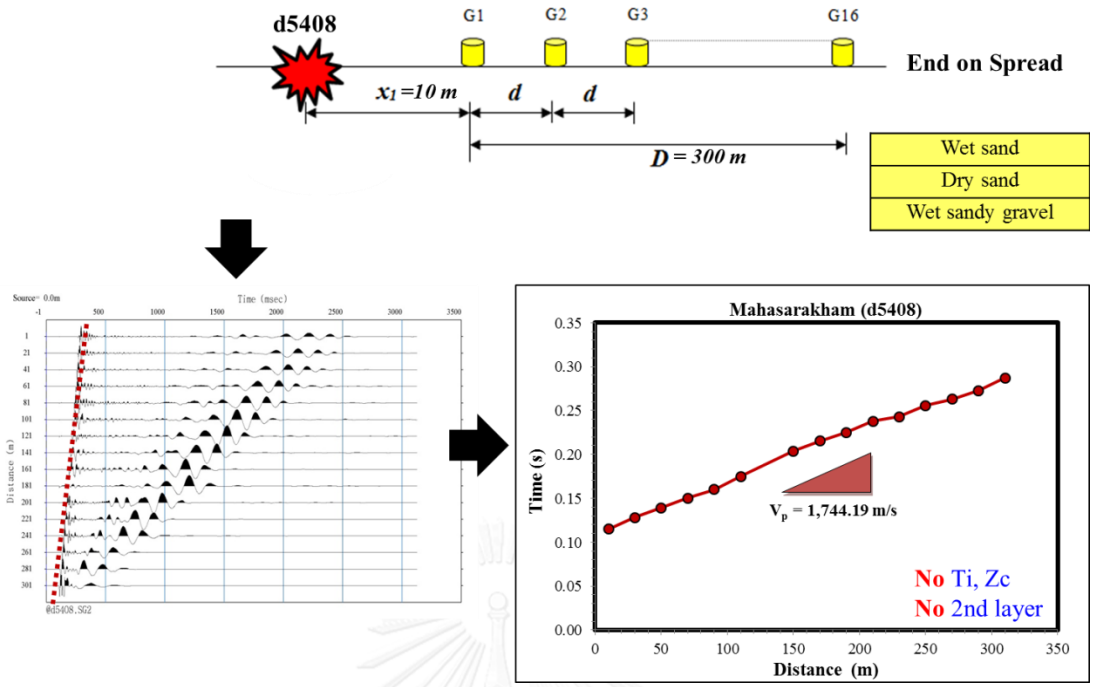

Figure 51 Data processing by Refraction seismic survey at Mahasarakham

4.4.1.2 Reflection seismic survey

This figure shown that the relation between square of time (t^2) and square of distance (x^2) is established a straight line with a slope ($1/V^2$) in term of y = mx + b, so we can find the P-wave velocity of soil-rock (1,202 m/s). If square of distance (x^2) is equal to zero, then t_0^2 and t_0 are equal to 20,484 and 143.12 ms, respectively. The depth of soil-rock can be calculated from eq. (15). From P-wave velocity equal to 1,202 can be classify as Wet sand, Dry sand, Wet sandy gravel, Dry sandy gravel, Wet clay or Dry clay (Table 2).

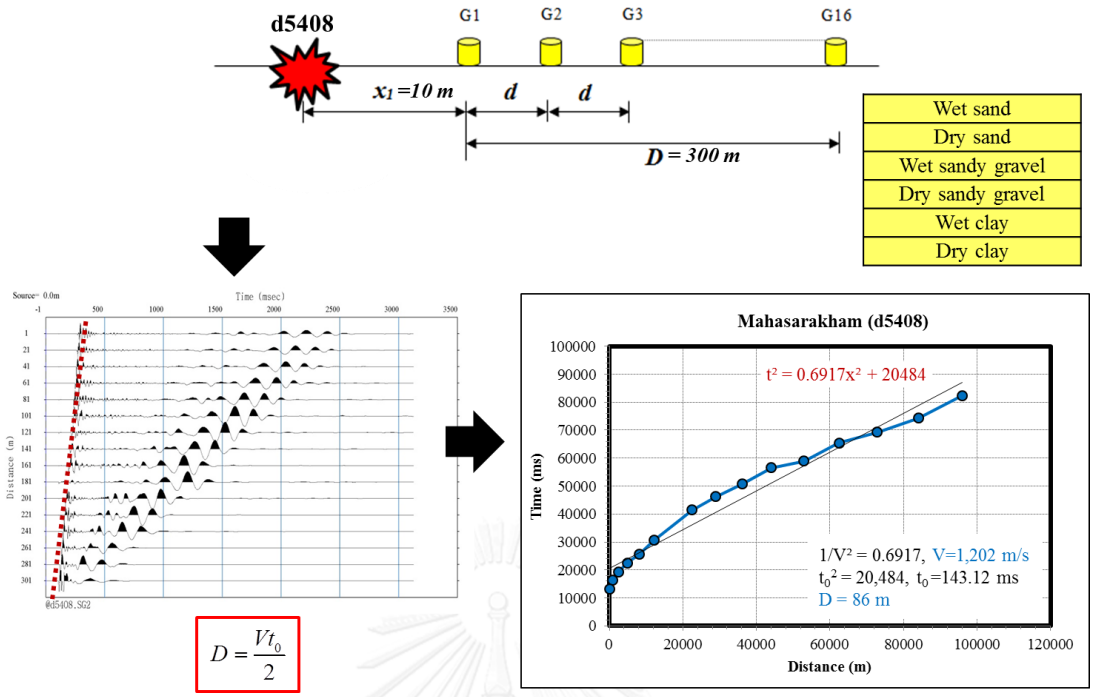

Figure 52 Data processing by Reflection seismic survey at Mahasarakham

4.4.1.3 The Simple Analysis of Surface Wave Method (SM)

The figure shows that the analyzed of the data by procedure described in Section 2.2.3.1 to establish the relationship between the phase velocity with frequency (Dispersion Curve), and inversion to determine the shear wave velocity at the depth of the soil layer using the principles and theories in Section 2.2.4.2.

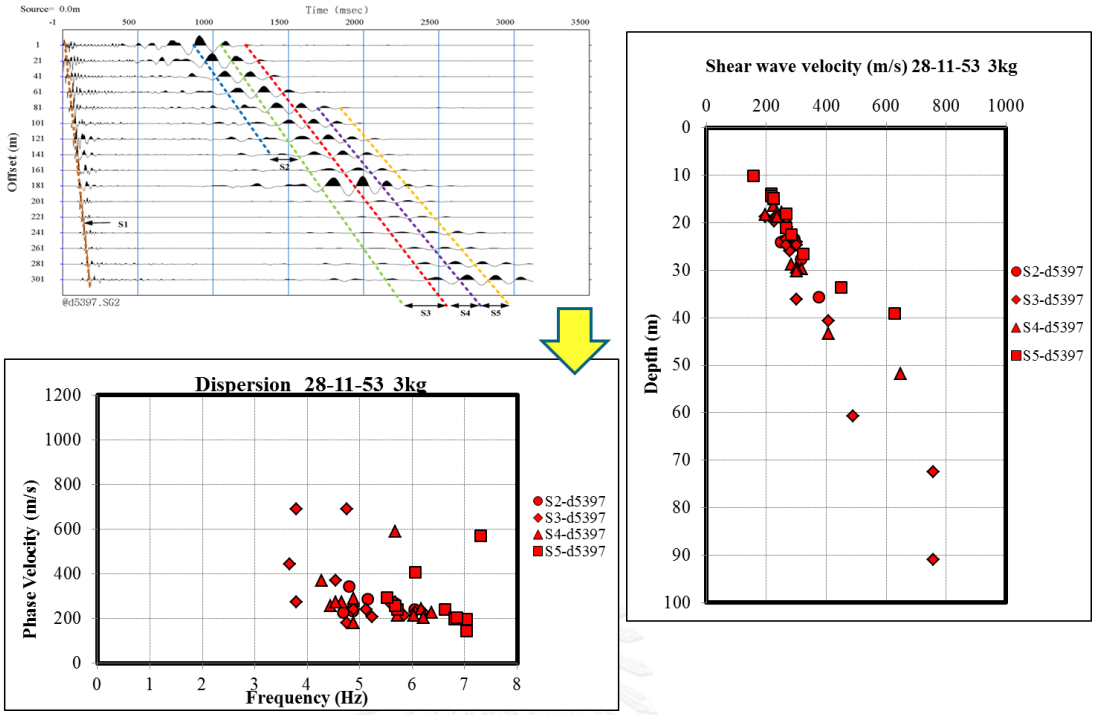

Figure 53 The SM data processing from field test (d5397)

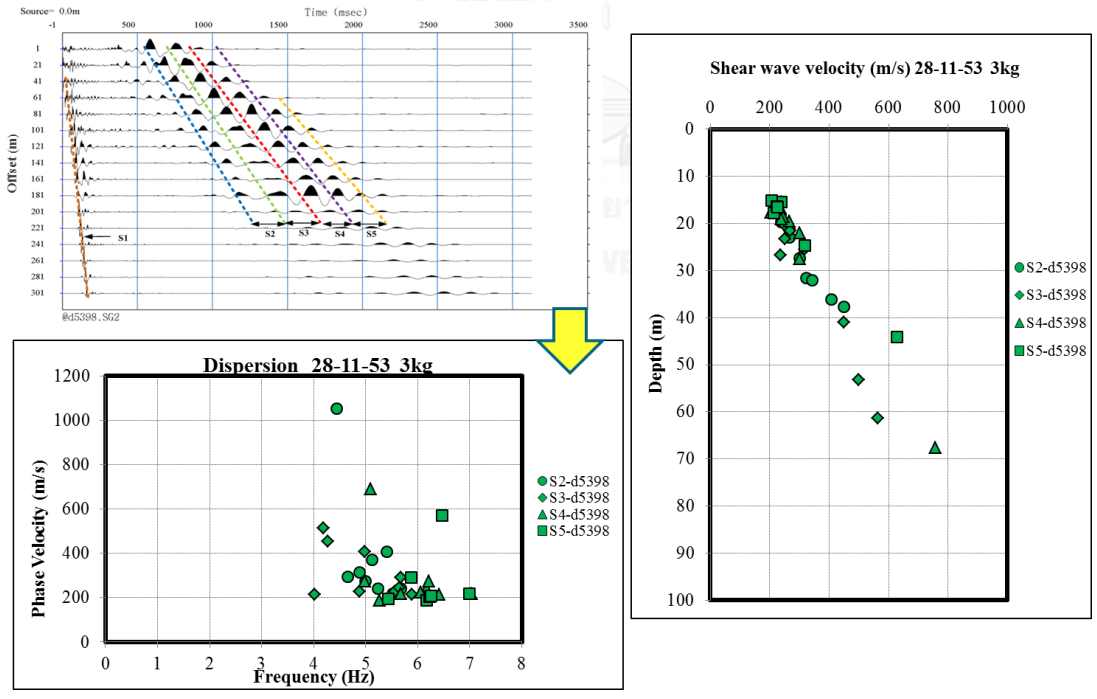

Figure 54 The SM data processing from field test (d5398)

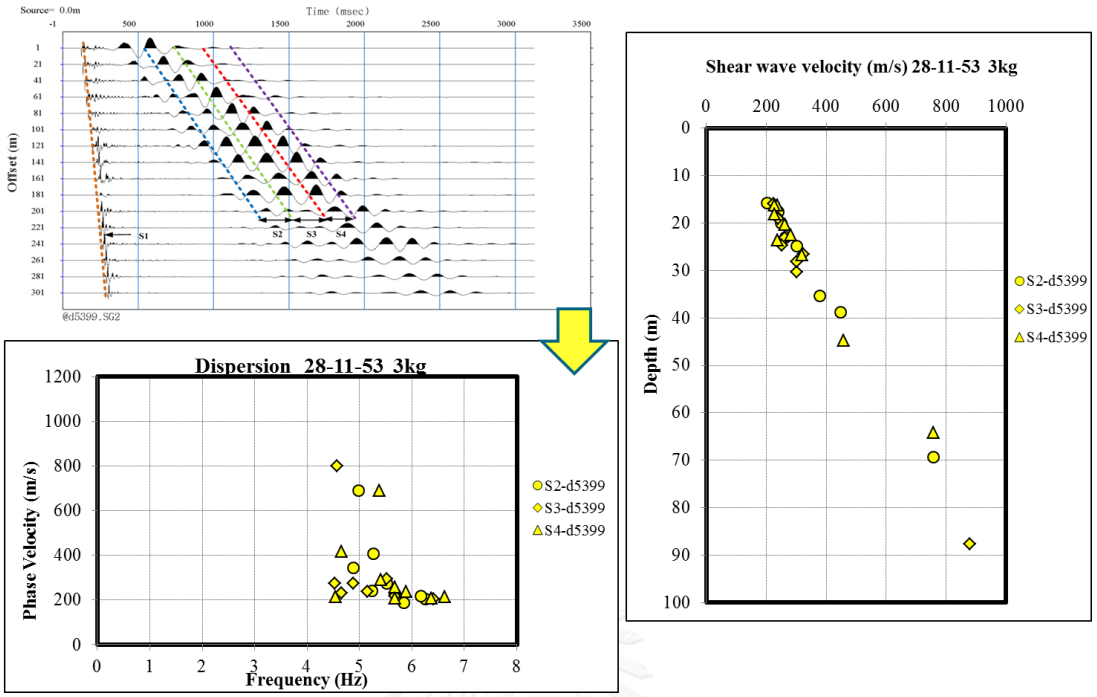

Figure 55 The SM data processing from field test (d5399)

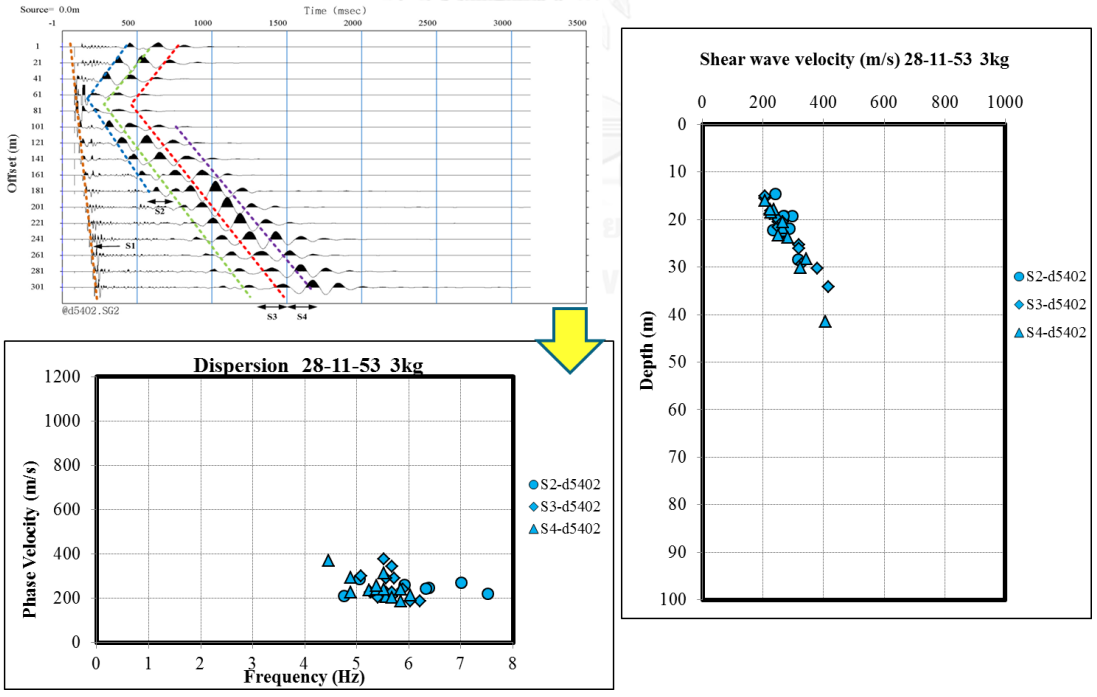

Figure 56 The SM data processing from field test (d5402)

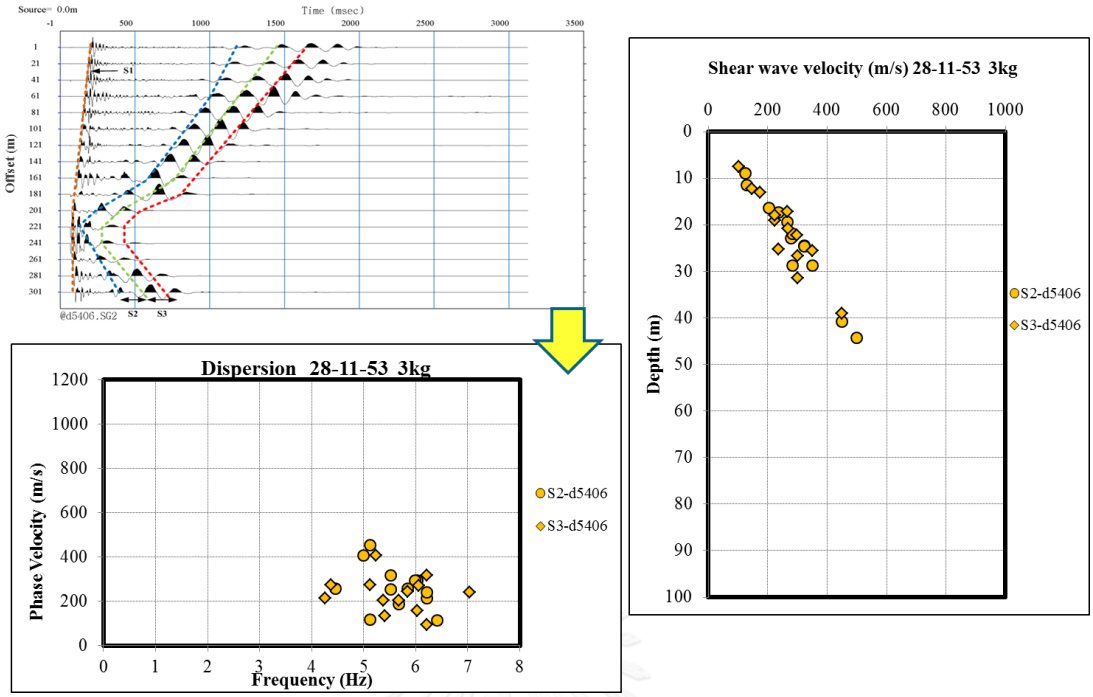

Figure 57 The SM data processing from field test (d5406)

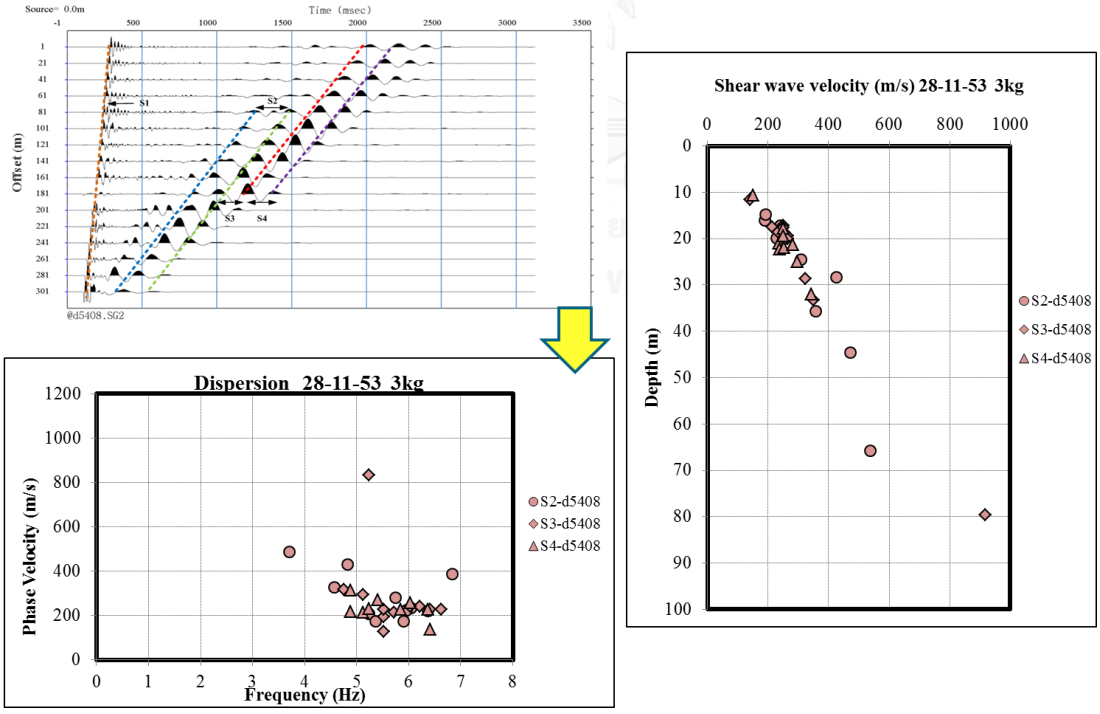

Figure 58 The SM data processing from field test (d5408)

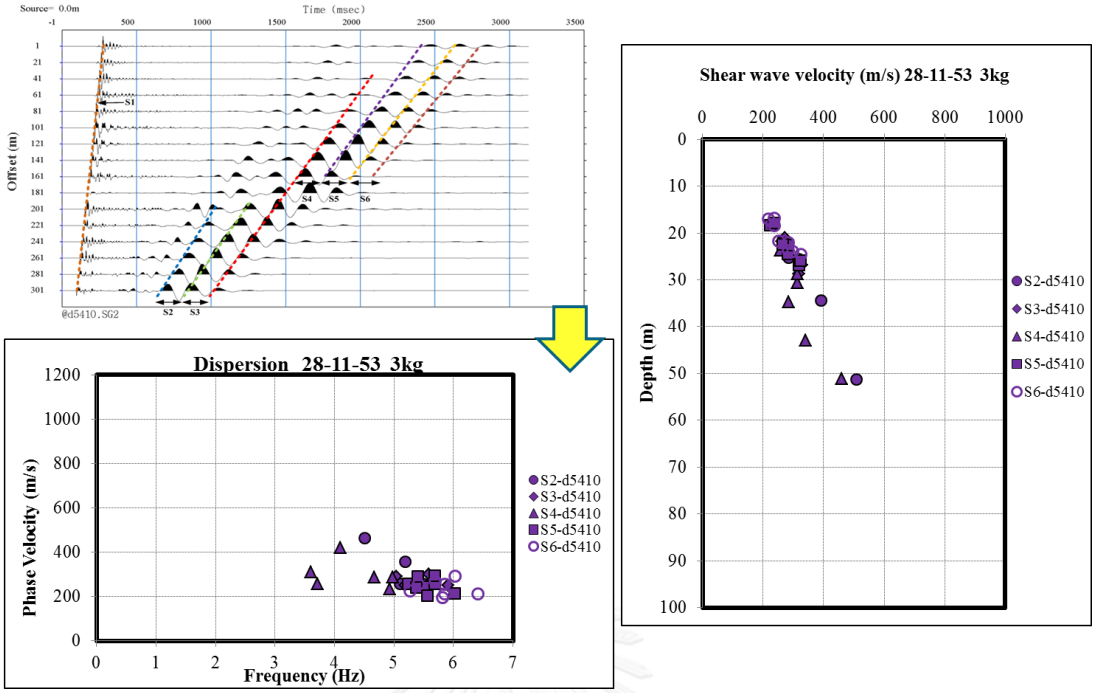

Figure 59 The SM data processing from field test (d5410)

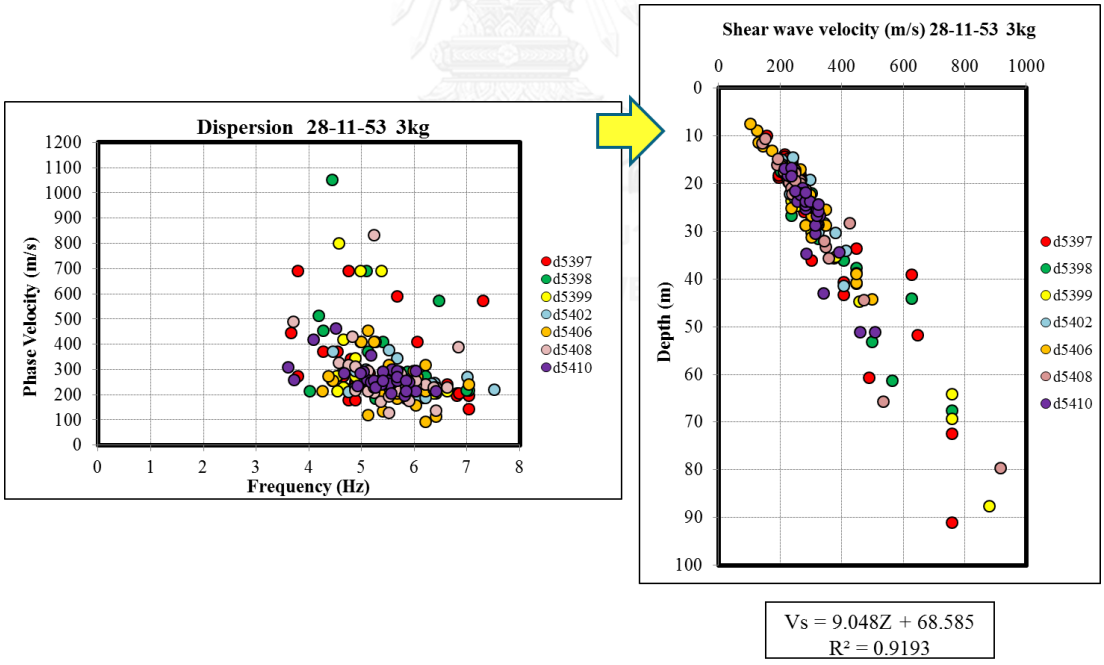

Figure 60 Shear wave velocity profile by SM at Mahasarakham

4.4.1.4 The Multichannel Analysis of Surface Wave Method (MASW)

The data obtained from measurements of the processed as described in Section 2.2.4.1 to established the relationship between the phase velocity with frequency (Dispersion Curve) as shown in this figure by the intensity of the color indicates the strength of the energy measurement (Image processing), and inversion to determine the shear wave velocity at the depth of the soil layer using the principles and theories. As discussed in Section 2.2.4.2.

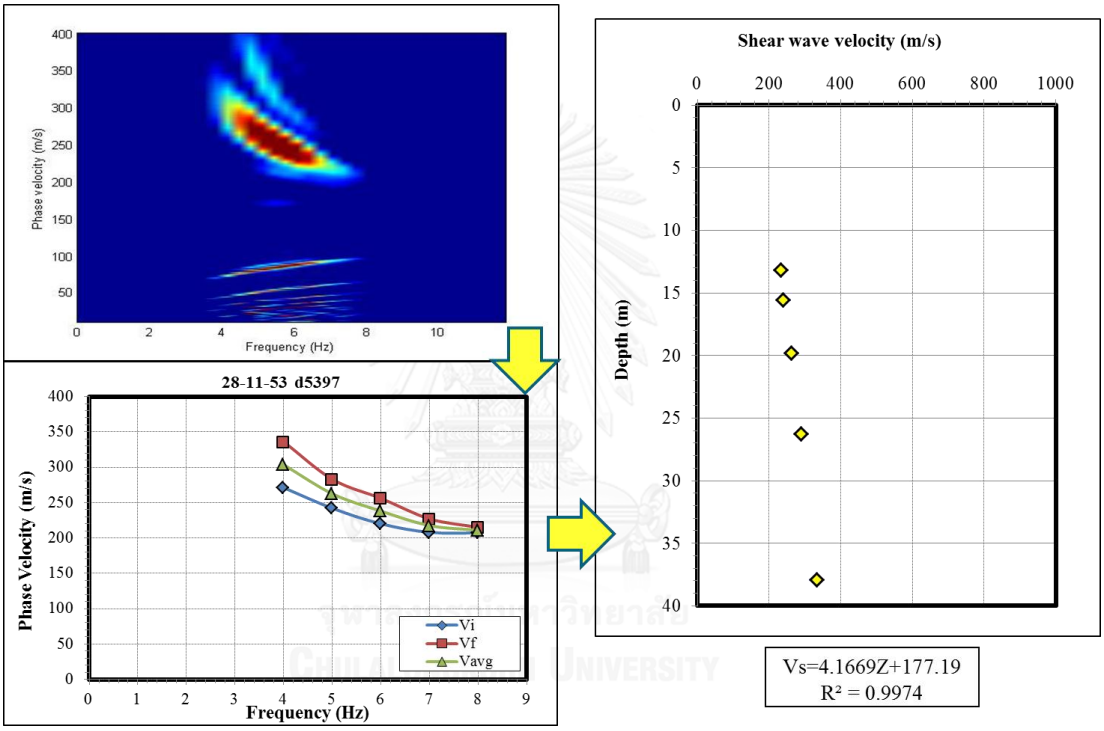

Figure 61 Shear wave velocity profile by MASW at Mahasarakham

4.4.1.5 Down-hole Seismic Method (DH)

The Vs can be calculated by Snell's Law Ray-Path Method in eq. (26), (27) and (28). The incidental angle (α_i) of the initial ray of a shear wave is randomly selected and used to compute the traveling time. Trial selection of is continued unless the computed travel time is equal to the recorded time. The calculation must be done sequentially from top to bottom of the borehole.

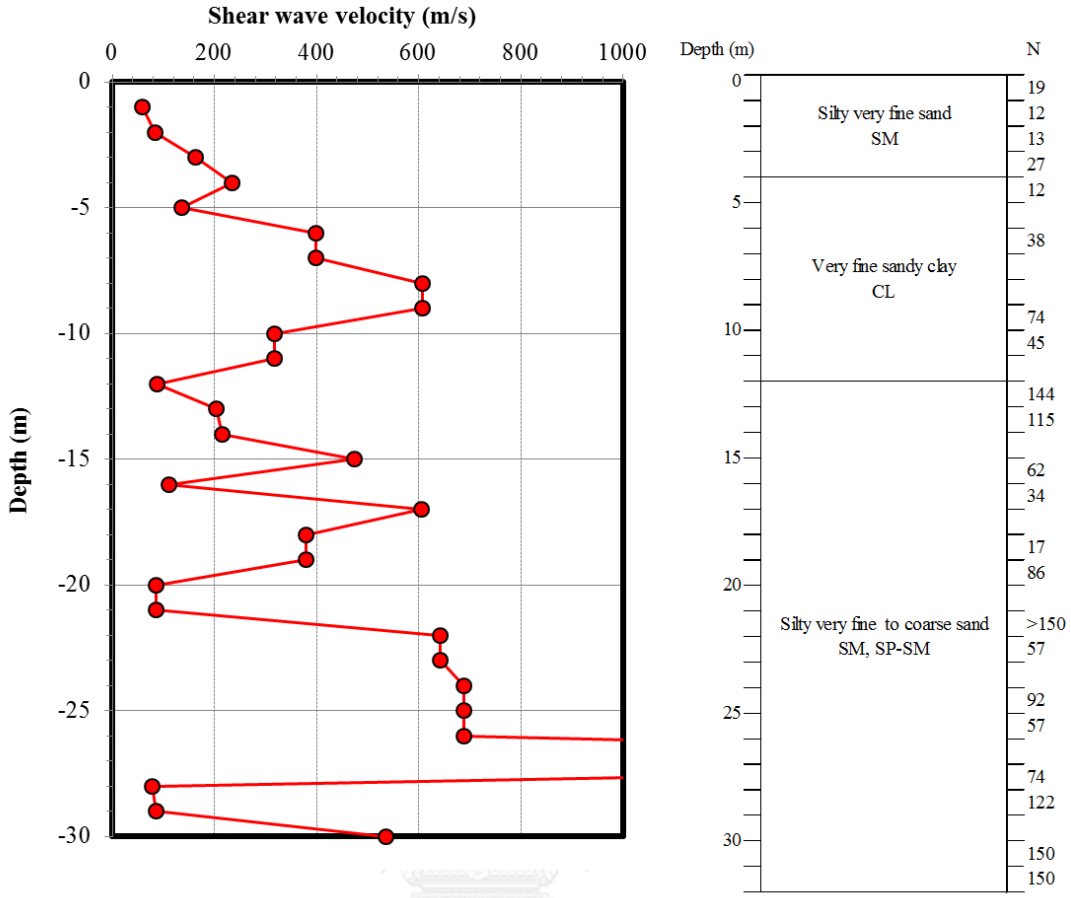

Figure 62 Shear wave velocity profile by DH at Mahasarakham

4.4.2 Estimation of shear wave velocity profile at Surin province

4.4.2.1 Refraction seismic survey

In this figure, the first arrival picks from the P-wave refraction survey shows one layer with a consistent P-wave velocity of 1,687.29 m/s. No second layer was found and it is postulated, due to the length of the line and weak energy source. With the absence of a second layer, the thickness of the initial layer cannot be calculated. Results from Refraction seismic survey, in this case velocity of the initial layer are used as input for the SM and MASW to drive inversion to more realistic results. From P-wave velocity can be classify as Wet sand, Dry sand or Wet sandy gravel (Table 2).

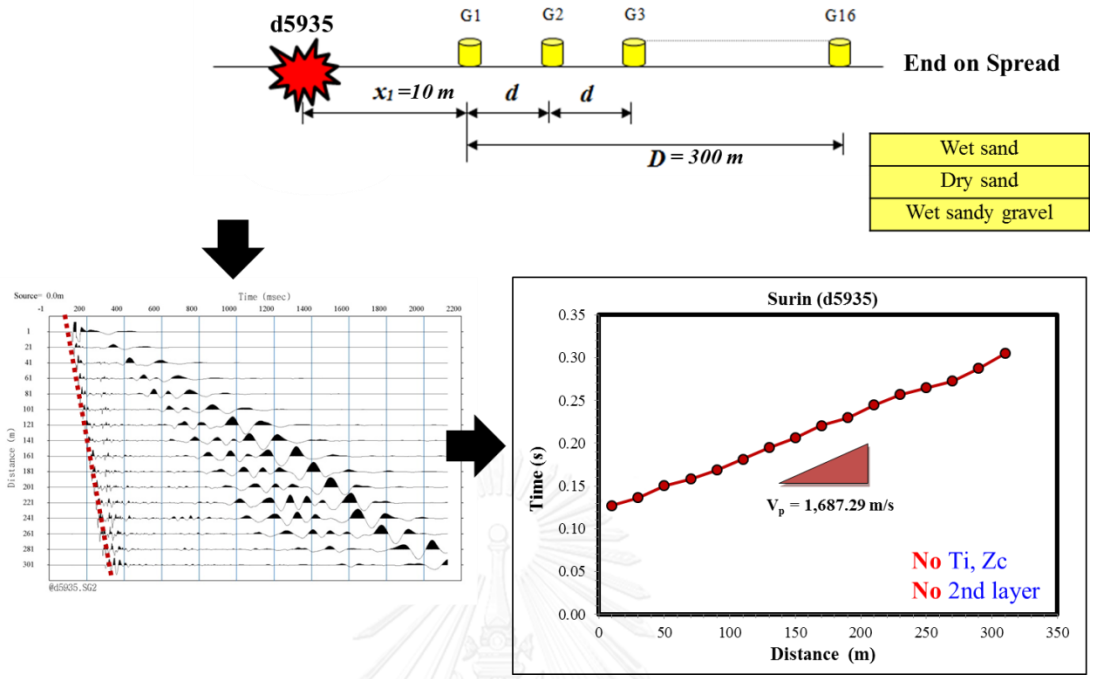

Figure 63 Data processing by Refraction seismic survey at Surin

4.4.2.2 Reflection seismic survey

This figure shown that the relation between square of time (t^2) and square of distance (x^2) is established a straight line with a slope ($1/V^2$) in term of y = mx + b, so we can find the P-wave velocity of soil-rock (1,148 m/s). If square of distance (x^2) is equal to zero, then t_0^2 and t_0 are equal to 22,407 and 149.169 ms, respectively. The depth of soil-rock can be calculated from eq. (15). From P-wave velocity equal to 1,148 can be classify as Wet sand, Dry sand, Wet sandy gravel, Dry sandy gravel, Wet clay or Dry clay (Table 2).

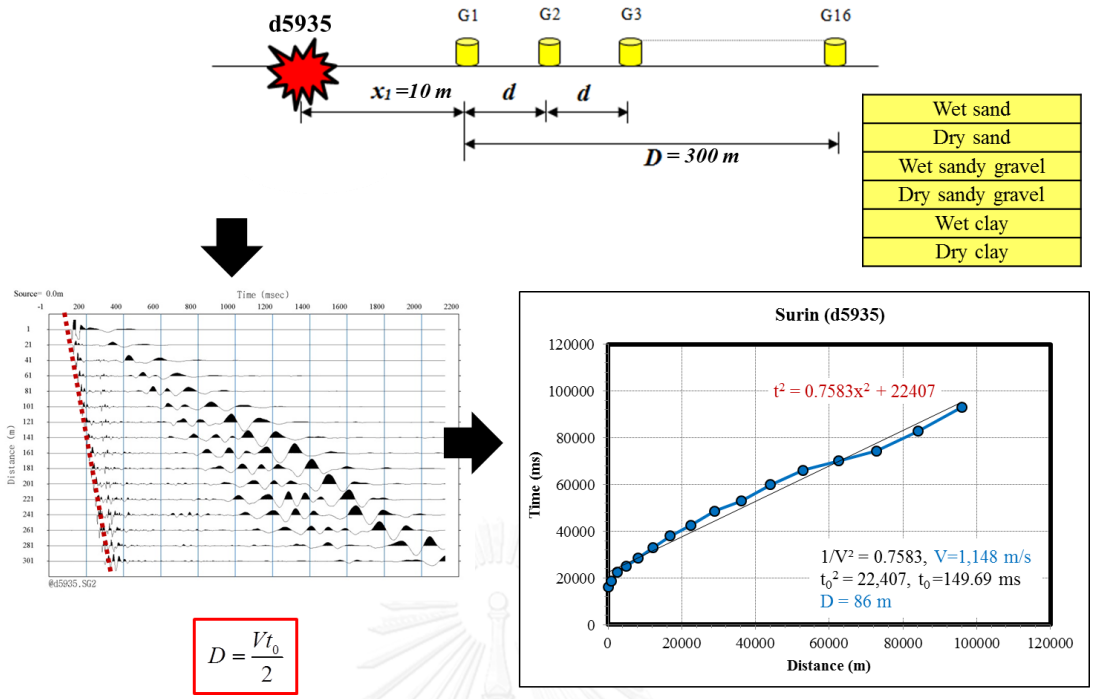

Figure 64 Data processing by Reflection seismic survey at Surin

4.4.2.3 The Simple Analysis of Surface Wave Method (SM)

The figure shows that the analysis of the data by procedure described in Section 2.2.3.1 to establish the relationship between the phase velocity with frequency (Dispersion Curve), and inversion to determine the shear wave velocity at the depth of the soil layer using the principles and theories in Section 2.2.4.2.

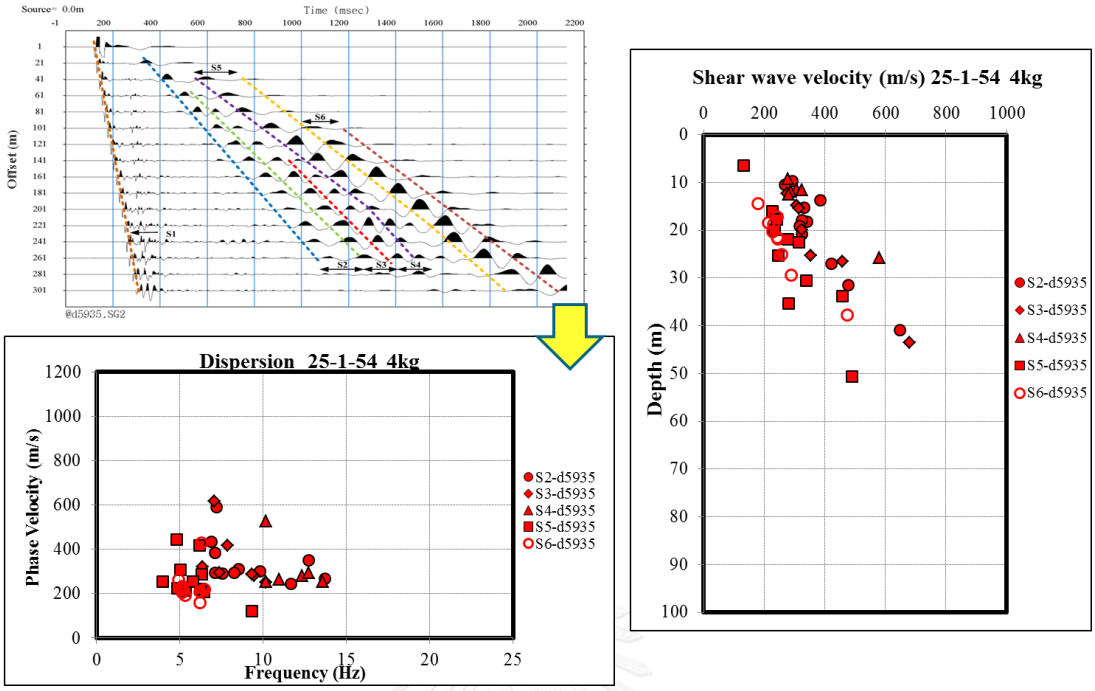

Figure 65 The SM data processing from field test (d5935)

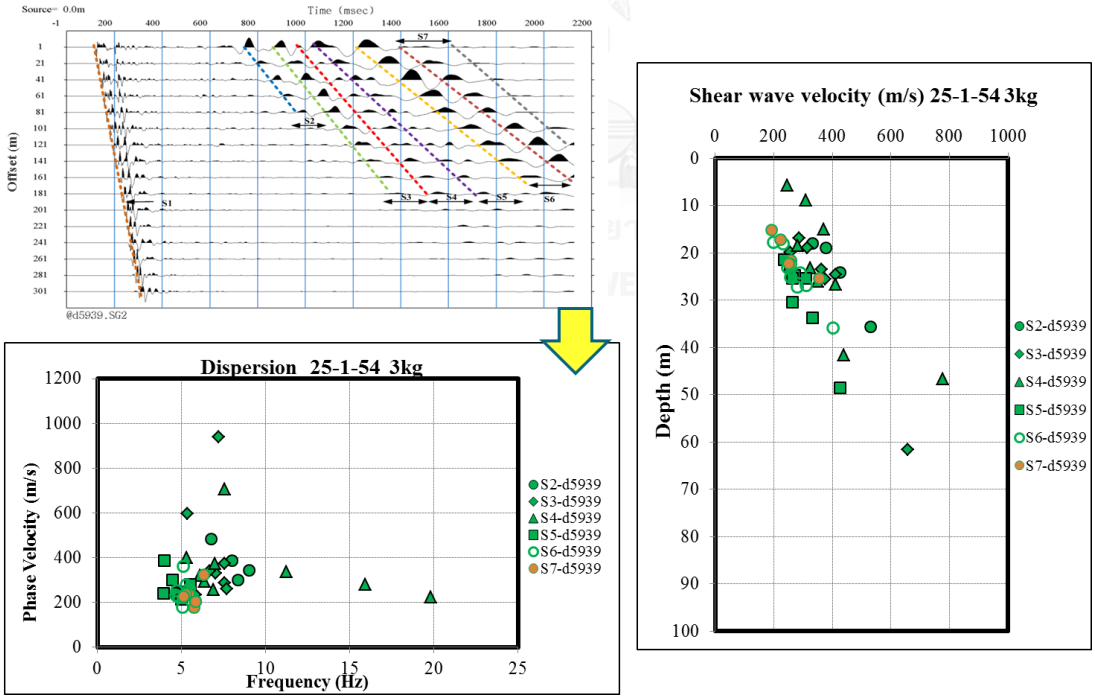

Figure 66 The SM data processing from field test (d5939)

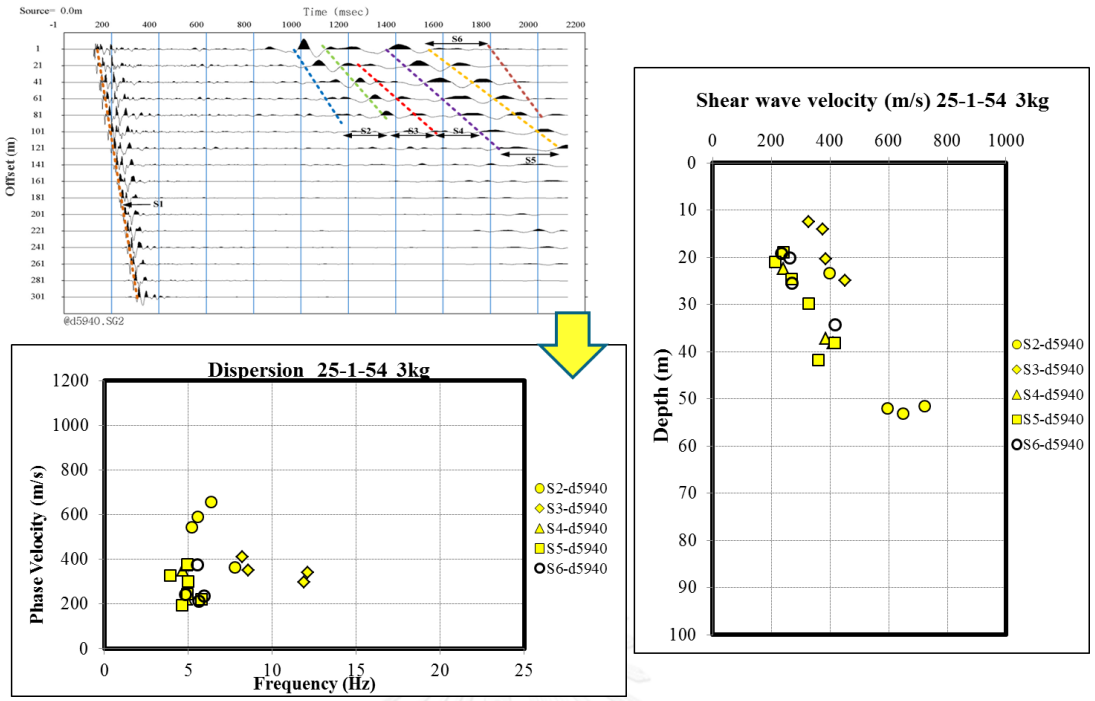

Figure 67 The SM data processing from field test (d5940)

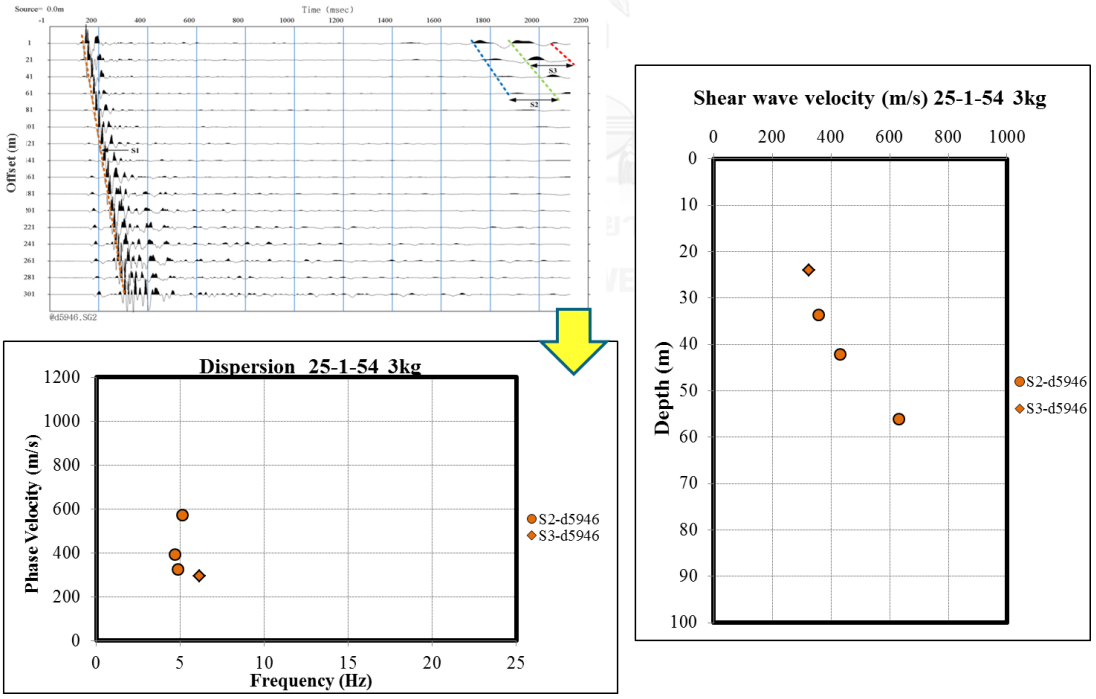

Figure 68 The SM data processing from field test (d5946)

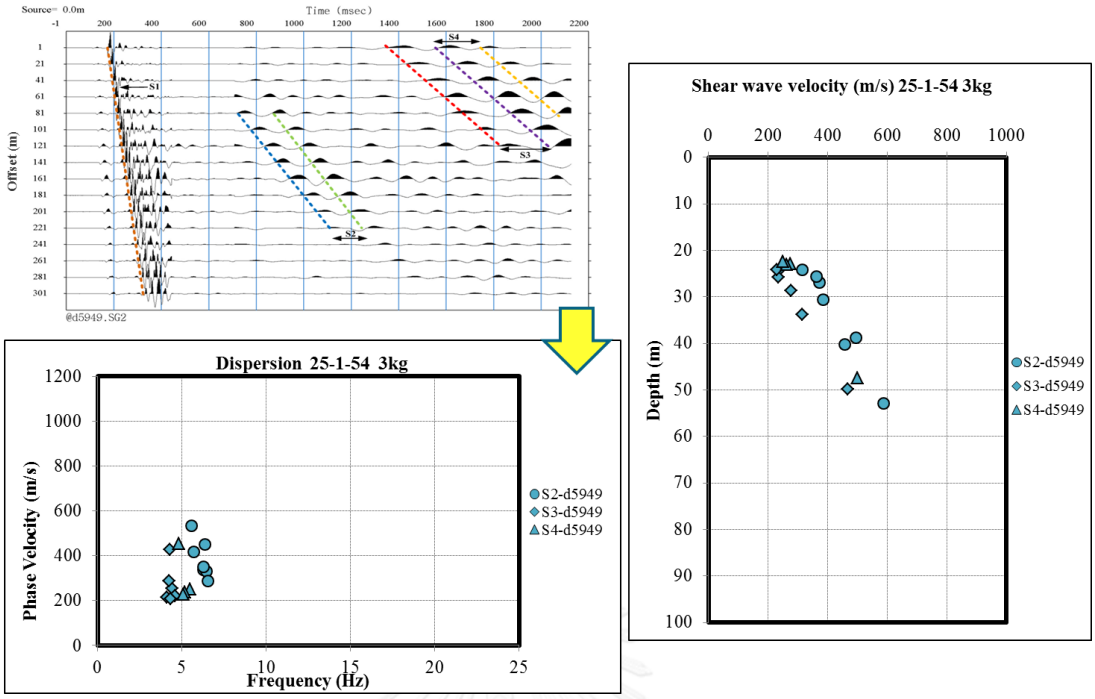

Figure 69 The SM data processing from field test (d5949)

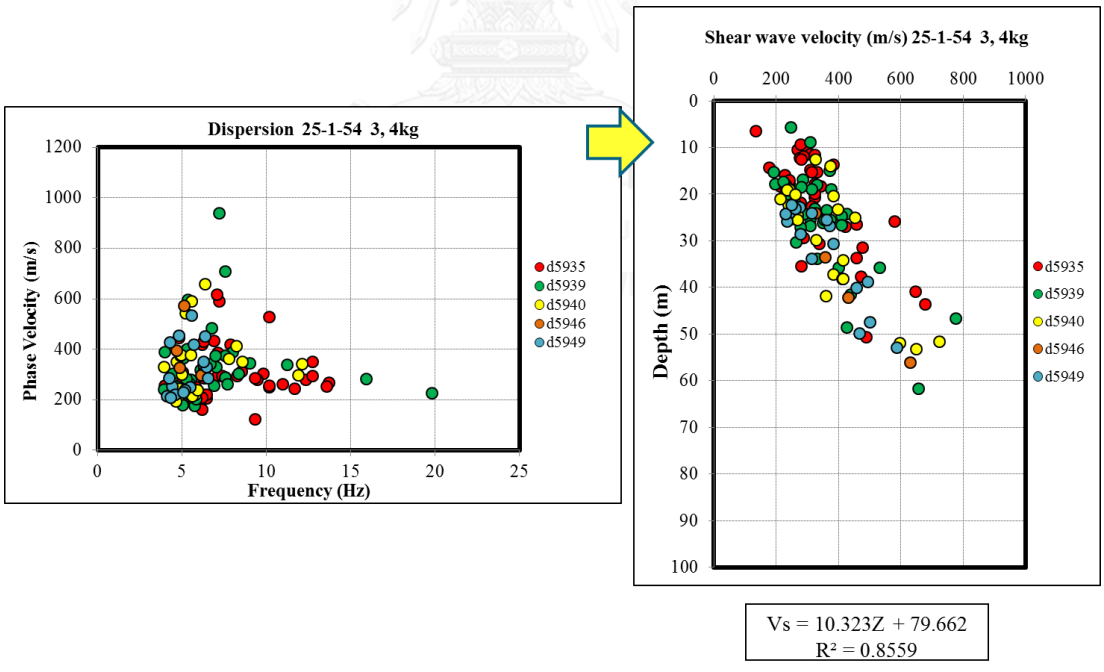

Figure 70 Shear wave velocity profile by SM at Surin

4.4.2.4 The Multichannel Analysis of Surface Wave Method (MASW)

The data obtained from measurements of the processed as described in Section 2.2.4.1 to established the relationship between the phase velocity with frequency (Dispersion Curve) as shown in this figure by the intensity of the color indicates the strength of the energy measurement (Image processing), and inversion to determine the shear wave velocity at the depth of the soil layer using the principles and theories. As discussed in Section 2.2.4.2.

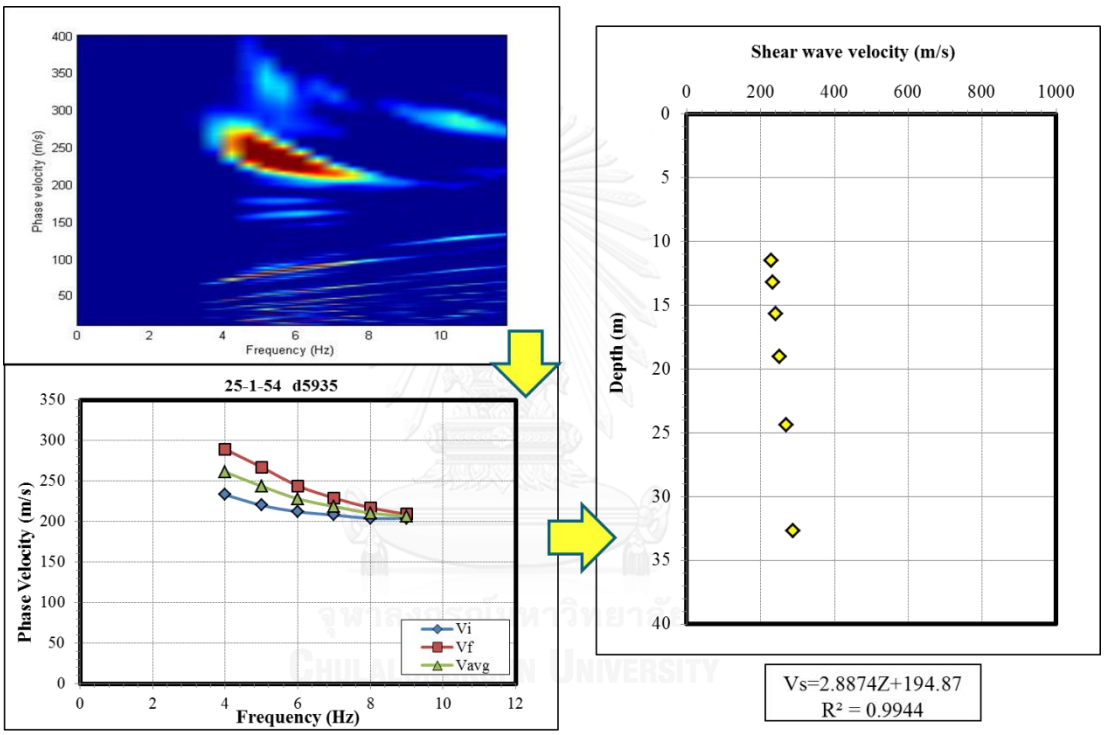

Figure 71 Shear wave velocity profile by MASW at Surin

4.4.2.5 Down-hole Seismic Method (DH)

The Vs can be calculated by Snell's Law Ray-Path Method in eq. (26), (27) and (28). The incidental angle (α_i) of the initial ray of a shear wave is randomly selected and used to compute the traveling time. Trial selection of is continued unless the computed travel time is equal to the recorded time. The calculation must be done sequentially from top to bottom of the borehole.

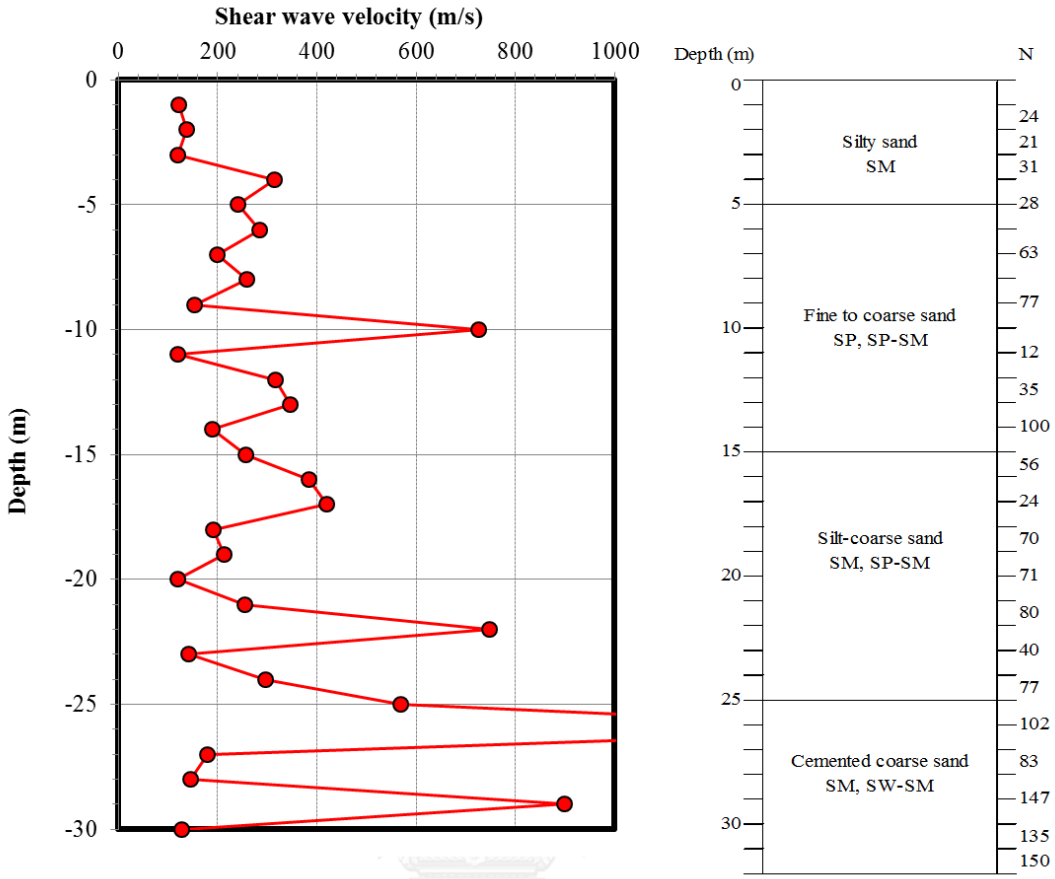

Figure 72 Shear wave velocity profile by DH at Surin

4.4.3 Estimation of shear wave velocity profile at Udonthani province

4.4.3.1 Refraction seismic survey

In this figure, the first arrival picks from the P-wave refraction survey shows one layer with a consistent P-wave velocity of 4,470.43 m/s. No second layer was found and it is postulated, due to the length of the line and weak energy source. With the absence of a second layer, the thickness of the initial layer cannot be calculated. Results from Refraction seismic survey, in this case velocity of the initial layer are used as input for the SM and MASW survey to drive inversion to more realistic results. From P-wave velocity can be classify as Granite, Gneiss, Andesite, Rhyolite, Marble, Limestone or Salt (Table 2).

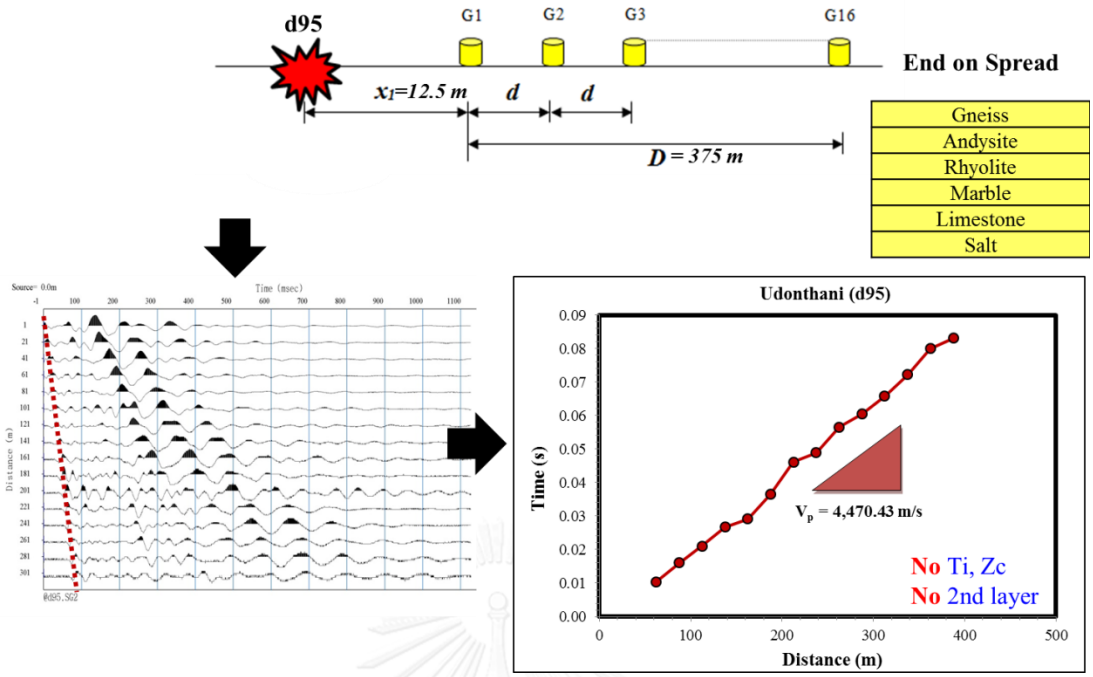

Figure 73 Data processing by Refraction seismic survey at Udonthani

4.4.3.2 Reflection seismic survey

This figure shows that the relation between square of time (t^2) and square of distance (x^2) is establish a straight line with a slope ($1/V^2$) in term of y = mx + b, so we can find the P-wave velocity of soil-rock (4,569 m/s). If square of distance (x^2) is equal to zero, then t_0^2 and t_0 are equal to 202.82 and 14.24 ms, respectively. The depth of soil-rock can be calculated from eq. (15). From P-wave velocity equal to 4,569 can be classify as Granite, Gneiss, Andesite, Rhyolite, Marble, Limestone or Salt (Table 2).

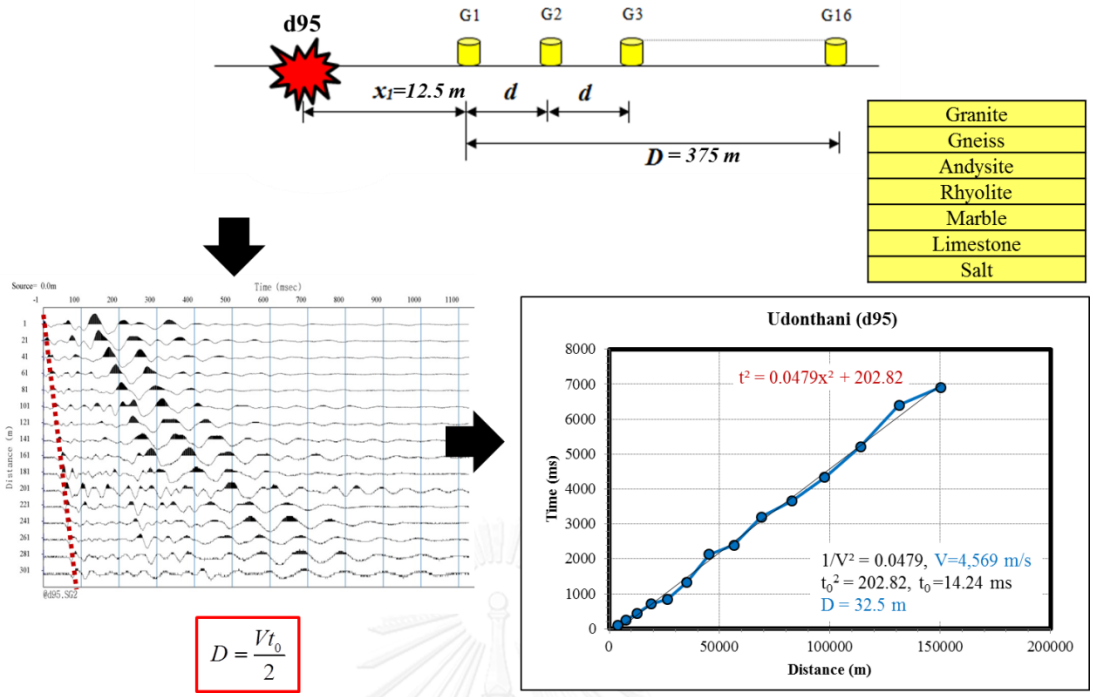

Figure 74 Data processing by Reflection seismic survey at Udonthani

4.4.3.3 The Simple Analysis of Surface Wave Method (SM)

The figure shows that the analysis of the data by procedure described in Section 2.2.3.1 to establish the relationship between the phase velocity with frequency (Dispersion Curve), and inversion to determine the shear wave velocity at the depth of the soil layer using the principles and theories in Section 2.2.4.2.

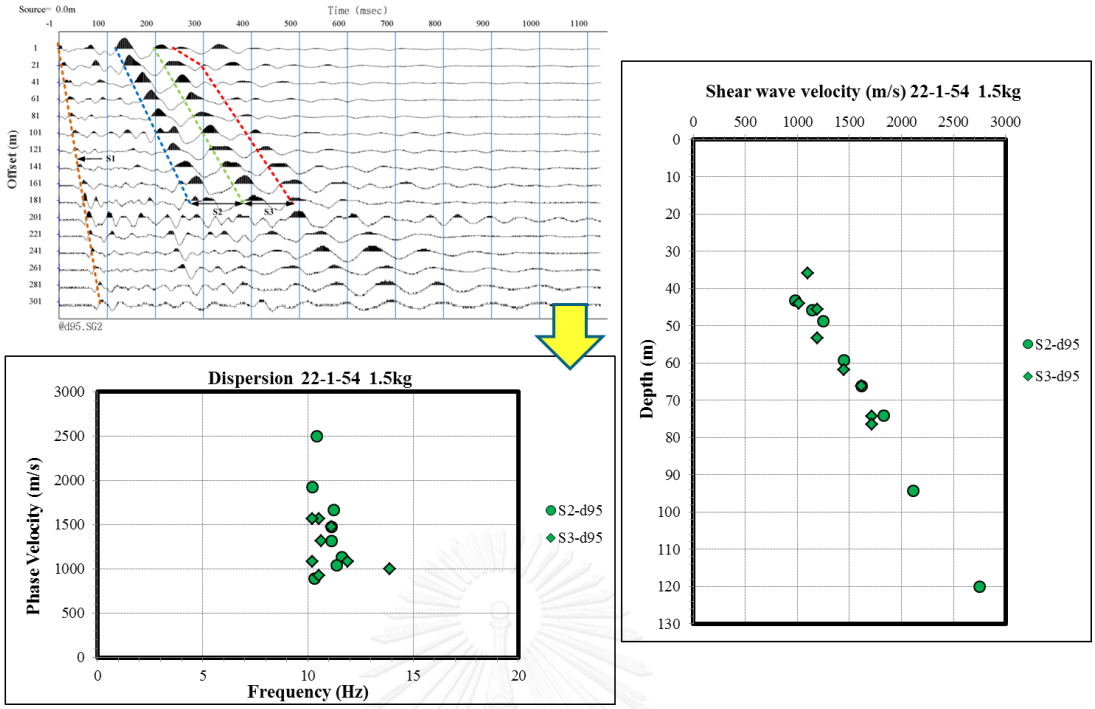

Figure 75 The SM data processing from field test (d95)

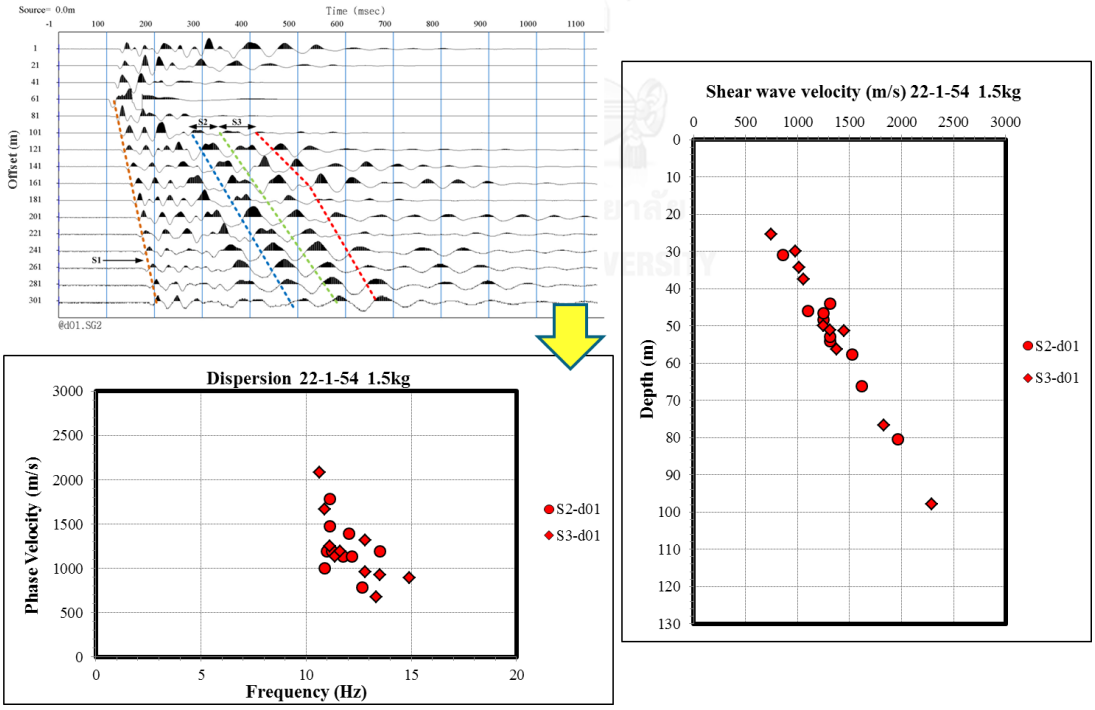

Figure 76 The SM data processing from field test (d01)

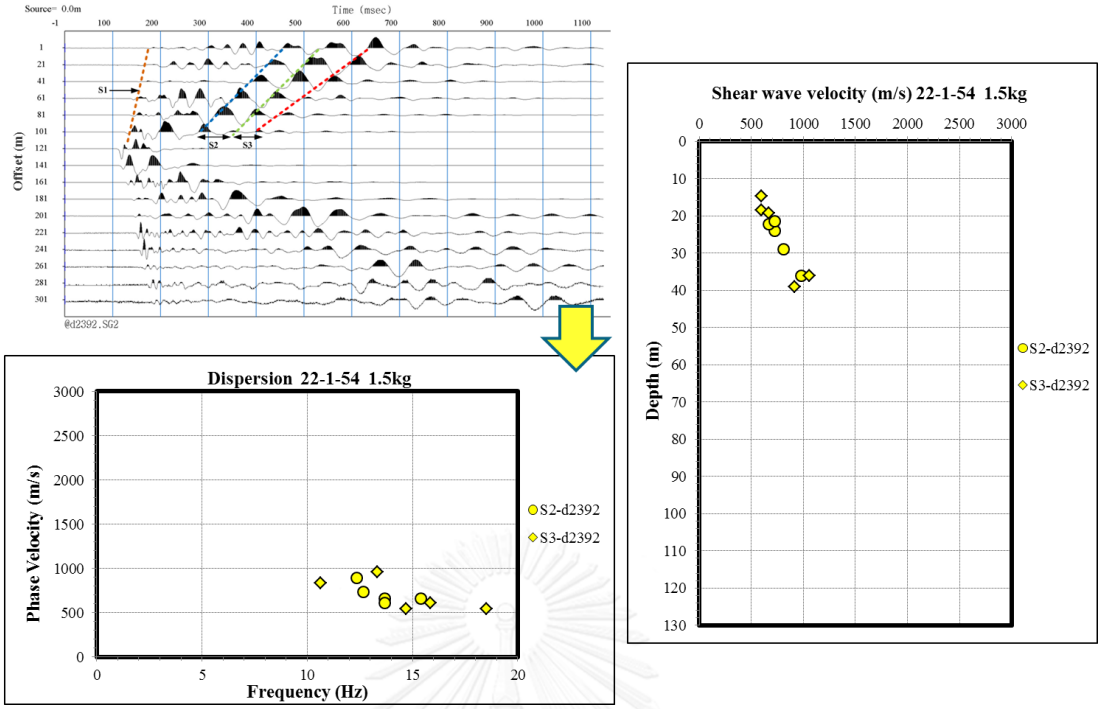

Figure 77 The SM data processing from field test (d2392)

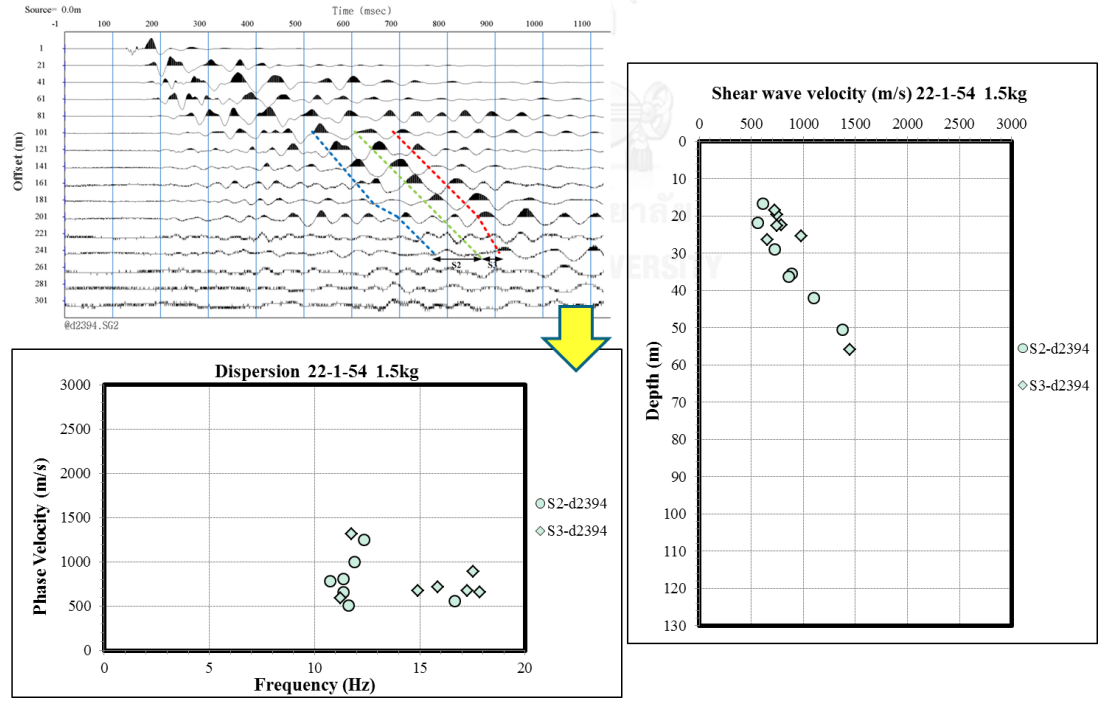

Figure 78 The SM data processing from field test (d2394)

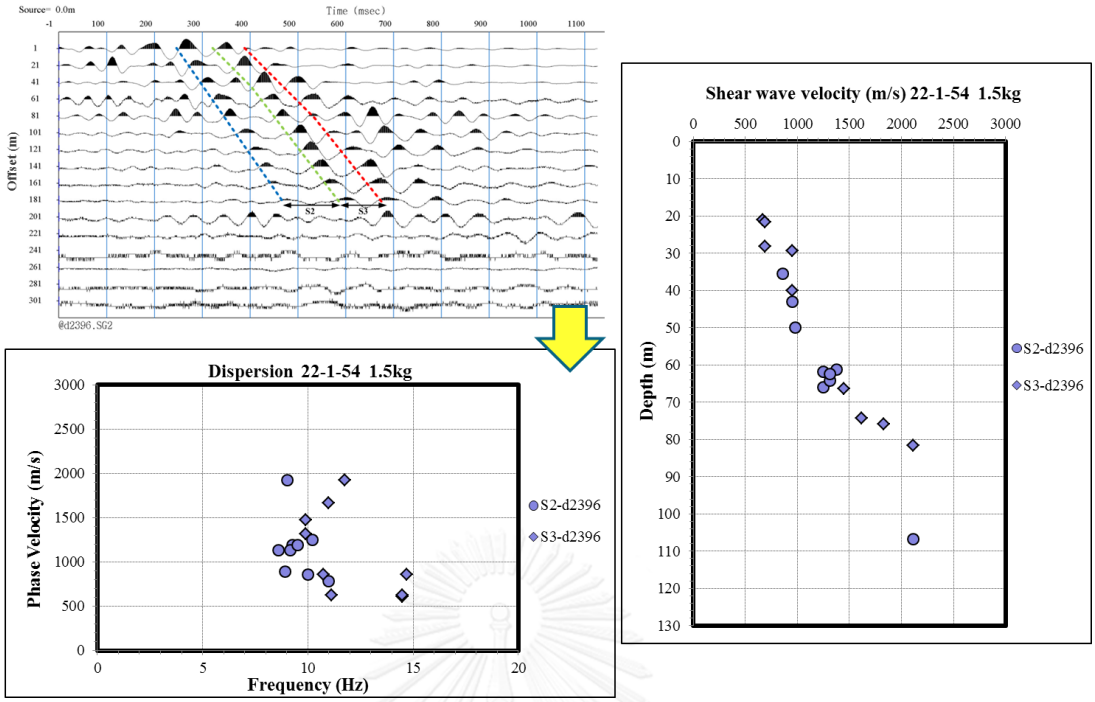

Figure 79 The SM data processing from field test (d2396)

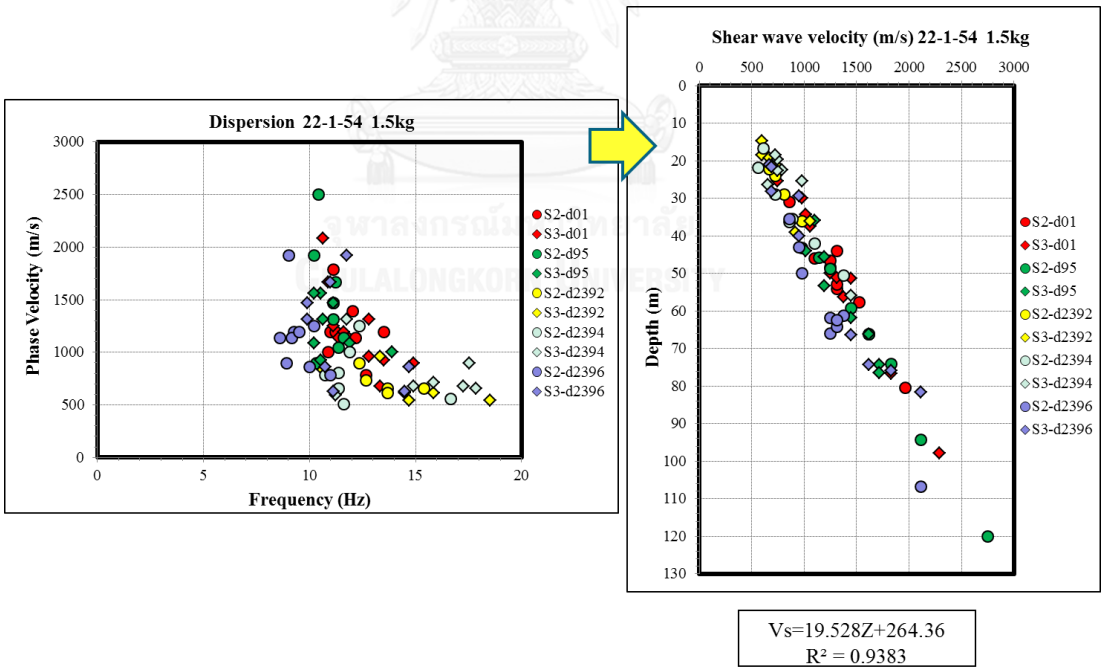

Figure 80 Shear wave velocity profile by SM at Udonthani

4.4.3.4 The Multichannel Analysis of Surface Wave Method (MASW)

The data obtained from measurements of the processed as described in Section 2.2.4.1 to established the relationship between the phase velocity with frequency (Dispersion Curve) as shown in this figure by the intensity of the color indicates the strength of the energy measurement (Image processing), and inversion to determine the shear wave velocity at the depth of the soil layer using the principles and theories. As discussed in Section 2.2.4.2.

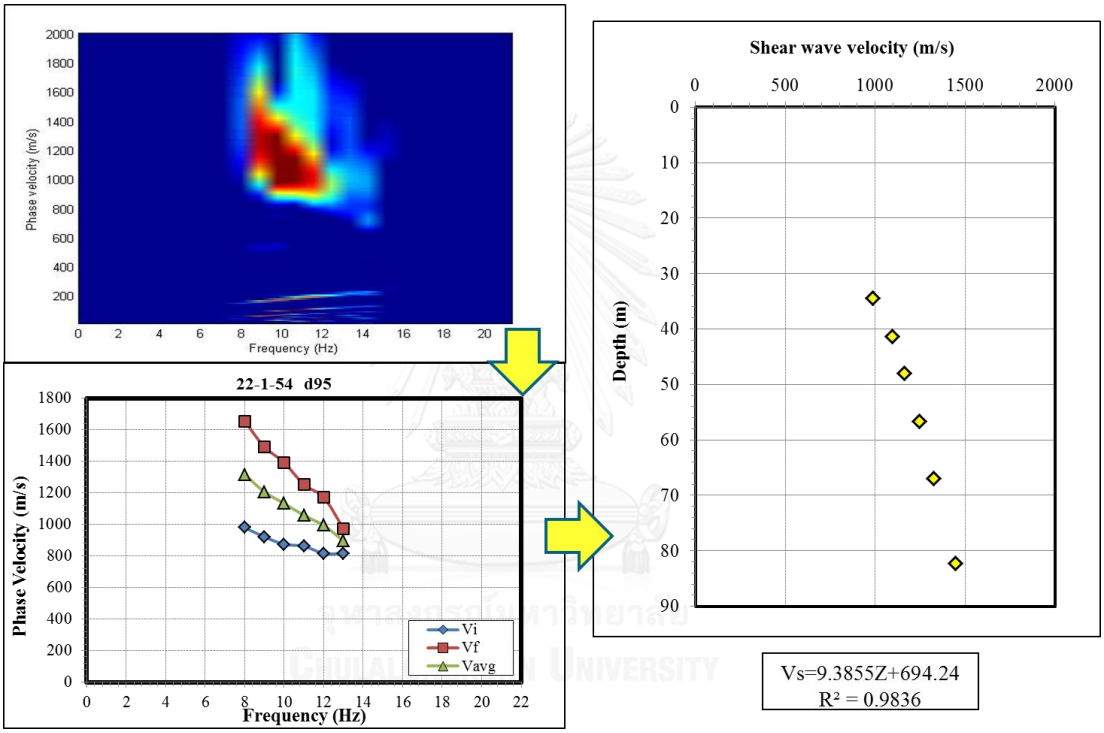

Figure 81 Shear wave velocity profile by MASW at Udonthani

4.4.3.5 Down-hole Seismic Method (DH)

The Vs can be calculated by Snell's Law Ray-Path Method in eq. (26), (27) and (28). The incidental angle (α_i) of the initial ray of a shear wave is randomly selected and used to compute the traveling time. Trial selection of is continued unless the computed travel time is equal to the recorded time. The calculation must be done sequentially from top to bottom of the borehole.

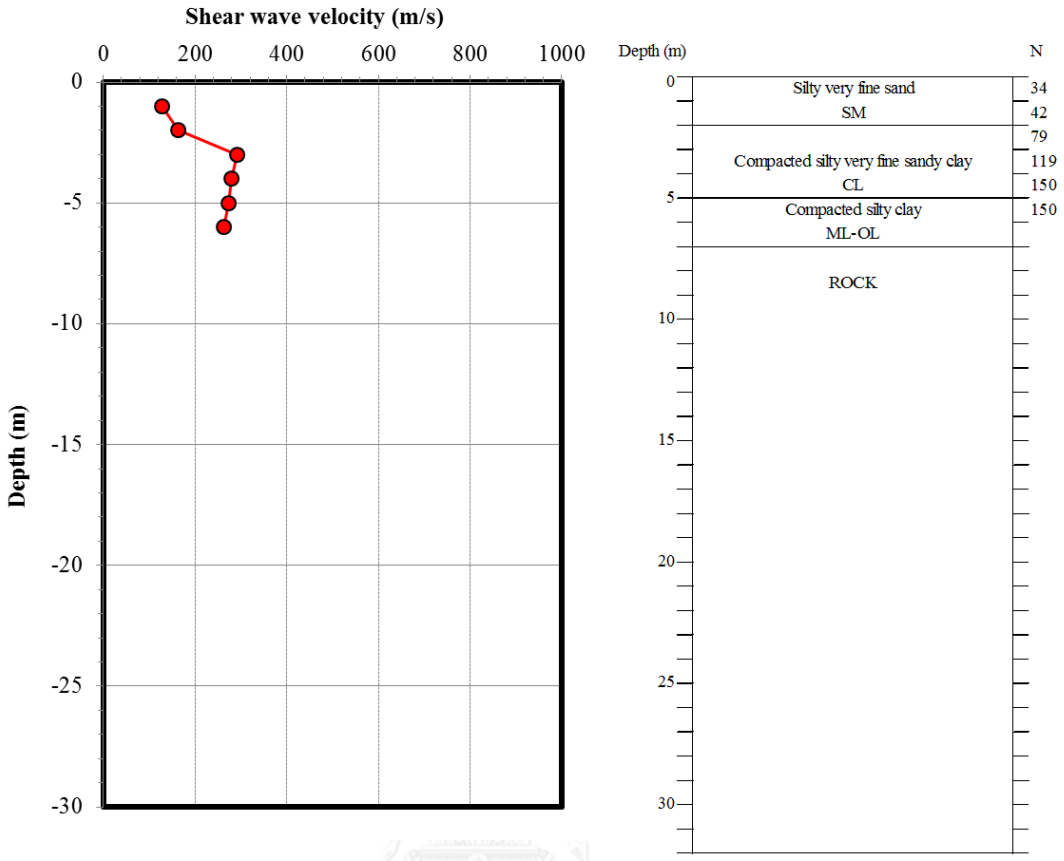

Figure 82 Shear wave velocity profile by DH at Udonthani

จุฬาลงกรณ์มหาวิทยาลัย
Chulalongkorn University

4.4.4 Estimation of shear wave velocity profile at Suphanburi province

4.4.4.1 Refraction seismic survey

In this figure, the first arrival picks from the P-wave refraction survey shows one layer with a consistent P-wave velocity of 1,874.94 m/s. No second layer was found and it is postulated, due to the length of the line and weak energy source. With the absence of a second layer, the thickness of the initial layer cannot be calculated. Results from Refraction seismic survey, in this case velocity of the initial layer are used as input for the SM and MASW survey to drive inversion to more realistic results. From P-wave velocity can be classify as Wet sand, Dry sand, Wet sandy gravel, Wet clay or Shale (Table 2).

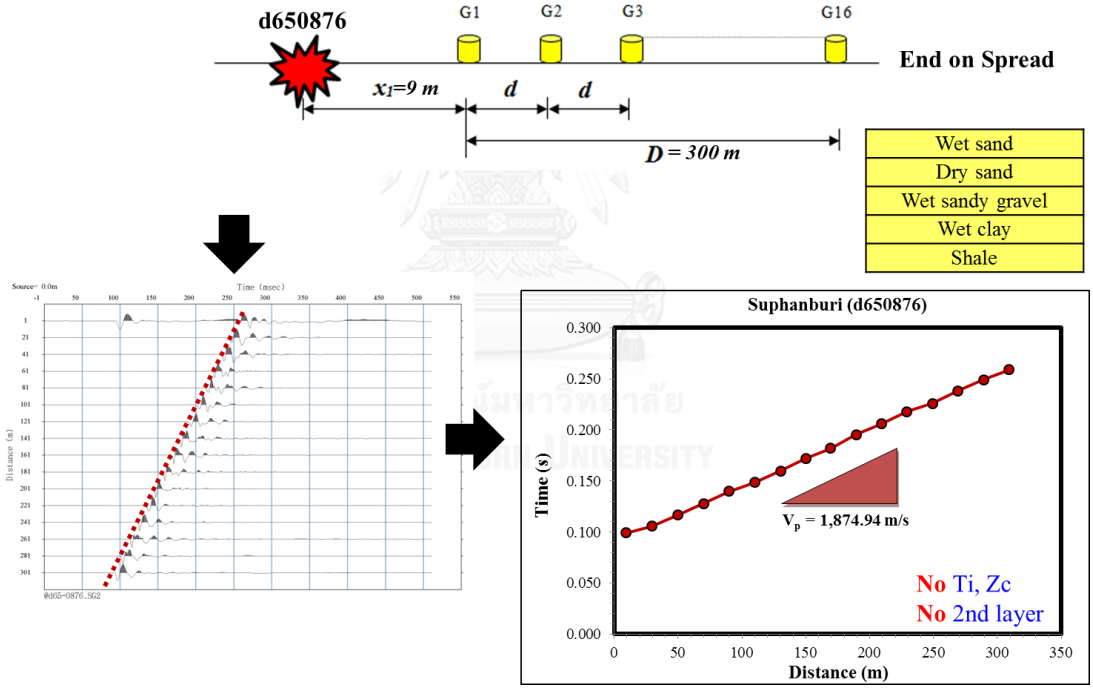

Figure 83 Data processing by Refraction seismic survey at Suphanburi

4.4.4.2 Reflection seismic survey

This figure shows that the relation between square of time (t^2) and square of distance (x^2) is established a straight line with a slope ($1/V^2$) in term of $y = mx + b$, so we can find the P-wave velocity of soil-rock (1,299 m/s). If square of distance (x^2) is

equal to zero, then t_0^2 and t_0 are equal to 14,013 and 118.38 ms, respectively. The depth of soil-rock can be calculated from eq. (15). From P-wave velocity equal to 1,202 can be classify as Wet sand, Dry sand, Wet sandy gravel, Dry sandy gravel, Wet clay or Dry clay (Table 2).

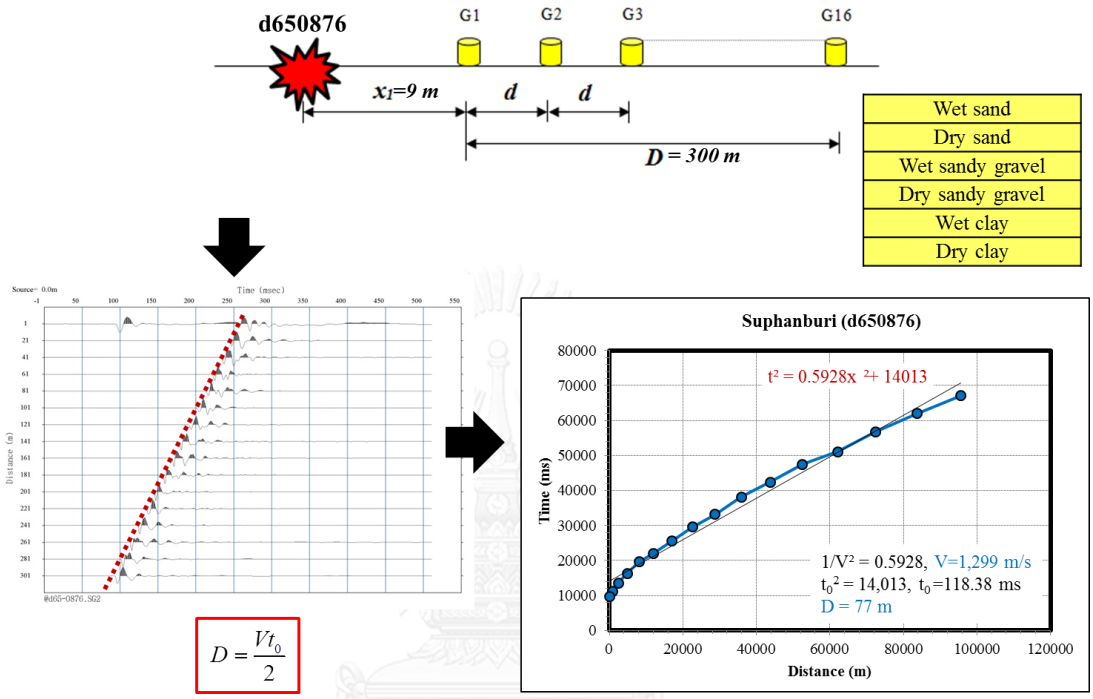

Figure 84 Data processing by Reflection seismic survey at Suphanburi

4.4.4.3 The Simple Analysis of Surface Wave Method (SM)

The figure shows that the analysis of the data by procedure described in Section 2.2.3.1 to establish the relationship between the phase velocity with frequency (Dispersion Curve), and should be inversion to determine only primary wave velocity at the depth of the soil layer using the principles and theories in Section 2.2.4.2.

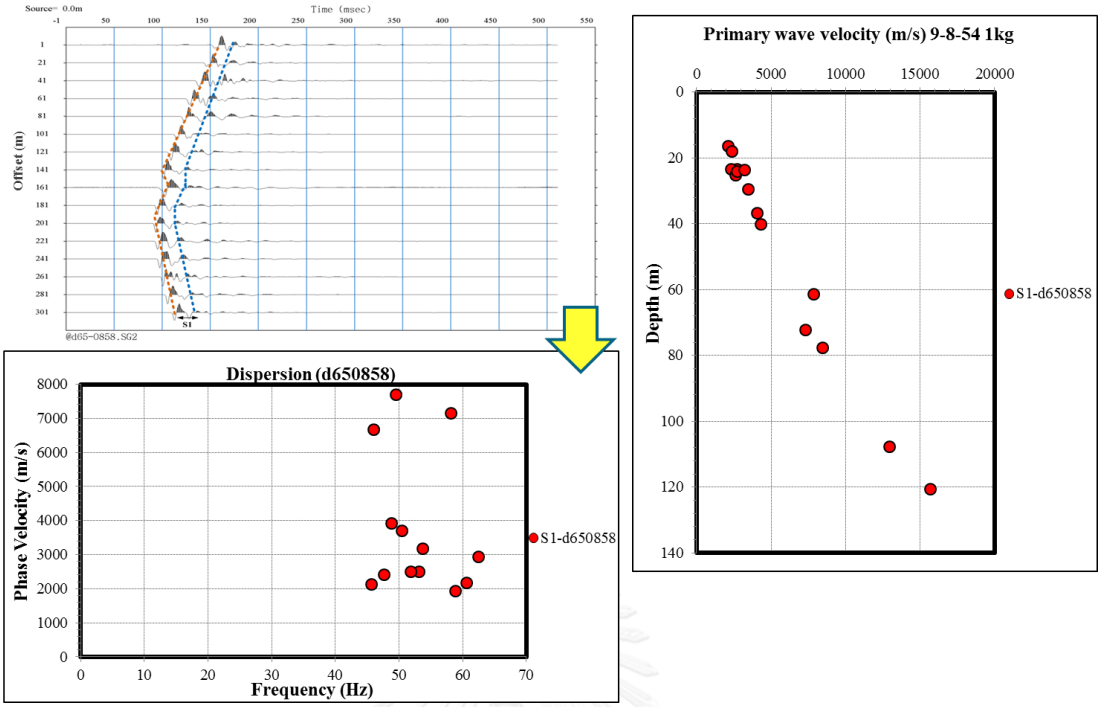

Figure 85 The SM data processing from field test (d650858)

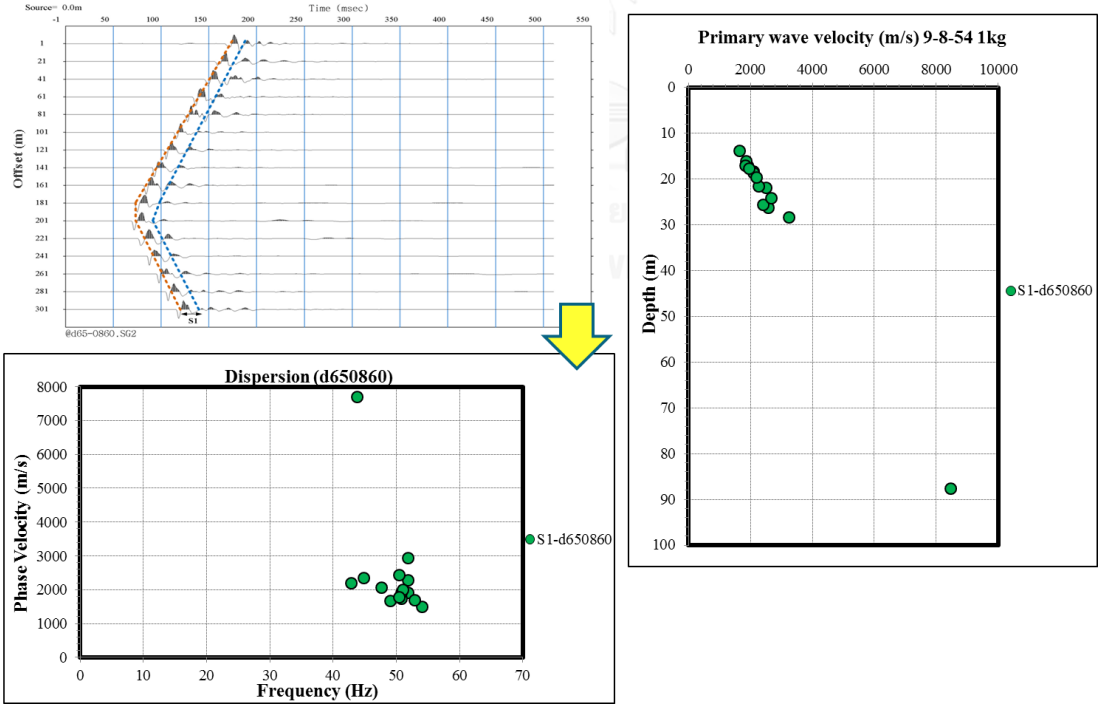

Figure 86 The SM data processing from field test (d650860)

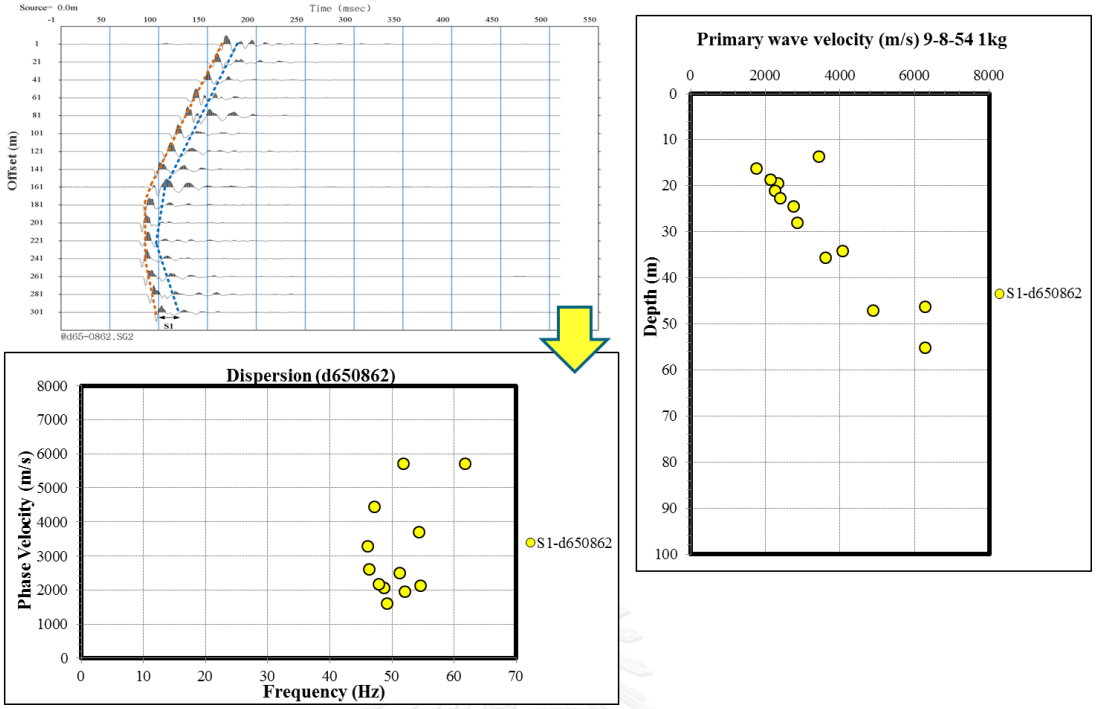

Figure 87 The SM data processing from field test (d650862)

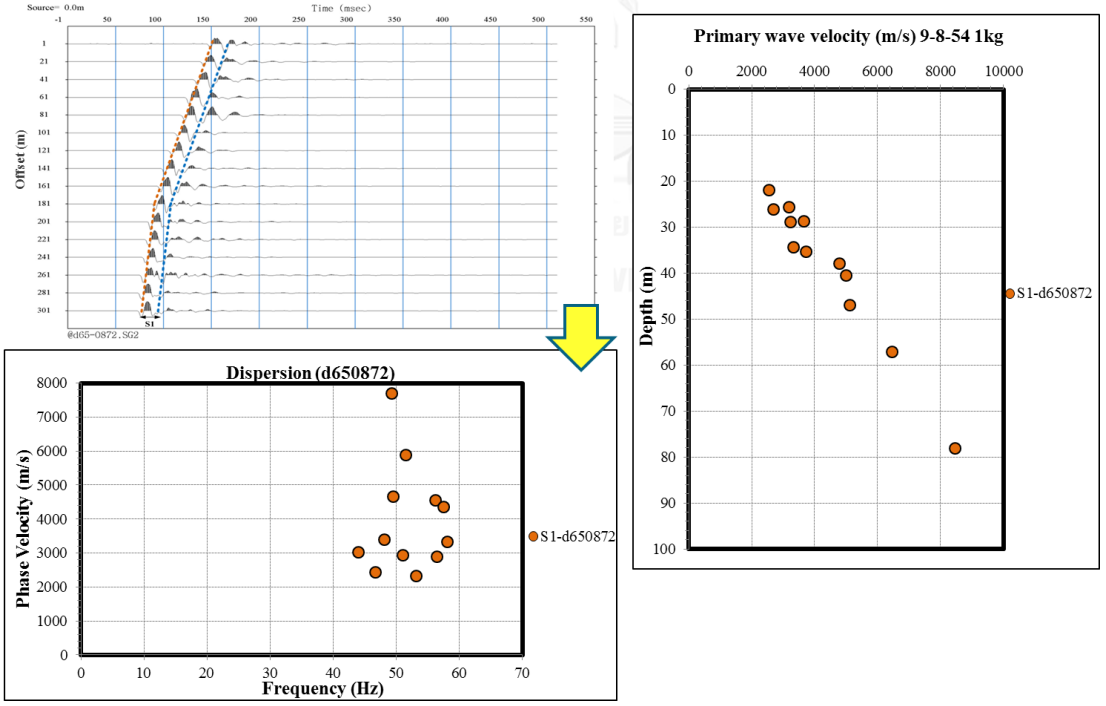

Figure 88 The SM data processing from field test (d650872)

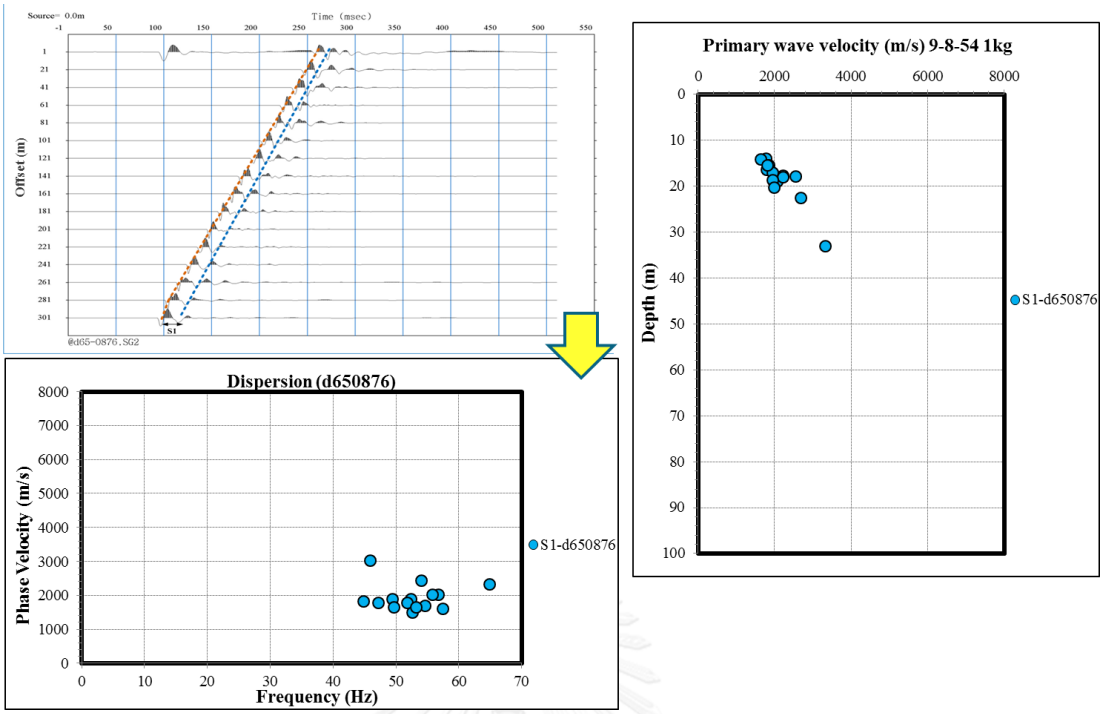

Figure 89 The SM data processing from field test (d650876)

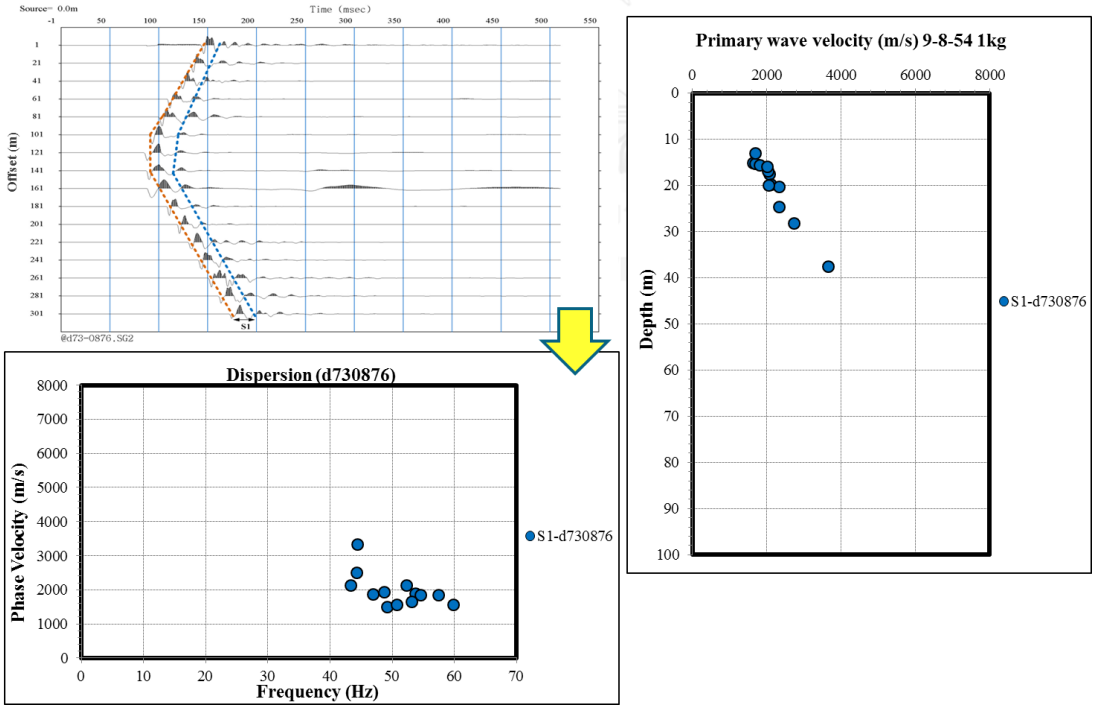

Figure 90 The SM data processing from field test (d730876)

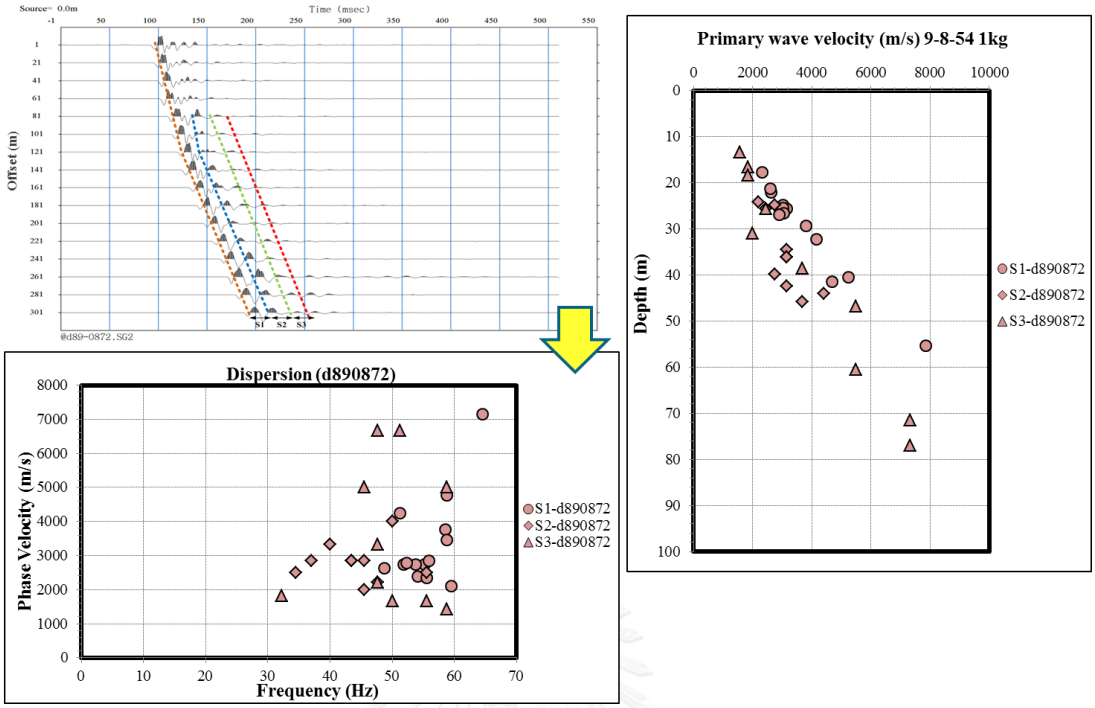

Figure 91 The SM data processing from field test (d890872)

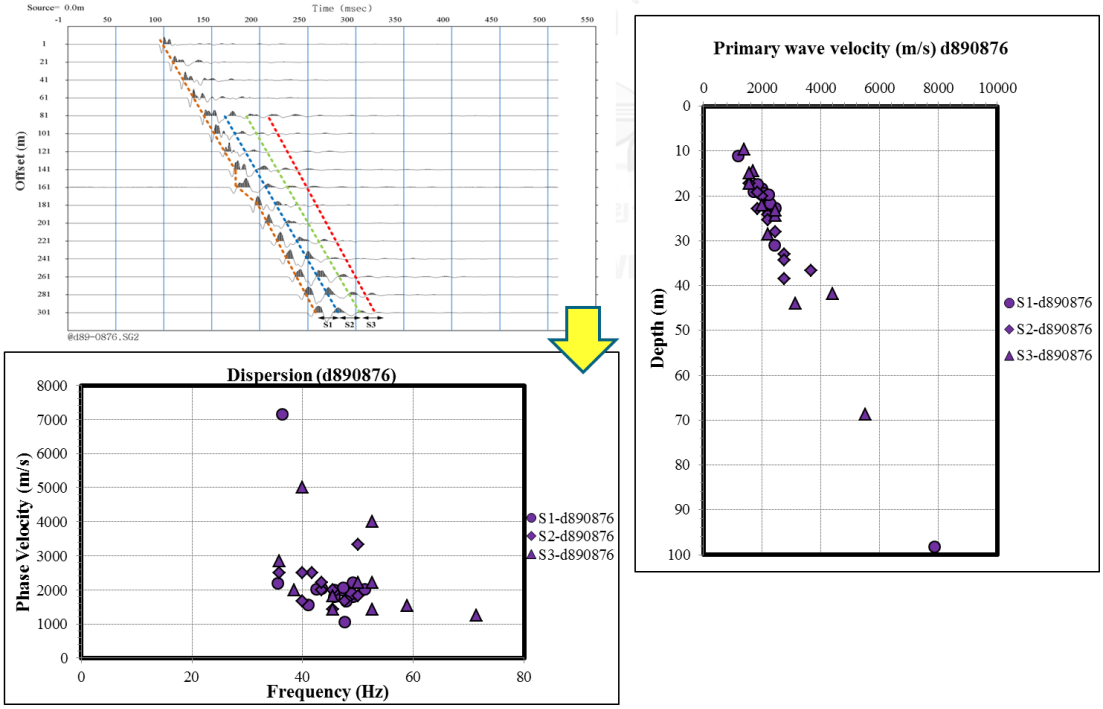

Figure 92 The SM data processing from field test (d890876)

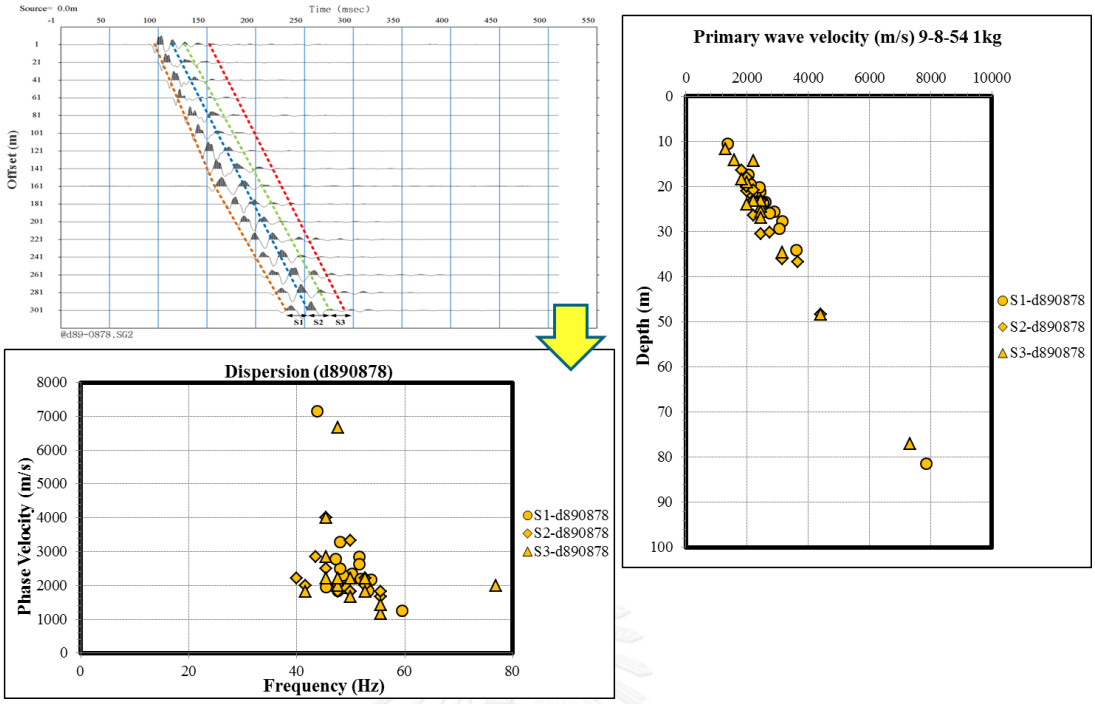

Figure 93 The SM data processing from field test (d890878)

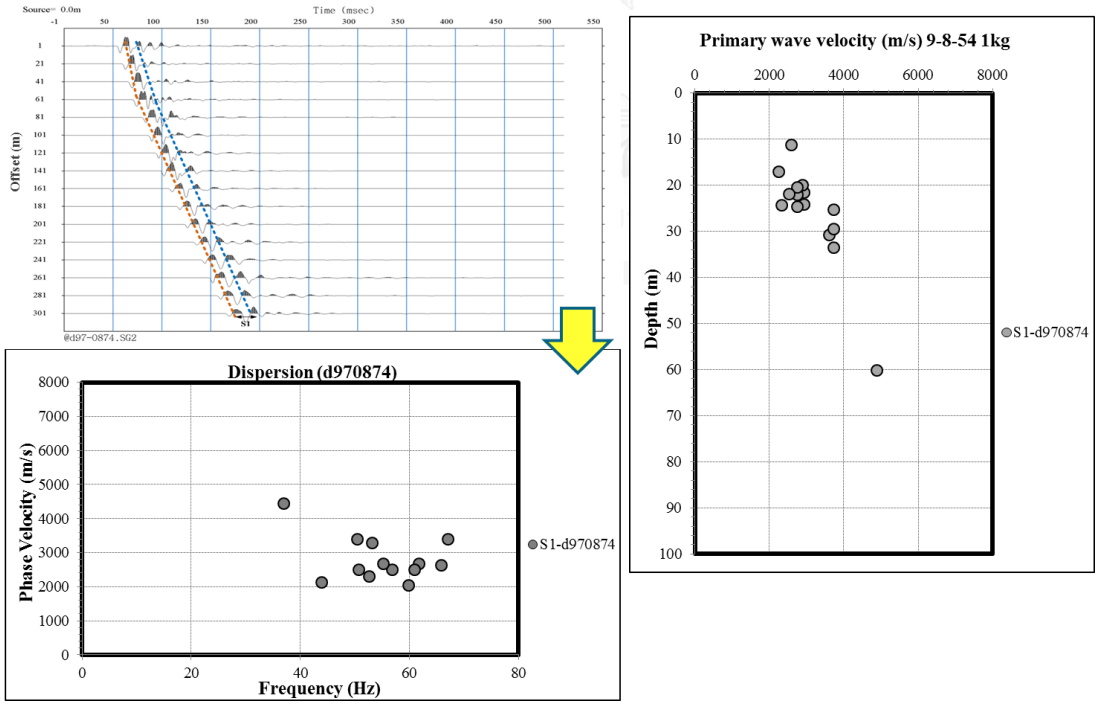

Figure 94 The SM data processing from field test (d970874)

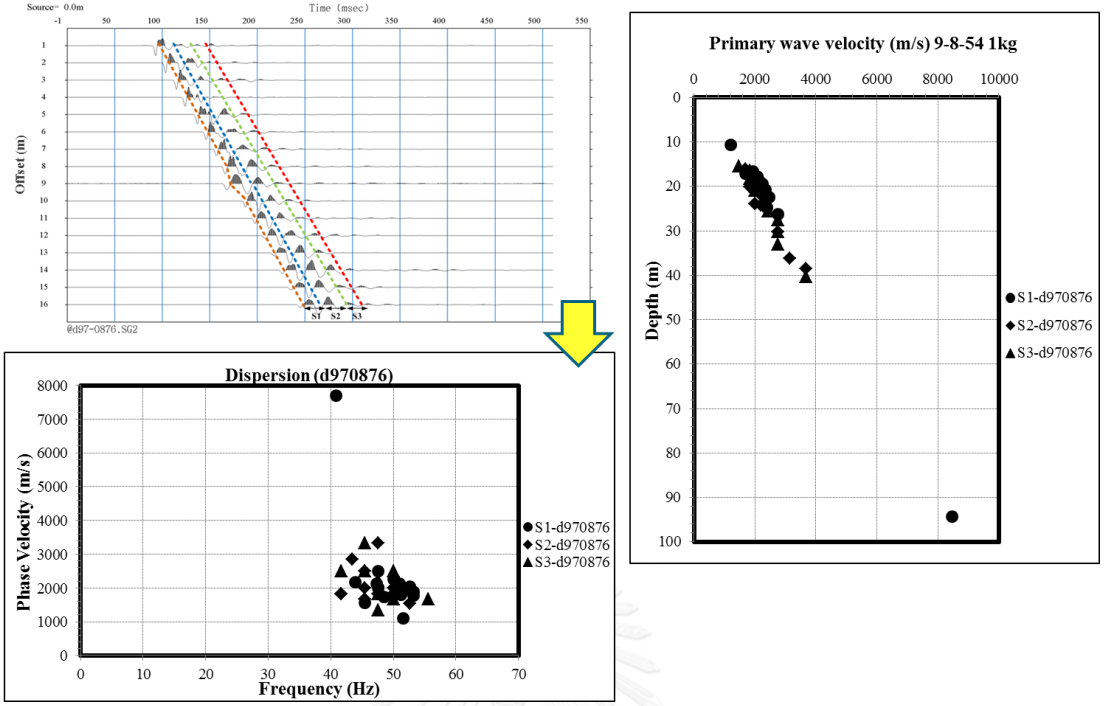

Figure 95 The SM data processing from field test (d970876)

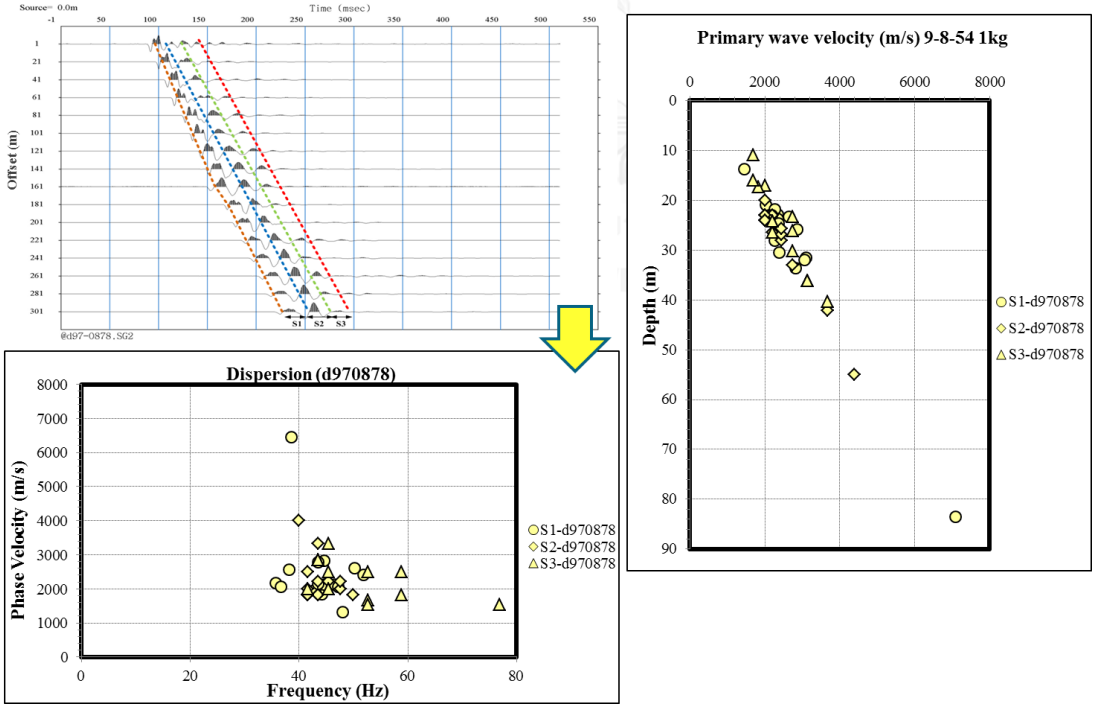

Figure 96 The SM data processing from field test (d970878)

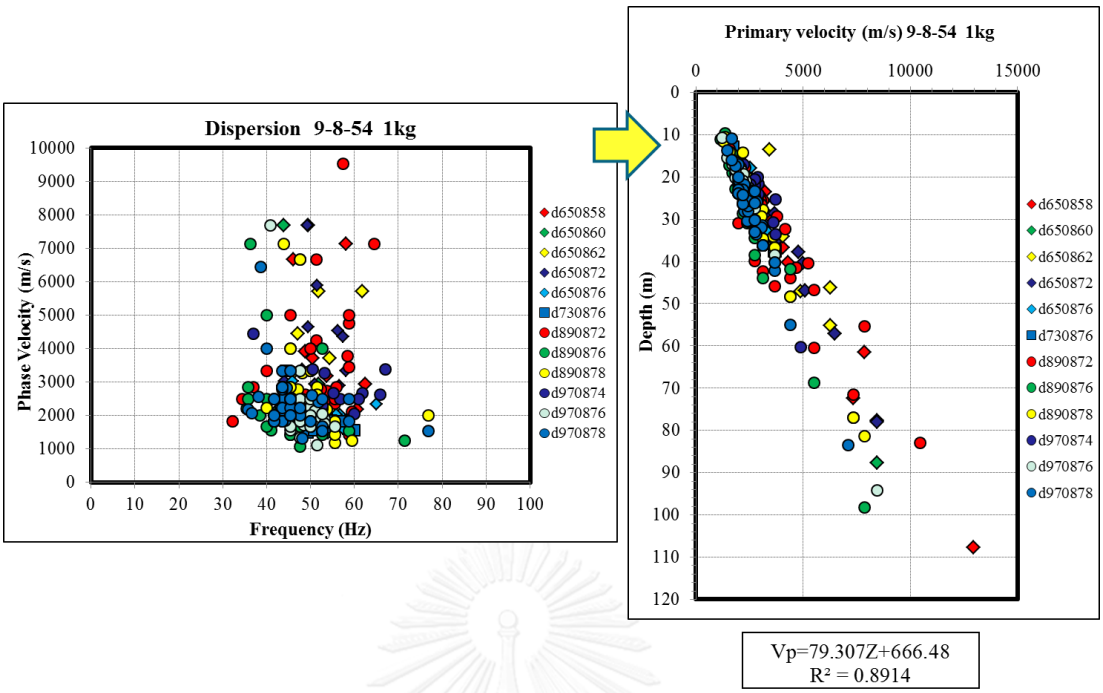

Figure 97 Primary wave velocity profile by SM at Suphanburi

4.4.4.4 The Multichannel Analysis of Surface Wave Method (MASW)

The data obtained from measurements of the processed as described in Section 2.2.4.1 to establish the relationship between the phase velocity with frequency (Dispersion Curve) as shown in this figure by the intensity of the color indicates the strength of the energy measurement (Image processing), and inversion to determine only primary wave velocity of the soil.

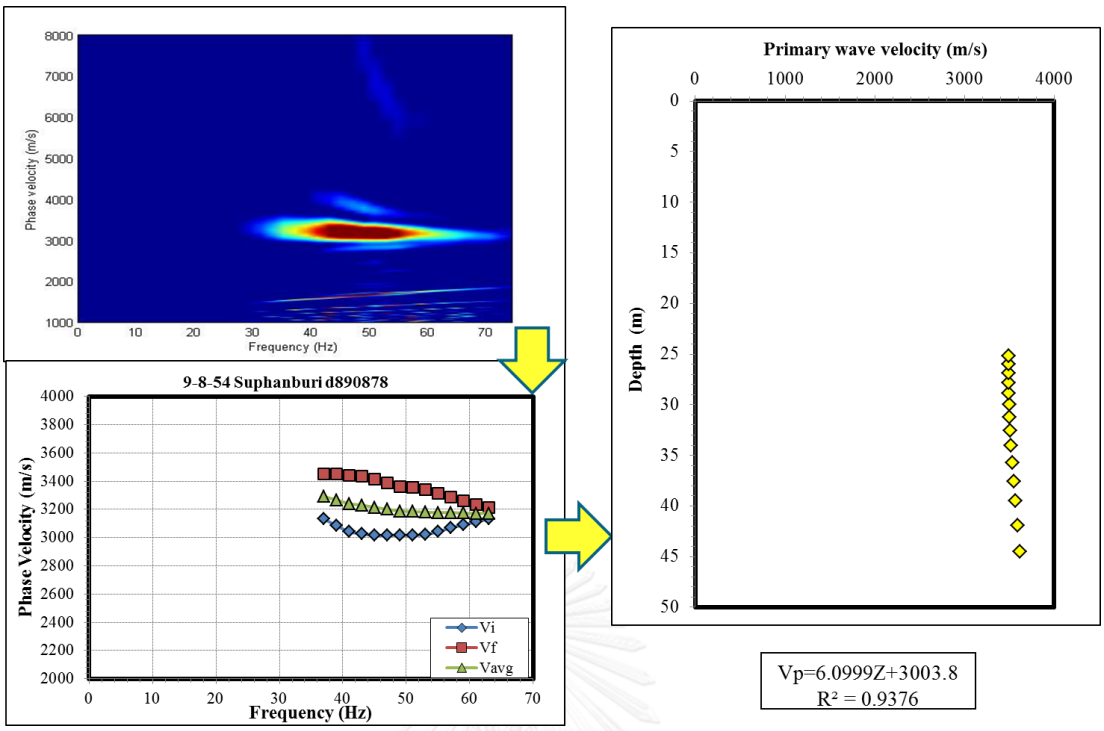

Figure 98 Primary wave velocity profile by MASW at Suphanburi

4.4.5 Estimation of shear wave velocity profile at Suratthani province

4.4.5.1 Refraction seismic survey

In this figure, the first arrival picks from the P-wave refraction survey shows one layer with a consistent P-wave velocity of 1,904.76 m/s. No second layer was found and it is postulated, due to the length of the line and weak energy source. With the absence of a second layer, the thickness of the initial layer cannot be calculated. Results from Refraction seismic survey, in this case velocity of the initial layer are used as input for the SM and MASW survey to drive inversion to more realistic results. From P-wave velocity can be classify as Sandstone, Shale or Wet sand (Table 2).

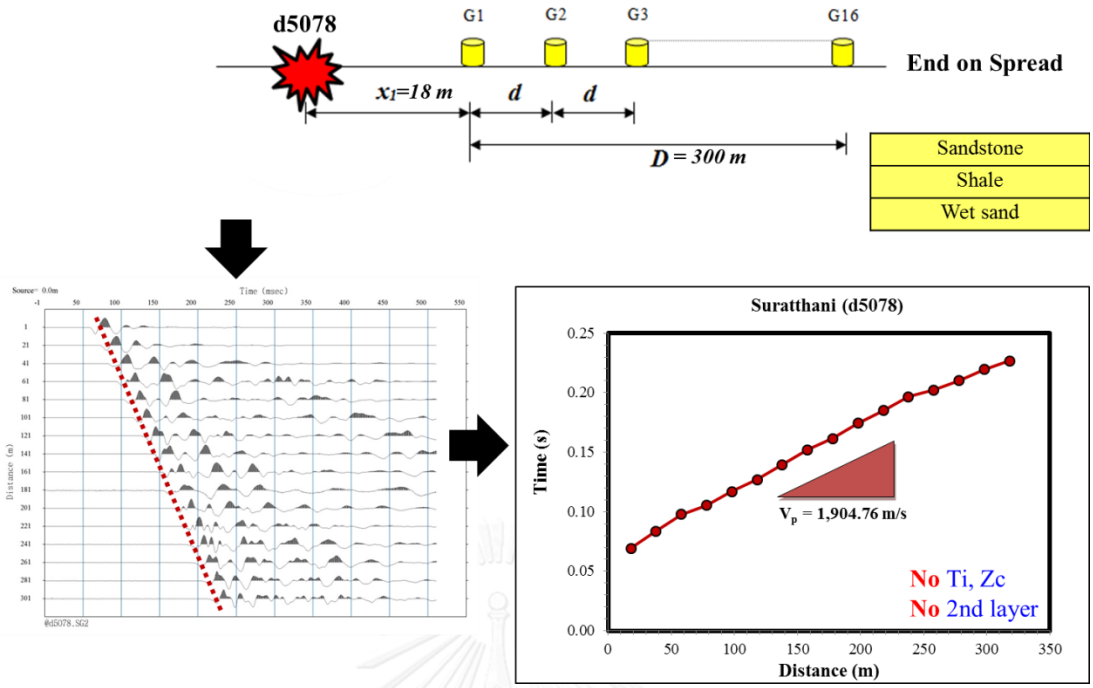

Figure 99 Data processing by Refraction seismic survey at Suratthani

4.4.5.2 Reflection seismic survey

This figure shows that the relation between square of time (t^2) and square of distance (x^2) establishes a straight line with a slope ($1/V^2$) in term of y = mx + b, so we can find the velocity of soil-rock (1,475 m/s). If square of distance (x^2) is equal to zero, then t_0^2 and t_0 are equal to 9,298.5 and 96.43 ms, respectively. The depth of soil-rock can be calculated from eq. (15). From P-wave velocity equal to 1,202 can be classify as Wet sand, Dry sand, Wet sandy gravel, Dry sandy gravel, Wet clay or Dry clay (Table 2).

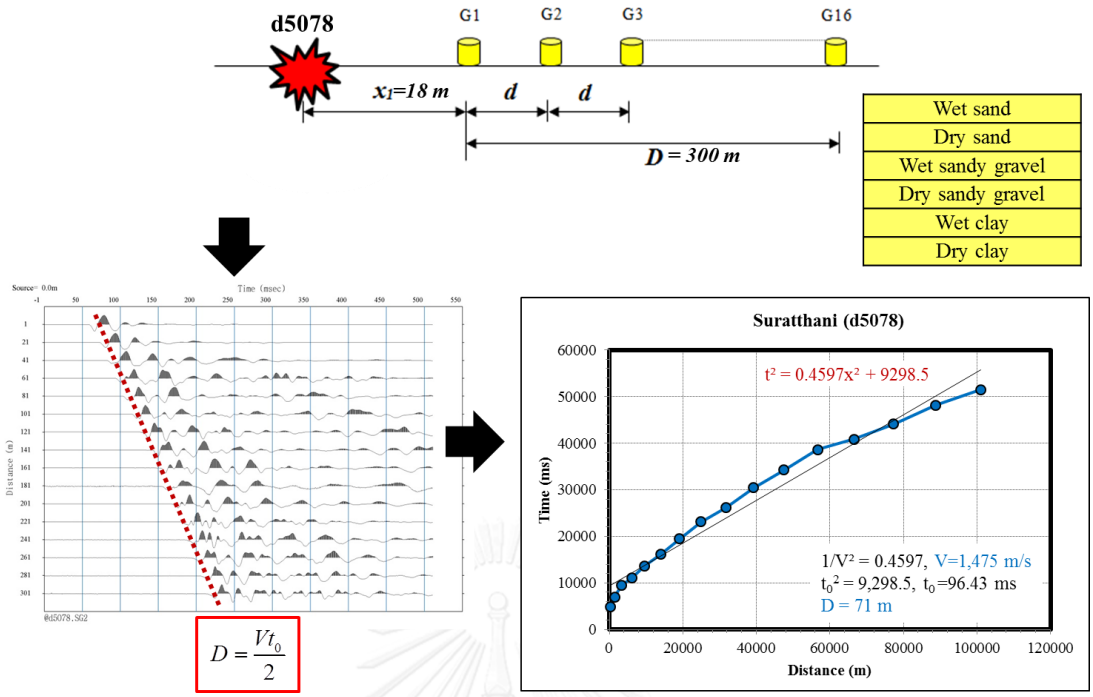

Figure 100 Data processing by Reflection seismic survey at Suratthani

4.4.5.3 The Simple Analysis of Surface Wave Method (SM)

The figure shows that the analysis of the data by procedure described in Section 2.2.3.1 to establish the relationship between the phase velocities with frequency (Dispersion Curve), and should be inversion to determine only primary wave velocity at the depth of the soil layer using the principles and theories in Section 2.2.4.2.

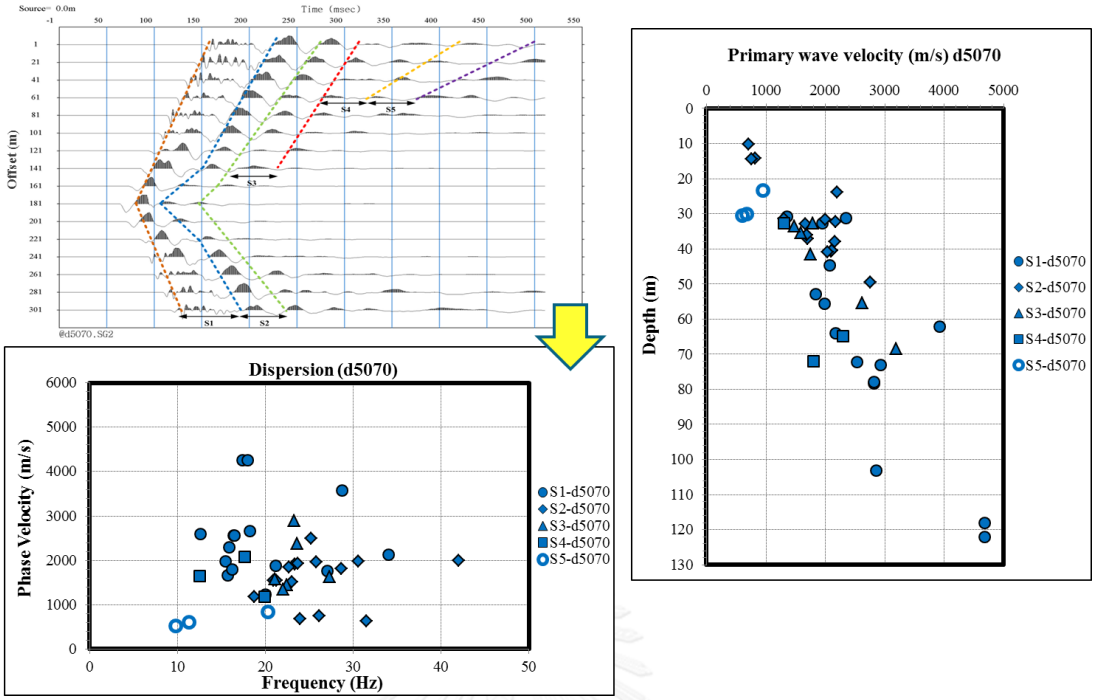

Figure 101 The SM data processing from field test (d5070)

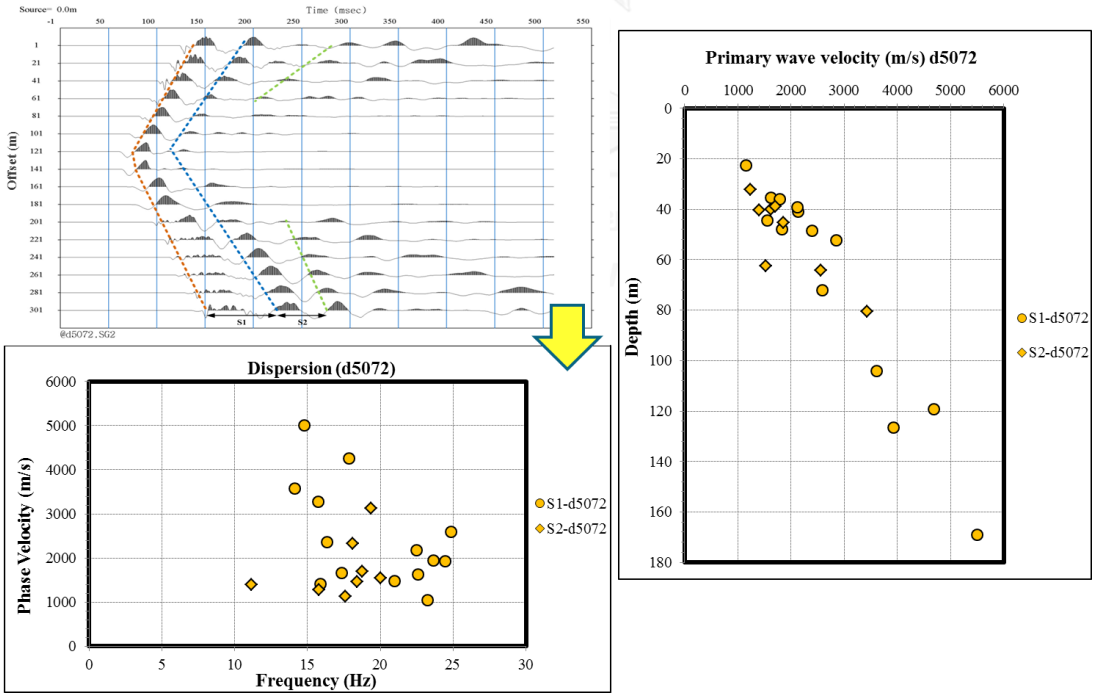

Figure 102 The SM data processing from field test (d5072)

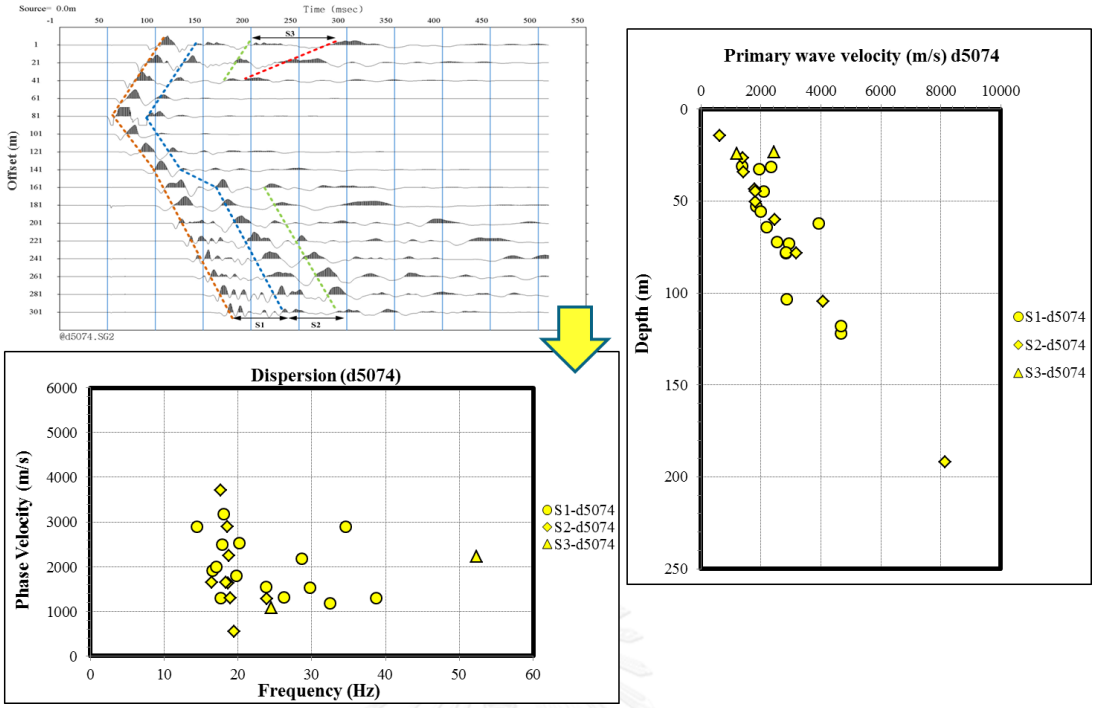

Figure 103 The SM data processing from field test (d5074)

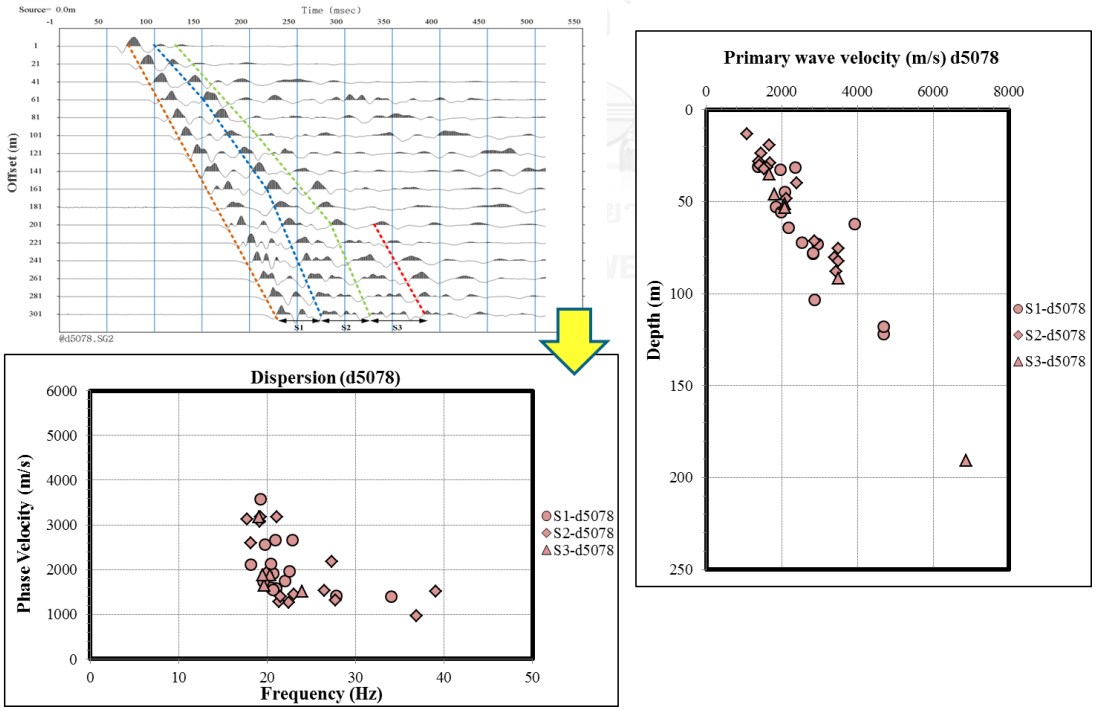

Figure 104 The SM data processing from field test (d5078)

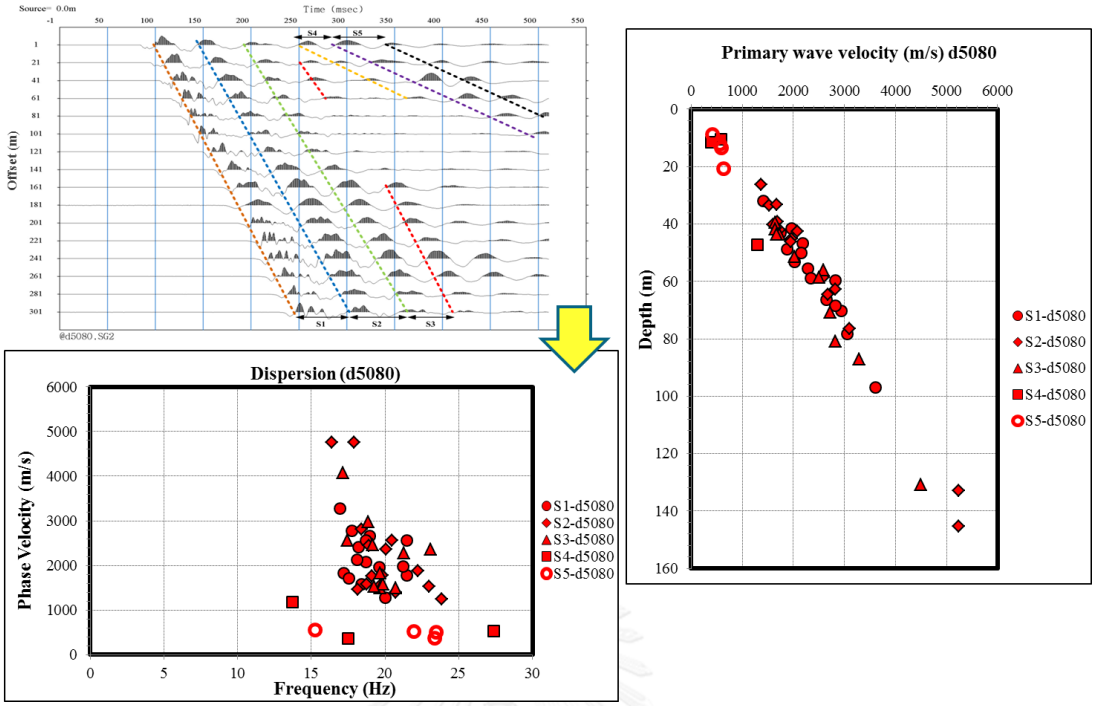

Figure 105 The SM data processing from field test (d5080)

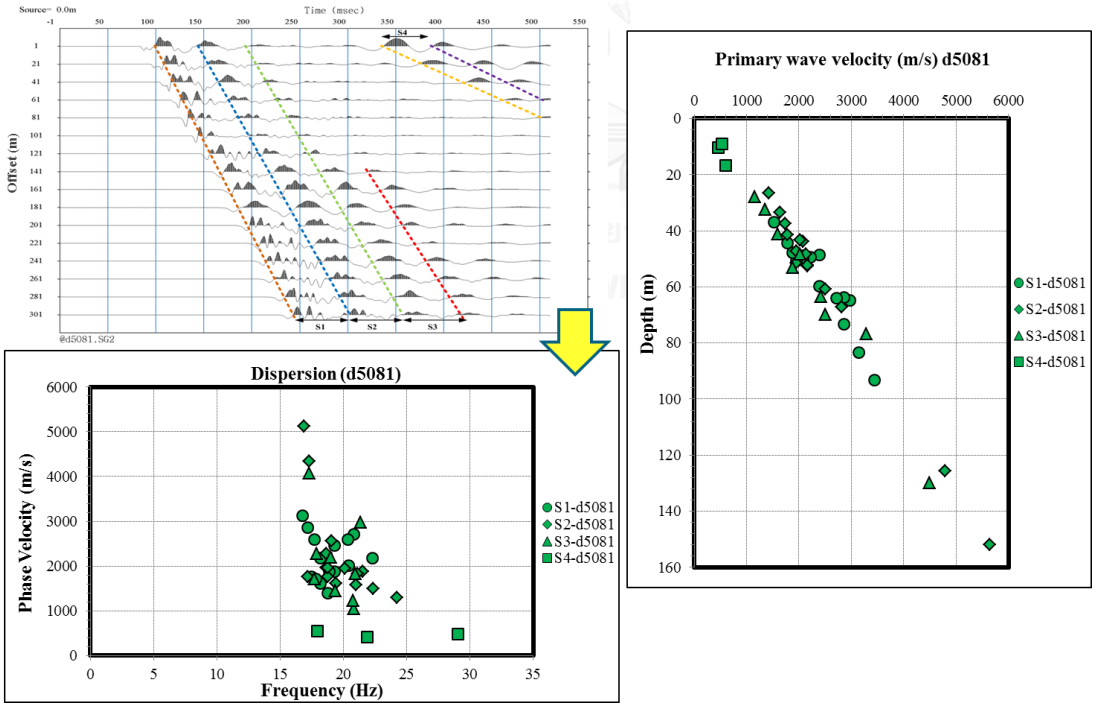

Figure 106 The SM data processing from field test (d5081)

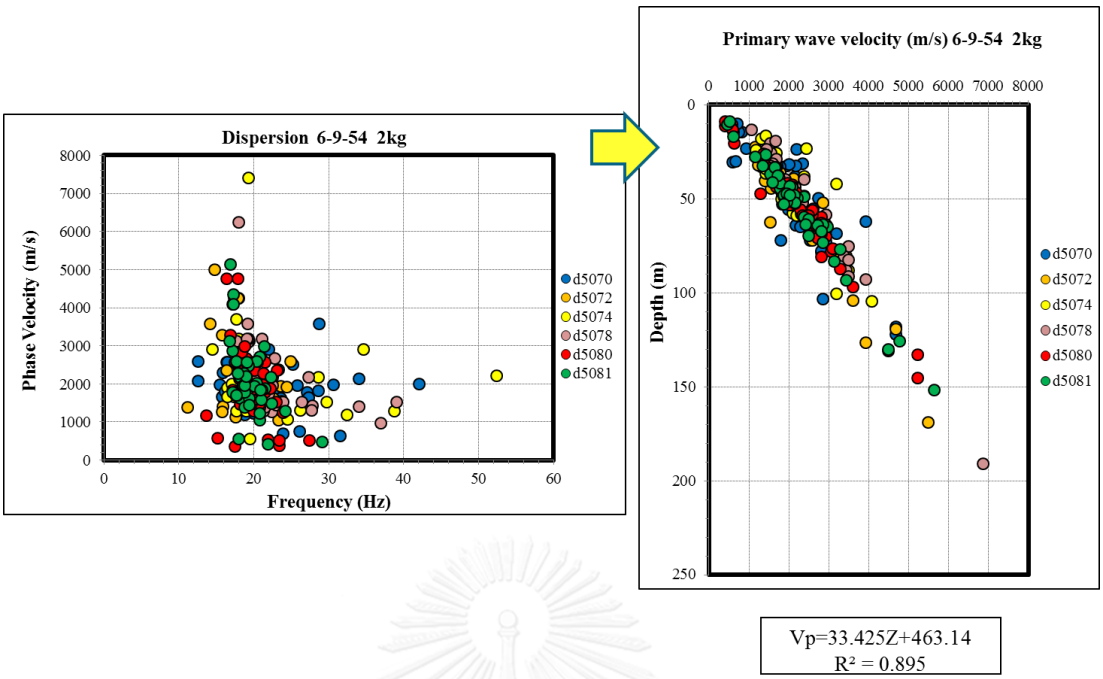

Figure 107 Primary wave velocity profile by SM at Suratthani

4.4.5.4 The Multichannel Analysis of Surface Wave Method (MASW)

The data obtained from measurements of the processed as described in Section 2.2.4.1 to establish the relationship between the phase velocity with frequency (Dispersion Curve) as shown in this figure by the intensity of the color indicates the strength of the energy measurement (Image processing), and inversion to determine only primary wave velocity of the soil.

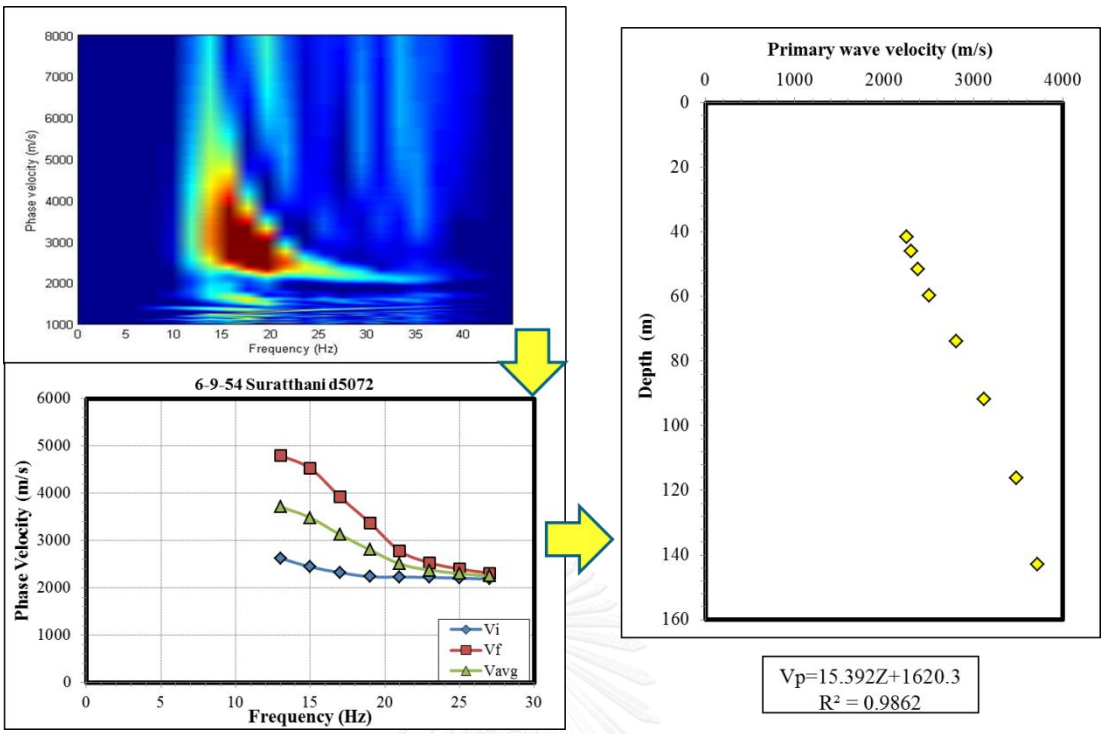

Figure 108 Primary wave velocity profile by MASW at Suratthani

จุฬาลงกรณ์มหาวิทยาลัย
Chulalongkorn University

4.5 The comparison of shear wave velocity profile between SM, MASW and DH

In figure 109-111 shows that shear wave velocity profile from SM corresponded with those obtained from MASW and DH, as did the primary waves with those obtained from MASW as shown as figure 112-113.

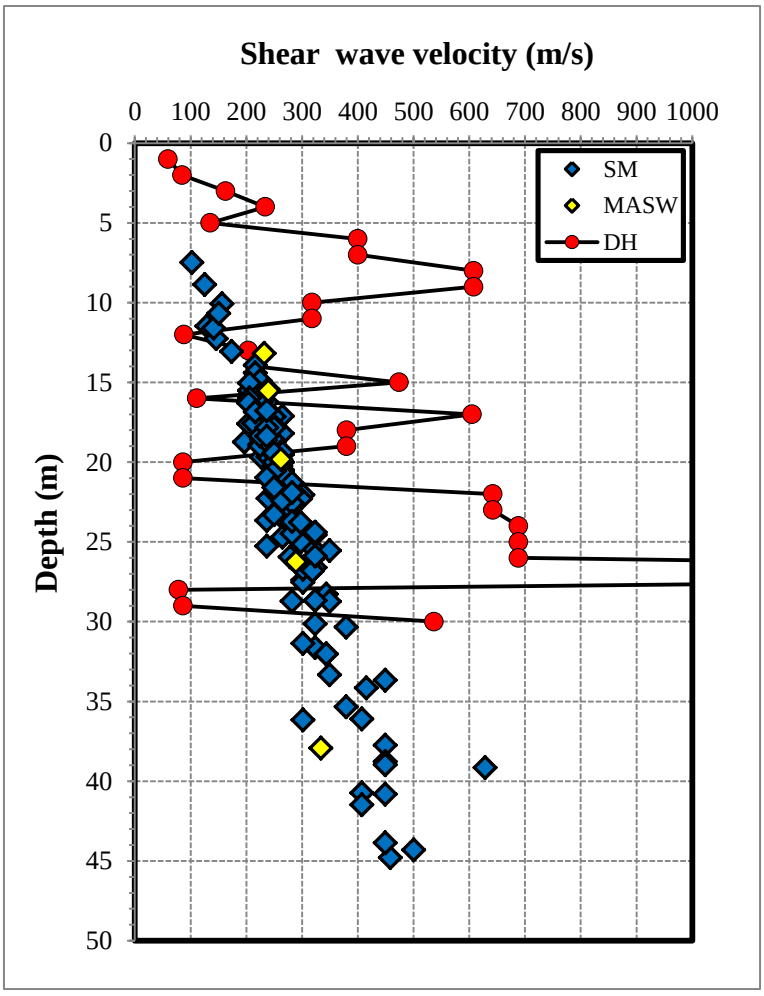

Figure 109 The comparison of shear wave velocity profile between SM, MASW and DH method at Mahasarakham

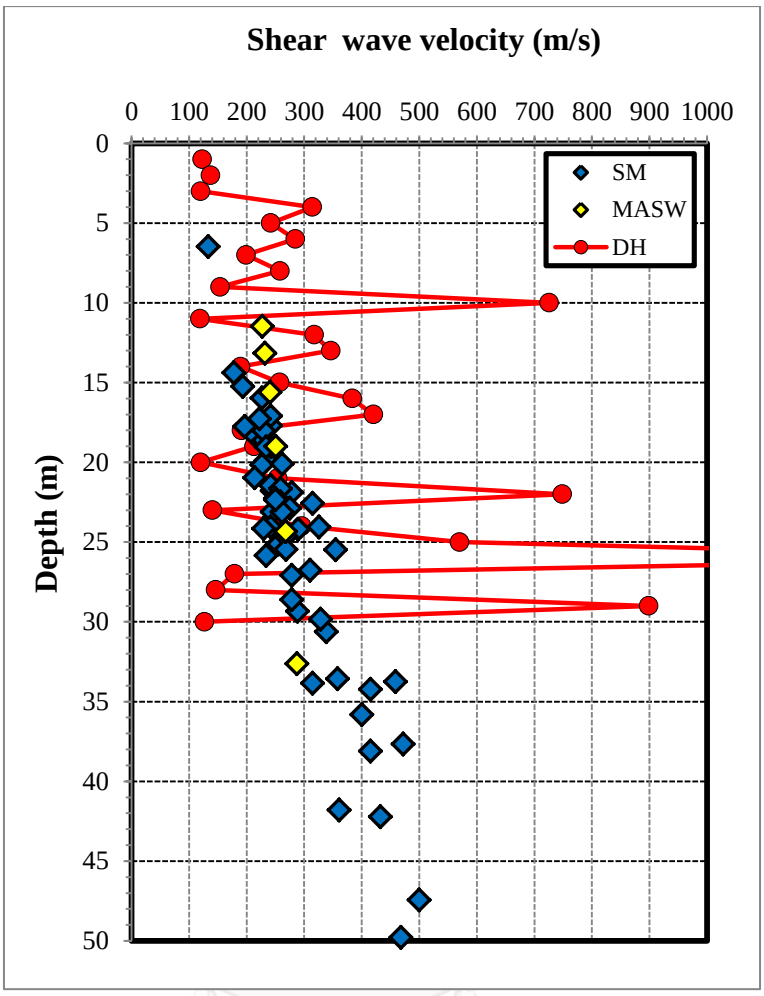

Figure 110 The comparison of shear wave velocity profile between SM, MASW and DH method at Surin

จุฬาลงกรณ์มหาวิทยาลัย
Chulalongkorn University

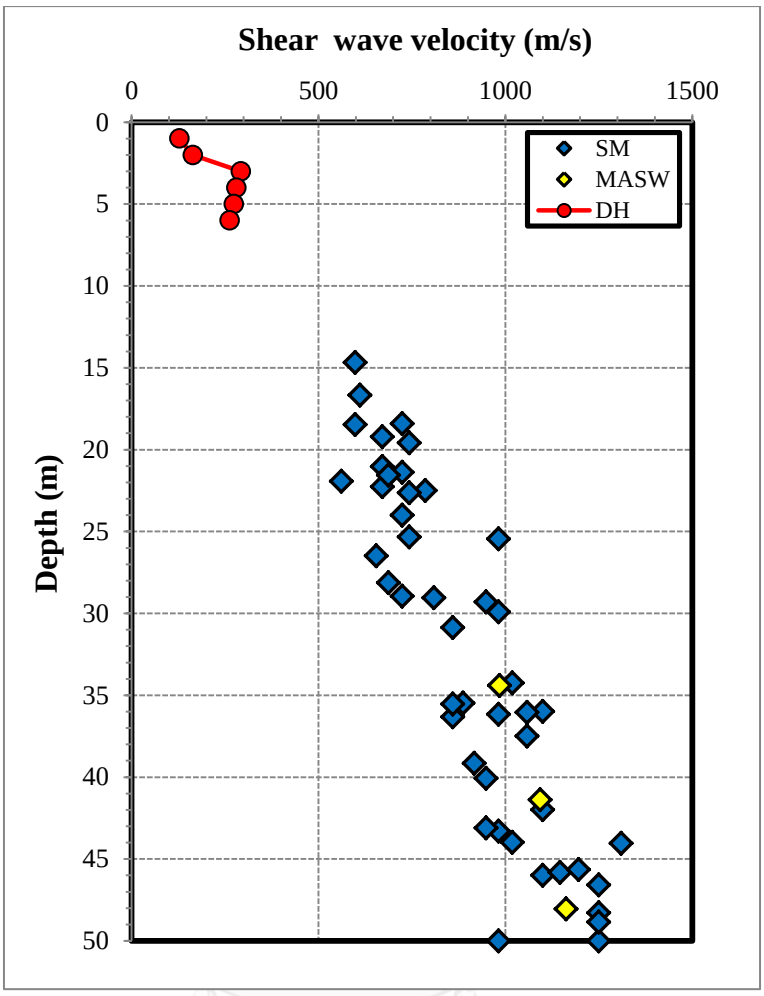

Figure 111 The comparison of shear wave velocity profile between SM, MASW and DH method at Udonthani

จุฬาลงกรณ์มหาวิทยาลัย
Chulalongkorn University

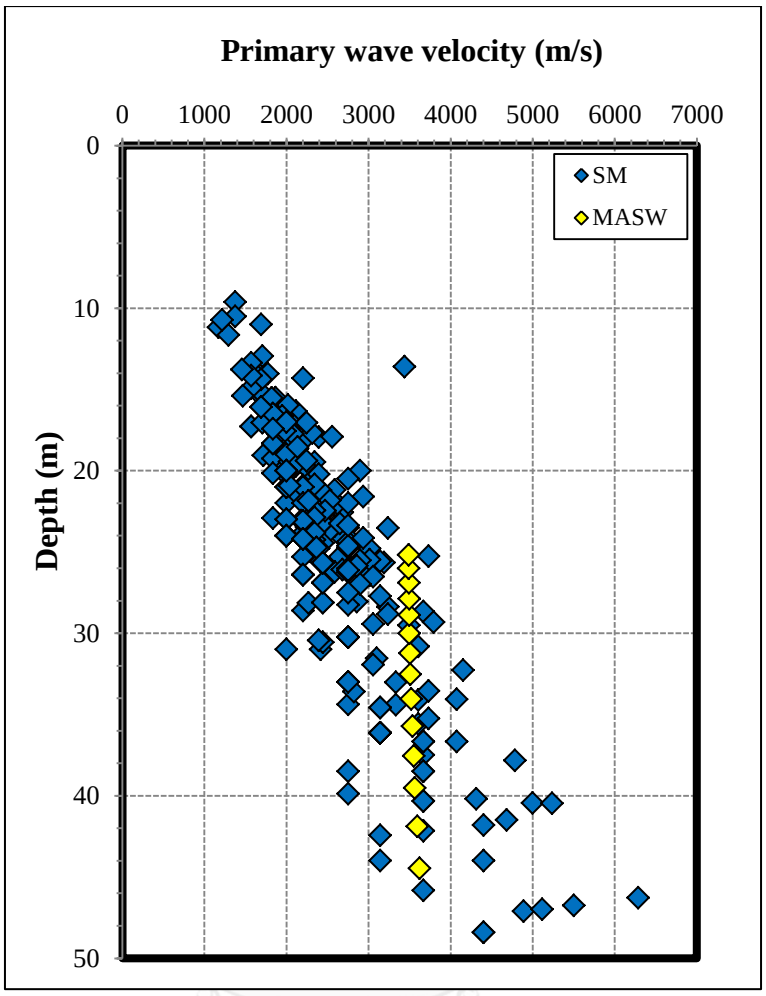

Figure 112 The comparison of primary wave velocity profile between SM and MASW method at Suphanburi

จุฬาลงกรณ์มหาวิทยาลัย
Chulalongkorn University

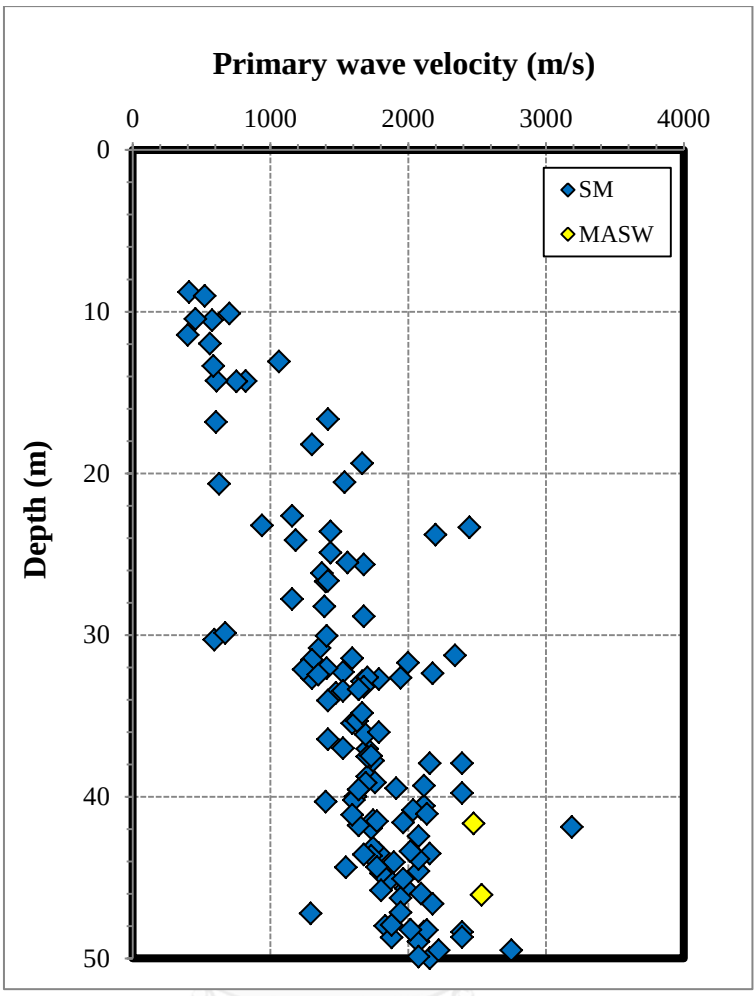

Figure 113 The comparison of primary wave velocity profile between SM and MASW method at Suratthani

จุฬาลงกรณ์มหาวิทยาลัย
Chulalongkorn University

4.6 The correlations between Vs and SPT-N value

The results of soil investigation data 3 case can be establish the relationship between Vs(DH) and SPT-N value at Mahasarakham, Surin and Udonthani province as shown in Figure 114-116.

$$Vs = aN^{b} \quad (28)$$

where N is Standard penetration test (blow/ft)

a, b are Site coefficients

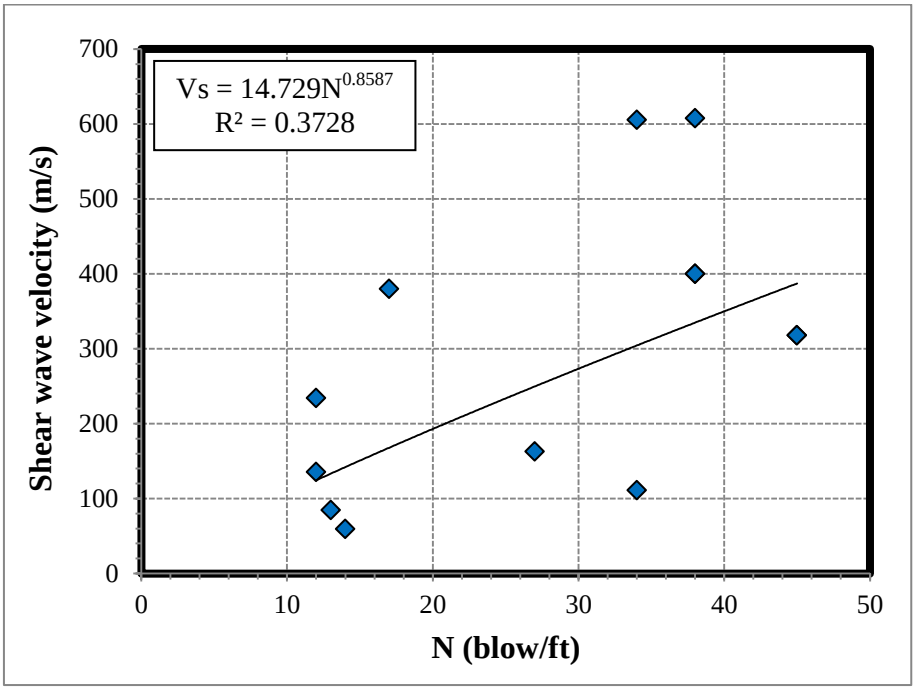

Figure 114 The correlations between Vs and SPT-N value at Mahasarakham province

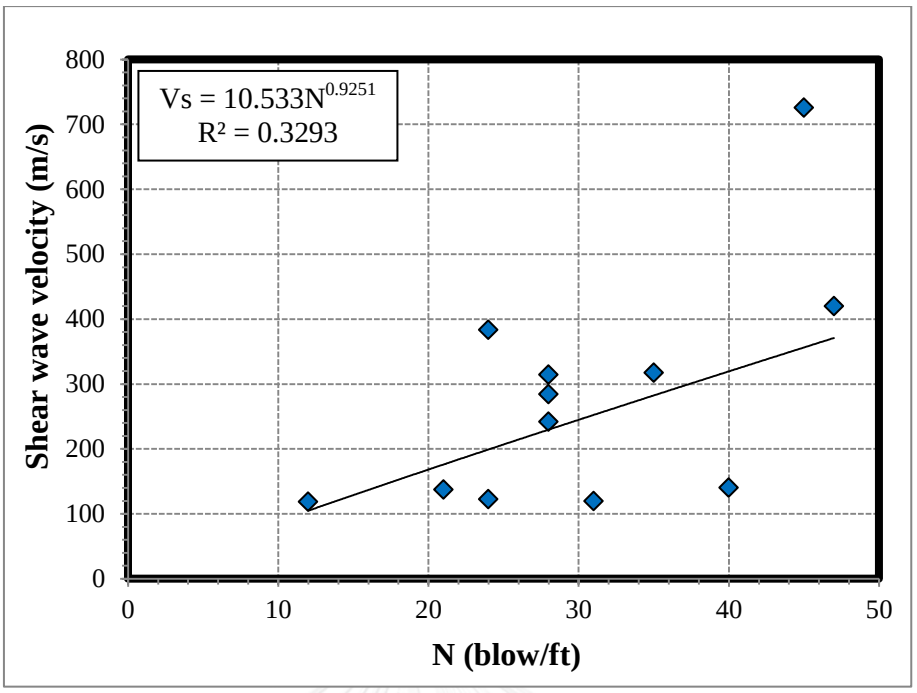

Figure 115 The correlations between Vs and SPT-N value at Surin province

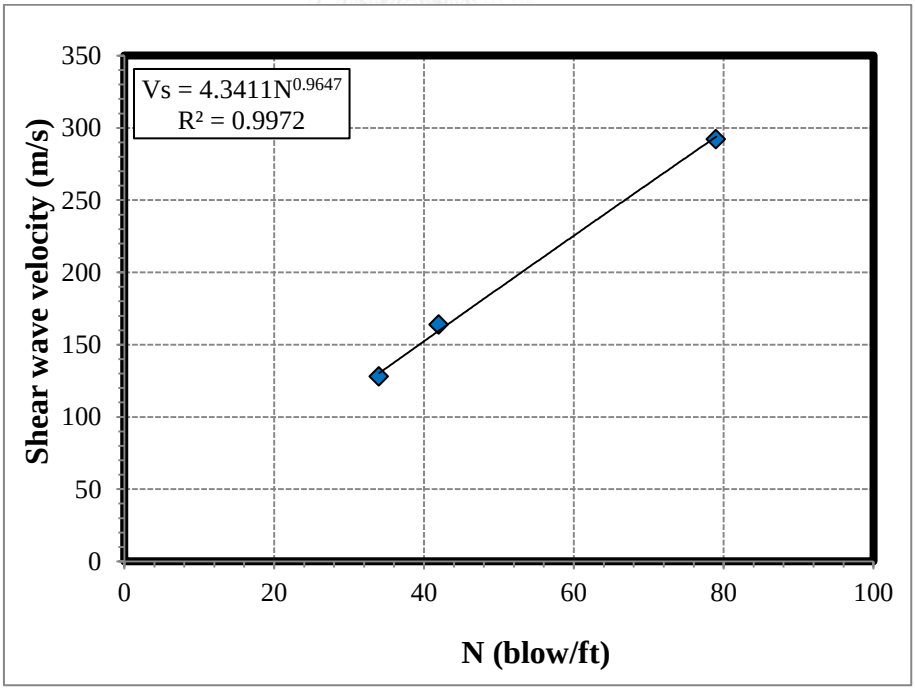

Figure 116 The correlations between Vs and SPT-N value at Udonthani province

CHAPTER 5

CONCLUSIONS AND RECOMMENDATIONS

5.1 Conclusions

5.1.1 The Simple Analysis of Surface Wave Method (SM) can be investigated the shear wave velocity profiles within 30 m depth from explosion source.

5.1.2 The shear wave velocity profiles by Simple Analysis of Surface Wave Method (SM) have similar values with Multichannel Analysis of Surface Wave Method (MASW) and Down-hole Seismic Method (DH).

5.1.3 The development of empirical correlations between shear wave velocity (Vs, DH) and SPT-N value at Mahasarakham, Surin and Udonthani, the coefficient of determination (R^2) are not well data fit.

5.1.4 The Simple Analysis of Surface Wave Method (SM) is the easiest to analyze and interpret the shear wave velocity profiles from explosion source.

5.1.5 The Simple Analysis of Surface Wave Method (SM) has been used to determine shear wave velocity profile for seismic hazard mapping, city planning, and economical technique for seismic survey projects.

5.1.6 There are abundant of ground motion records from seismic surveys (i.e. the petroleum source survey), the shear wave velocity profile can be easily obtained as a byproduct from such projects.

5.2 Recommendations

5.2.1 The shear wave velocity profiles at Suphanburi and Suratthani could not be concluded because those areas had high signal frequency, high underground water level, and deep blast holes.

5.2.2 The further research should be varying distance (x_1) and geophone spacing (d) for explosion source.

5.2.3 The researcher can change seismic source (i.e. sledge hammer, vibroseis)

จุฬาลงกรณ์มหาวิทยาลัย
Chulalongkorn University

REFERENCES

American Society for Testing and Materials. (2010). Standard Guide for Using the Seismic-Reflection Method for Shallow Subsurface Investigation (D7128-05). West Conshohocken: ASTM International.

American Society for Testing and Materials. (2011). Standard Guide for Using the Seismic Refraction Method for Subsurface Investigation (D5777-00). West Conshohocken: ASTM International.

American Society for Testing and Materials. (2014). Standard Test Methods for Downhole Seismic Testing. West Conshohocken: ASTM International.

Bruce, B. R. (1973). Seismic Refraction Exploration for Engineering Site Investigations. California: Explosive excavation research laboratory livermore.

Clark, D. A., & Emerson, D. W. (1999). Self-demagnetization: a preview. *Exploration Geophysics, 79*, 22-25.

Dobrin, M. B., & Savit, C. H. (1988). *Introduction to geophysical prospecting*. New York: McGraw-Hil.

Foti, S. (2000). *Multi Station Methods for Geotechnical Characterisation Using Surface Waves.* (Ph.D.), Politecnico di Torino.

Huntera, J. A., Benjumeaa, B., Harrisb, J. B., Millerc, R. D., Pullana, S. E., Burnsa, R. A., & Gooda, R. L. (2002). Surface and downhole shear wave seismic methods for thick soil site investigations. *Soil Dynamics and Earthquake Engineering, 22*, 931–941.

Imai, T., & Tonouchi, K. (1982). *Correlation of N-value with S- Wave Velocity and Shear Modulus*. Paper presented at the Proceedings of the Second European Symposium on Penetration Testing, Amsterdam,.

Kim, D. S., Bang, E. S., & Kim, W. C. (2008). Evaluation of Various Downhole Data Reduction Methods for Obtaining Reliable Vs Profiles. *Geotechnical Testing Journa, 27*, 1-13.

Kramer, S. L. (1996). *Geotechnical Earthquake Engineering*. United State: Prentice hall.

Lippus, C. (2007). *Fundamentals of Seismic Refraction*: Geometric,Inc.

Mayne, P. W., & Rix, G. J. (1995). Correlations between shear wave velocity and cone tip resistance in natural clays. *Soils and Foundations, 35*(2), 107-110.

Ohta, Y., & Goto, N. (1978). Empirical Shear Wave Velocity Equations in Terms of Characteristics Soil Indexes. *Earthquake Engineering and Structural Dynamics, 6*, 167-187.

Park, C. B., Miller, R. D., & Xia, J. (1999). Multichannel analysis of surface waves. *GEOPHYSICS, 64*(3), 800-808.

Sattarak, P. (2007). *Exploration Geophysics*. Faculty of Technology: Khonkaen University.

Siam moeco limited. (2005). Final Report for The Onshore Seismic Survey 2-D and 3-D (No. L10/43 and L11/43). Bangkok.

Sykora, D. W., & Stokoe, K. H. (1983). Correlations of In-Situ Measurements in Sands with Shear Wave Velocity. Texas: The University of Texas at Austin.

Teachavorasinskun, S., & Lukkunaprasit, P. (2004). A simple correlation for shear wave velocity of soft Bangkok clays. *Geotechnique, 54*(5), 323-326.

Telford, W. M., Geldart, L. P., & Sheriff, R. E. (1990). *Apply Geophysics*. England: Cambridge University.

Xia, J., Miller, R. D., & Park, C. B. (1999). Estimation of near-surface shear-wave velocity by inversion of Rayleigh wave. *GEOPHYSICS, 64*, 691-700.

Zhang, S. X., Chan, L. S., & Xia, J. (2004). The Selection of Field Acquisition Parameters for Dispersion Images from Multichannel Surface Wave Data. *Pure and Applied Geophysics, 161*, 185-201.

จุฬาลงกรณ์มหาวิทยาลัย
CHULALONGKORN UNIVERSITY

APPENDIX

จุฬาลงกรณ์มหาวิทยาลัย
Chulalongkorn University

VITA

PITHAN PAIROJN

Postal Address: 50/68 Ladprao Road, Saphansong, Wangthonglang, Bangkok, 10310

Tel: +66840705220

E-mail: dr.pithan@gmail.com

EDUCATION:

- M.Eng. (2010), Chulalongkorn University Major in Civil Engineering (Geotechnical Engineering)
- B.B.A. (2010), Sukhothai Thummathirat Open University Major in Business Administration (Construction Management)
- B.Eng. (2008), Srinakharinwirot University Major in Civil Engineering

EXTRA-CURRICULAR ACTIVITIES:

- Researcher, Center of Excellence in Earthquake Engineering and Vibration, Faculty of Engineering, Chulalongkorn University (2012-Present)
- Researcher, Joint Venture Chulalongkorn University and Department of Mineral Fuels, Ministry of Energy (2010-2012)
- Teaching Assistant, Department of Civil Engineering, Chulalongkorn University (2009-2011)